THE QUARTERLY JOURNAL OF MECHANICS AND APPLIED MATHEMATICS

VOLUME II
1949

OXFORD
AT THE CLARENDON PRESS

Oxford University Press, Amen House, London E.C. 4
GLASGOW NEW YORK TORONTO MELBOURNE WELLINGTON
BOMBAY CALCUTTA MADRAS CAPE TOWN
Geoffrey Cumberlege, Publisher to the University

PRINTED IN GREAT BRITAIN
AT THE UNIVERSITY PRESS, OXFORD
BY CHARLES BATEY, PRINTER TO THE UNIVERSITY

THE QUARTERLY JOURNAL OF MECHANICS AND APPLIED MATHEMATICS

VOLUME II PART 1
MARCH 1949

OXFORD
AT THE CLARENDON PRESS
1949

Price 12*s.* 6*d. net*

PRINTED IN GREAT BRITAIN BY CHARLES BATEY AT THE UNIVERSITY PRESS, OXFORD

THE QUARTERLY JOURNAL OF MECHANICS AND APPLIED MATHEMATICS

THE QUARTERLY JOURNAL OF MECHANICS AND APPLIED MATHEMATICS is published at 12*s.* 6*d.* net for a single number with an annual subscription (for four numbers) of 40*s.* post free.

NOTICE TO CONTRIBUTORS

1. *Communication.* Papers should be communicated to one or other of the Executive Editors, by name, at King's College, Strand, London, W.C. 2.

2. *Presentation.* Manuscripts should preferably be typewritten, and each paper should be preceded by a summary not exceeding 300 words in length. References to literature should be given in standard order, *author, title of journal, volume number, date, page.* These should be placed at the end of the paper and arranged according to the order of reference in the paper.

3. *Diagrams.* The number of diagrams should be kept to the minimum consistent with clarity. The lines of the figures should be drawn in ink either on draughtsman's paper or on good quality white paper. Each individual line in the figure should bear reducing to one-half of the size of the original, and great care should be exercised to see that the lines are regular in thickness, especially where they meet. Lettering of the figure should be in pencil and should be sufficient to define clearly the lines and curves in it. The writing of formulae or of explanations on the diagram itself should be avoided. All explanations of symbols, etc., should be given in underline. Contributors should indicate on their manuscripts where figures should be inserted.

4. *Tables.* Tables should preferably be arranged so that they can be printed with the columns parallel to the longer edge of the page.

5. *Vector Notation.* All single letters used to denote vectors in the manuscript should be marked by underlining with a wavy line. Scalar and vector products should be denoted by $\underset{\sim}{a} . \underset{\sim}{b}$ and $\underset{\sim}{a} \wedge \underset{\sim}{b}$ respectively.

6. *Offprints.* Authors of papers will be entitled to 25 free offprints.

7. All correspondence other than that dealing with contributions should be addressed to the Publisher:

GEOFFREY CUMBERLEGE
OXFORD UNIVERSITY PRESS
AMEN HOUSE, LONDON, E.C. 4

ICS

es is
tion

ative

ould
ture
age.
r of

with
per
ing
the
uld
The
All
di-

the

uld
be

ed

By

INT
PA
AN
OF
PA
SM
1
2
3

4
APP
C
RE

T
gau
cha
imp
gau
teri
the
T
supe
in te
the
whil
prob
the s
acco
publ
abou
Th
is als
lence
are f
upst
redu
the c

[Qu
50

THE EFFECT OF WIRE GAUZE ON SMALL DISTURBANCES IN A UNIFORM STREAM

By G. I. TAYLOR *and* G. K. BATCHELOR (*Trinity College, Cambridge*)

(*With an Appendix by* H. L. DRYDEN *and* G. B. SCHUBAUER)

[Received 29 December 1947]

CONTENTS

SUMMARY

The paper sets out to give a comprehensive account of the effect of woven wire gauze on small disturbances to a uniform stream. The relevant aerodynamic characteristics of gauze are the pressure drop and deviation in direction which it imposes on a uniform stream incident at an arbitrary angle to the plane of the gauze. Measurements by Dryden and Schubauer suggest that these two characteristics may be uniquely related for all gauzes and Reynolds numbers, and enable the deviation to be determined when the pressure drop is known.

The effect of placing a gauze at right angles to a uniform stream, on which is superimposed a small steady disturbance to the longitudinal velocity, is determined in terms of the gauze characteristics. The limitation to a small disturbance linearizes the problem and the effect of gauze is to reduce the intensity of the disturbance while leaving its (arbitrary) shape unchanged. Previous attempts to solve this problem have been made; it is shown that they all make special assumptions about the side-force exerted by the gauze and that Collar's analysis is incorrect on another account. The theoretical reduction in the disturbance is consistent with the few published measurements. There is one gauze—with a pressure-drop coefficient of about 2·8—which entirely removes all small steady longitudinal disturbances.

The effect of gauze on a small arbitrary unsteady disturbance—i.e. on turbulence—is also determined, on the assumption that the gauze wires produce no wake turbulence. The intensities of fluctuations parallel and normal to the plane of the gauze are found to be reduced by different amounts, and if the turbulence is isotropic far upstream from the gauze it is axially symmetrical downstream from the gauze. The reduction in turbulent energy depends on the three-dimensional energy spectrum of the oncoming turbulence and is thus not unique, even when the oncoming turbulence

is isotropic. Some estimates of the reduction in intensity obtained from an approximation to the spectrum function in isotropic turbulence are presented. They are found to be close to the reduction factors appropriate to a simplified type of turbulence in which the longitudinal velocity does not vary in the direction of the stream. It is possible to deduce the effect of gauze on other characteristics of the turbulence; one immediate result is that the longitudinal integral scale is reduced to zero by the gauze which removes steady longitudinal disturbances.

Introduction

It has long been known that when a turbulent stream of fluid passes through a wire gauze it becomes less turbulent, and that steady disturbances are reduced in intensity. Several attempts have been made (Prandtl, **1**; Collar, **2**; Batchelor, **3**; Dryden and Schubauer, **4**) to give a theoretical description of these effects and recently some measurements (Dryden and Schubauer, **4**) showing the effect of gauze on wind-tunnel turbulence have been published. In all theoretical discussions the gauze has been supposed to offer a resistance to the component of flow normal to its plane. If a pressure difference p_1-p_2 is required to drive fluid of density ρ through a gauze at velocity U, the drag coefficient k is defined as

$$k = \frac{p_1-p_2}{\frac{1}{2}\rho U^2},$$

and it has been assumed that k measures the only aerodynamic property of gauze which is effective in reducing turbulence.

It was to be expected that different values of the ratio of the disturbance velocity in front to that behind the gauze might be obtained when different types of disturbance are considered, but two quite different expressions for this ratio in terms of k were obtained by Prandtl (**1**) on the one hand, and by Collar (**2**) and by one of us (**3**) on the other, for exactly the same disturbance. It will be shown later that the difference is due to the fact that these authors left out of consideration the force which the gauze exerts on the fluid in directions parallel to its surface. Prandtl and Collar, in fact, make different implicit assumptions about this force. It will be found that when allowance is made for this side-force Prandtl's and Collar's expressions are special cases of a more general formula.

The work falls into three parts. In Part I a method is described by which the side-force as well as the drag of a gauze can be measured when a stream passes obliquely through it. Measurements made at the National Physical Laboratory by Simmons and Cowdrey (**5**) using this method are described and discussed. The results of more recent and more extensive measurements of the same kind by Dryden and Schubauer at the National Bureau of Standards have been communicated to the present authors and are reproduced in an appendix to this paper. Part II contains a solution

of Prandtl's and Collar's problem, viz. the effect of gauze on a small steady longitudinal disturbance, and a comparison with some experimental results. There is one particular value of k for which longitudinal disturbances are entirely removed by the gauze. In Part III we discuss the effect of a gauze (whose mesh is so small that it creates no turbulence) on a general unsteady disturbance, i.e. on stream turbulence, and expressions for the reduction of the mean-squares of the velocity components are derived. These reduction factors depend on the energy spectrum of the turbulence approaching the gauze. In the case of isotropic turbulence, previous measurements enable us to postulate a spectrum function which is likely to be approximately valid under certain conditions, and the effect of gauze can be calculated. A comparison with the experimental results of Dryden and Schubauer (**4**) is given, though owing to the nature of these experiments it is not possible to draw any definite conclusions.

PART I

Measurement of side-force and drag on a gauze sheet set obliquely to a uniform wind

In the first instance it will be assumed that the flow is confined to one plane perpendicular to the gauze. This assumption implies that the gauze has aerodynamic properties which are symmetrical about the plane of flow. The flow through the gauze gives rise to a pressure difference p_1-p_2 across its two sides. If U denotes the velocity of the stream approaching the gauze and θ the angle its direction makes with the normal to the plane of the gauze, the results of experiments in which p_1-p_2, U, and θ are measured can be expressed in the form

$$p_1-p_2 = k_\theta \cdot \tfrac{1}{2}\rho U^2. \tag{1.1}$$

The coefficient k_θ is identical with the k previously used when $\theta = 0$. Measurements show that k_θ is a function of θ and U for any particular gauze.

The force parallel to the gauze gives rise to a change in the component of velocity parallel to its plane as the fluid passes through it. To measure this force it is sufficient to measure the change in direction of the stream on passing through the gauze. If ϕ is the angle which the stream makes with the normal to the gauze on its leeward side (see Fig. 1), the air emerges from the gauze with velocity $U\cos\theta\sec\phi$ and the side-force per unit area of the gauze is

$$\rho U^2(\sin\theta\cos\theta - \sin\phi\cos^2\theta\sec\phi) = \rho U^2\cos\theta\sec\phi\sin(\theta-\phi).$$

If ϕ can be measured, the results of experiment can therefore be expressed in the form

$$F_\theta = 2\cos\theta\sec\phi\sin(\theta-\phi), \tag{1.2}$$

where F_θ is a force coefficient parallel to the plane of the gauze. In cases where steady or unsteady disturbances are producing transverse components of velocity which are small compared with the mean velocity, θ and ϕ are small, and (1.2) can be written

$$F_\theta/\theta = 2\{1-(\phi/\theta)\}. \tag{1.3}$$

This form is useful because the experimental results show that ϕ/θ tends to a finite limit as θ tends to 0. The value of ϕ/θ for small values of θ

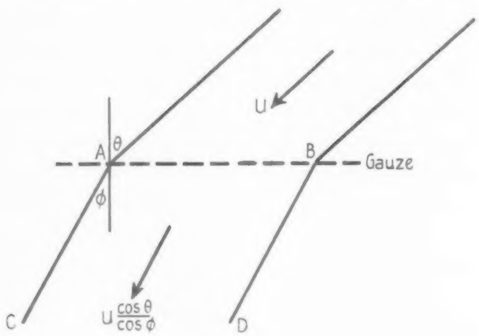

Fig. 1.

($=\alpha$, say) and the resistance coefficient k are the two parameters which will later be taken as specifying the effect of gauze on small disturbances.

In general, if a gauze is set up at angle θ to a stream in a wind tunnel with rigid walls, the direction of flow will vary along the length of the gauze on both sides of it. For convenience in measurement it is best to try to arrange matters so that the velocity and direction of the stream, and consequently the pressure, are uniform on both sides of the gauze. One way in which this may be done is by turning the walls of the channel (shown as AC, BD in Fig. 1) about hinges at A and B till they make the appropriate angle ϕ with the normal to the gauze. When the walls AC, BD are set at this angle, it is possible for the velocity, direction, and pressure of the streams on the two sides to be uniform. In practice the experiment consists in determining the angle ϕ at which the walls must be set in order to make the variation along the length of the gauze as small as possible.

This method was adopted by Simmons and Cowdrey (**5**) for measuring the values of k_θ and F_θ over a series of values of θ and U for three gauzes, referred to by them as G_2, G_4, and G_6, the geometrical characteristics of which are given in Table 1. The directions of flow up- and down-stream from the gauze lay in a vertical plane in each case. The measurements

TABLE 1

Geometrical characteristics of gauzes used by Simmons and Cowdrey, and Dryden and Schubauer

Source	*Gauze*	*Wire diameter*	*Number of wires per inch*
		in.	
Simmons and Cowdrey	G_2	0·0053	40
	G_4	0·0067	52 (horiz.) 60 (vert.)
	G_6	0·0075	40
Dryden and Schubauer	60-mesh	0·0065	60
	54-mesh	0·0055	54
	40-mesh	0·0065	40
	24-mesh	0·0075	24

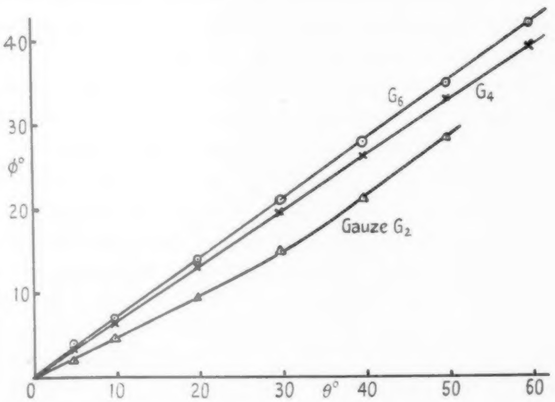

FIG. 2. Measurements of ϕ and θ made by Simmons and Cowdrey.

of ϕ for a given value of θ were found to be insensitive to variations of U over the range 8 to 34 ft. per sec. Their results for the three gauzes are shown with their permission in Fig. 2. It will be seen that in all three cases ϕ/θ is nearly constant over a large range of values of θ, viz.

$$\text{for gauze } G_2, \quad \phi/\theta = 0{\cdot}48 \quad (0 < \theta < 20^\circ),$$
$$\text{for gauze } G_4, \quad \phi/\theta = 0{\cdot}66 \quad (0 < \theta < 60^\circ),$$
$$\text{for gauze } G_6, \quad \phi/\theta = 0{\cdot}70 \quad (0 < \theta < 60^\circ).$$

Dryden and Schubauer have recently adopted the simpler plan of eliminating the walls of the duct downstream from the gauze so that the stream discharges into free air. The jet emerges at an angle ϕ to the normal to the gauze and this angle can readily be observed. Dryden and Schubauer have been kind enough to send to us an account of their

experiments which is reproduced as an appendix to this paper. The significant feature of this extensive series of measurements is that F_θ/θ appears to be uniquely related to k_θ for the four gauzes and the various wind speeds used.† An empirical relation which seems to fit the measurements sufficiently well over the range $k_\theta > 0{\cdot}7$ is

$$F_\theta/\theta = 2-2{\cdot}2(1+k_\theta)^{-\frac{1}{2}} \tag{1.4}$$

which is shown in Fig. 5 in the Appendix. In our discussions of the effect of gauze on small disturbances, we shall be concerned only with small values of θ, for which (1.4) leads to (see (1.3))

$$\alpha = 1{\cdot}1(1+k)^{-\frac{1}{2}}. \tag{1.5}$$

It would be very useful if, as the evidence seems to suggest, this relation were valid for all wire gauzes and Reynolds numbers in common use, for the aerodynamic 'smoothing' properties of a gauze would then be completely specified by the easily measured quantity k.

It is probable that the above experiments were confined to the case of gauzes possessing geometrical symmetry about the plane of flow, i.e. one of the lines of wires was in the plane of flow while the other was perpendicular. We have no experimental evidence that if the gauze were rotated in its plane the downstream flow would remain in the same direction or even in the plane containing the upstream flow and the perpendicular to the gauze. However, for simplicity in the succeeding analysis, we assume that the gauze has aerodynamical properties which are rotationally symmetrical about the perpendicular to its plane. It will also be assumed that the same value of α applies at each point of the gauze in cases when the flow velocity is uniform neither in space nor time, and that the distance between the wires of the gauze is small compared with the scale of non-uniformities in the stream passing through it.

PART II

Effect of gauze on a small steady disturbance

1. Solution of the problem

The disturbance investigated by both Prandtl and Collar is a small steady spatial variation in the magnitude, but not the direction, of the velocity of a stream, and so affects all points along a streamline. According to Prandtl (**1**) the ratio of the velocity increment (u_2) to the mean velocity at any point downstream to that upstream on the same streamline (u_1) is

$$\frac{u_2}{u_1} = \frac{1}{1+k}, \tag{2.1}$$

† A plot of $F_\theta/\sin\theta$ against k shows that these quantities can equally well be represented by a single relation.

whereas Collar's result (**2**) for the same type of disturbance is

$$\frac{u_2}{u_1} = \frac{2-k}{2+k}. \tag{2.2}$$

More recently one of us has obtained the result (2.2) by a different method (**3**). Prandtl and Collar considered the way in which the longitudinal velocity is altered by the gauze without considering the lateral velocity which must be acquired by the stream both upstream and downstream in the neighbourhood of the gauze in order to satisfy the condition of continuity as the longitudinal velocity varies. Batchelor took the induced lateral velocities into account but made the assumption, now known to be incorrect, that these lateral velocities are continuous across the gauze.

A complete solution of the steady disturbance problem can be given if it is assumed that the disturbance velocity u_1 is small compared with the mean velocity U, and that the gauze behaves as in the experiments already described, so that when θ and ϕ are small

$$\phi = \alpha\theta, \tag{2.3}$$

where α is a constant for a particular gauze and for arbitrary small azimuthal angles of the streamlines impinging on the gauze.

Consider first the case when the initial disturbance velocity, i.e. the increment to the mean speed far upstream, depends on the lateral coordinate y only, and has a sinusoidal variation, so that

$$u = u_1 \cos py. \tag{2.4}$$

The distribution of disturbance velocity near the gauze must also be periodic in y with wave-length $2\pi/p$. If the effect of viscosity be neglected except in so far as it is instrumental in giving rise to resistance at the gauze, the equation of motion can be written

$$\left[(U+u)\frac{\partial}{\partial x}+v\frac{\partial}{\partial y}\right]\nabla^2\psi_1 = 0, \tag{2.5}$$

where ψ_1 is the stream function for the upstream disturbance velocity, x represents distance in the downstream direction from the gauze, and

$$u = -\frac{\partial\psi_1}{\partial y}, \qquad v = \frac{\partial\psi_1}{\partial x}.$$

Neglecting terms containing squares of small quantities, (2.5) assumes the form

$$\frac{\partial}{\partial x}(\nabla^2\psi_1) = 0, \tag{2.6}$$

so that $\nabla^2\psi_1$ is a function of y only. Far upstream u is given by (2.4), so that the flow near the gauze is given by

$$\nabla^2\psi_1 = u_1 p \sin py. \tag{2.7}$$

The solution of this equation which does not become infinite for large negative values of x is

$$\psi_1 = -\frac{u_1}{p}\sin py + Ae^{px}\sin py. \tag{2.8}$$

(The other solution $A'e^{px}\cos py$ is not needed in view of the symmetry of the flow about $y = 0$. Nor are the solutions representing higher harmonics needed since all the equations are linear and their coefficients would be found to be zero.) Similar considerations show that the stream function ψ_2 for the disturbance downstream of the gauze must be

$$\psi_2 = -\frac{u_2}{p}\sin py + Be^{-px}\sin py, \tag{2.9}$$

where $u_2\cos py$ is the disturbance velocity far downstream and A and B are constants to be determined.

Now there are three conditions available for the determination of A, B, and u_2/u_1. The condition of continuity requires that u should be continuous across the gauze, with value $u_3\cos py$, say, so that

$$u_3 = u_1 - pA = u_2 - pB. \tag{2.10}$$

The equation for the change in v on passing through the gauze is, from (2.3),

$$\frac{\partial\psi_2}{\partial x} = \alpha\frac{\partial\psi_1}{\partial x} \quad \text{at } x = 0,$$

i.e.

$$B + \alpha A = 0, \tag{2.11}$$

and (2.10) becomes

$$u_3 = \frac{\alpha u_1 + u_2}{1+\alpha}. \tag{2.12}$$

Bernoulli's equation for an arbitrary streamline equates the difference in the total pressures far upstream and far downstream to the drop in static pressure at the gauze. Thus, to the first order of small quantities,

$$p_1 + \rho U u_1\cos py - p_2 - \rho U u_2\cos py = k\tfrac{1}{2}\rho(U^2 + 2Uu_3\cos py). \tag{2.13}$$

But since the streamlines are initially and finally straight, the asymptotic static pressures p_1 and p_2 are independent of y, and $p_1 - p_2$ must have the value $k\frac{1}{2}\rho U^2$. Hence

$$u_1 - u_2 = ku_3. \tag{2.14}$$

From (2.10), (2.11), and (2.14) it will be found that

$$A = \frac{u_1}{p}\left(\frac{k}{1+\alpha+k}\right), \qquad B = -\frac{u_1}{p}\left(\frac{\alpha k}{1+\alpha+k}\right), \tag{2.15}$$

and†

$$\frac{u_2}{u_1} = \frac{1+\alpha-\alpha k}{1+\alpha+k}. \tag{2.16}$$

† In the course of Collar's work (**2**) he had some correspondence with one of us (G. I. T.), who pointed out that the difference between his formula and that of Prandtl was associated with the transverse force on the gauze. In a letter (9 Feb. 1939) Collar then proposed the formula (2.16) as a possible general expression containing both formulae.

Though it has been assumed that the disturbance is sinusoidal in y, the wave-length p does not appear in the result; and since in the first-order analysis small disturbances are superposable, it appears that any disturbance of the Prandtl–Collar type will be exactly reproduced in shape far downstream from the gauze but with the velocity altered in the ratio

$$\frac{1+\alpha-\alpha k}{1+\alpha+k}.$$

One particular case of a small steady disturbance to a uniform stream which is not covered by the preceding analysis consists of a disturbance in which the motion is purely lateral. A longitudinal vortex in which the lateral velocity is everywhere small compared with U is of this type. In this case there is no superposed irrotational flow near the gauze and the effect of the gauze is simply to reduce all lateral velocities to a fraction α of their value upstream of the gauze. The effect of the gauze is here independent of the resistance coefficient k, except in so far as α and k are related, because to the first order the magnitude of the velocity is U everywhere and the pressure-drop across the gauze is the same for all streamlines. It follows from the linearity of the problem that for a disturbance consisting of both longitudinal and lateral motion (the former of which must be steady, i.e. independent of x) the gauze alters all longitudinal velocities in the ratio $(1+\alpha-\alpha k)/(1+\alpha+k)$ and all lateral velocities in the ratio α. The shape of the flow pattern far downstream will not be the same as that far upstream in this general case.

2. Comparison with previous analysis

It will be noticed that (2.16) reduces to Prandtl's result that

$$\frac{u_2}{u_1}=\frac{1}{1+k},$$

when $\alpha = 0$, and to the result obtained by Collar and by Batchelor, viz.

$$\frac{u_2}{u_1}=\frac{2-k}{2+k},$$

when $\alpha = 1$. In his proof Prandtl assumes that the flow downstream of the gauze is parallel to the mean flow, and that the pressure there is consequently uniform. This condition is fulfilled only when $\alpha = 0$, which is likely to be true for real gauzes only when $k = \infty$. Batchelor's proof, which is not unlike that used in the preceding section, involved explicitly the assumption that the lateral velocities are continuous at the gauze, i.e. that $\alpha = 1$, which is also untrue, in general, for real gauzes with a finite resistance coefficient.

On the other hand, Collar's analysis, which leads to the correct result for the particular case $\alpha = 1$, appears to contain an error which we shall examine for its intrinsic interest.† He discusses the flow in a parallel-walled channel in which a narrow filament has velocity u_1 in excess of that of the main stream. The filament passes through the gauze with velocity u_3 and finally settles down to velocity u_2 far downstream. The rate of change of momentum of the filament is then equated to the excess drag at the gauze due to the fact that the filament is not moving with the same speed as the mean flow. In this way Collar derives an equation which, when associated with the equation

$$u_1 - u_2 = ku_3 \tag{2.17}$$

representing the effect of applying Bernoulli's equation (see (2.14)), yields the result

$$u_1 + u_2 = 2u_3, \tag{2.18}$$

which is identical with (2.12) in the case $\alpha = 1$.

This method of Collar's depends on the assumption that the change in momentum of the stream outside the filament is zero. This assumption is not true.‡ The change in momentum of the stream outside the filament is, so far as the first-order term is concerned, exactly equal and opposite to that of the filament. If U is the mean velocity, and the stream has constant total width b, and if u_1 is the variable disturbance-velocity far upstream, while u_2 is that far downstream, the rate of change in momentum of the stream is

$$\rho \int_0^b [(U+u_1)^2 - (U+u_2)^2]\, dy.$$

By definition of U,

$$\int_0^b u_1\, dy = 0 \quad \text{and} \quad \int_0^b u_2\, dy = 0,$$

so that the rate of increase in momentum is a small quantity of the second order when u_1/U is small. The expression used by Collar is the part of the momentum integral lying within the filament. This is of the first order and therefore, when u_1/U is small, is large compared with the true expression which is of the second order. The same considerations show that the difference between the resistance of the gauze when opposing a uniform stream, and that which occurs when the stream has a small

† Professor Collar informs us that he originally obtained his result by another approach, in which he used a single filament and adopted the assumptions of the well-known Rankine–Froude momentum theory of propellers: these assumptions are consistent with the results obtained by us for the particular case $\alpha = 1$. Subsequently he obtained experimental support for his formula, and realizing the objections to his original theoretical approach, published a different analysis which was wrongly used to obtain the same result.

‡ H. L. Dryden has also drawn attention to the error in private correspondence.

variable velocity, is also of the second order of small quantities. Thus the momentum equation applied to a parallel-walled channel merely gives a null result so far as the first-order terms are concerned.

Though Collar appears to apply his momentum condition to the whole stream, by neglecting the change in momentum outside a stream tube he really only applies the condition to the fluid inside the tube, thus virtually making the assumption that the pressure on all parts of the wall of the tube upstream of the gauze is p_1 and on all parts downstream p_2, p_1 and p_2 being the mean pressures on the two sides of the gauze. The fact is that the pressure varies along the surface of the stream-tube. This variable pressure makes a contribution to the momentum equation for the stream-tube which Collar's proof takes to be zero. The contribution would in fact be zero if and only if the distributions of difference in pressure from the mean on the two sides of the gauze were mirror images of one another with a change in sign. When only first-order terms are considered, such a distribution of pressure implies that the gauze produces a disturbance which is antisymmetrical on opposite sides, so that a velocity $(U+u_1+u, v)$ at the point $(-x, y)$ on the upstream side corresponds to a velocity $(U+u_2-u, v)$ at the point $(+x, y)$ on the downstream side; this is just the type of flow shown by (2.8), (2.9), and (2.11) to exist in the case $\alpha = 1$. At the gauze the x-component of velocity is the same on both sides and equal to $U+u_3$, so that

$$U+u_1+(u)_{x=0} = U+u_2-(u)_{x=0} = U+u_3.$$

This implies that

$$u_1+u_2 = 2u_3, \tag{2.19}$$

which is identical with (2.18). Thus Collar is virtually assuming (2.19) to be true and his proof obtains the correct result (for $\alpha = 1$) by virtue of the fact that (2.19) is in fact valid for a gauze which exerts no side force.

3. The flow in the neighbourhood of the gauze

We have seen that the assumption of antisymmetrical disturbance-velocities on opposite sides of the gauze includes the assumption that v is unchanged on passing through the gauze, or, in other words, that $\alpha = 1$. This raises the query, How is the antisymmetry modified when $\alpha \neq 1$? The answer is to be found in the analysis which we have already given, as shown by the following considerations.

From (2.6) it is seen that to the first order of small quantities the effect of the gauze on the upstream flow can be represented by superposing on the flow at infinity an irrotational motion specified by the potential $\phi(x, y)$. Similarly the downstream flow can be represented by a combination of the flow far downstream and an irrotational motion $\phi'(x, y)$ in the neighbour-

hood of the gauze. If the transverse velocity is continuous across the gauze at $x = 0$, the appropriate relation between the two potential flows is

$$\phi'(x,y) = \phi(-x,y).$$

Likewise in the case when $\alpha \neq 1$ the required change in transverse velocity across the gauze will be satisfied by

$$\phi'(x,y) = \alpha\phi(-x,y). \tag{2.20}$$

The condition of continuity of the u-component of velocity at the gauze gives

$$u_3 = u_1 + \left[\frac{\partial\phi(x,y)}{\partial x}\right]_{x=0} = u_2 + \left[\frac{\partial\phi'(x,y)}{\partial x}\right]_{x=0} = u_2 - \alpha\left[\frac{\partial\phi(x,y)}{\partial x}\right]_{x=0}$$

in the general case. Hence

$$\alpha(u_3 - u_1) = u_2 - u_3, \tag{2.21}$$

which is identical with equation (2.12) already established, and together with the Bernoulli equation (2.14) yields

$$\frac{u_2}{u_1} = \frac{1+\alpha-\alpha k}{1+\alpha+k} \tag{2.16}$$

as before. It will be noticed that $\phi(x,y)$ is determined by the distribution of u far upstream, for from (2.21) and (2.16)

$$\left[\frac{\partial\phi(x,y)}{\partial x}\right]_{x=0} = u_3 = u_1\left(\frac{1+\alpha}{1+\alpha+k}\right). \tag{2.22}$$

These formulae are still applicable if u_1 is a function of y and z, provided that the gauze has the property that the change in direction of the stream on passing through it is a function only of the angle between its plane and the direction of the incident stream.

4. Comparison with experiment

Measurements of the effect of gauze on a small steady disturbance are difficult to make for several reasons, not the least of which is the fact that wire gauzes tend to distort, producing non-uniformity in k. Two sets of measurements have been published, and although there is considerable scatter of the points, they provide some support for the validity of the result (2.16). Collar (**2**) measured the reduction in amplitude of a single disturbance for a number of gauzes, whose geometrical characteristics are given in Table 2, and his results are shown in Fig. 3. MacPhail (**6**) tested the effect of several gauzes (specified in Table 2) on a complex disturbance in a small water tunnel, and obtained the reduction in magnitude of the whole disturbance. His measuring points were at equal distances upstream and downstream from the gauze, and since with no gauze present the

TABLE 2

Geometrical characteristics of gauzes used by Collar and by MacPhail

Source	*Gauze*	*Wire diameter*	*Number of wires per inch*
		in.	
Collar	1	0·016	16
	2	0·0105	30
	3	0·0065	60
MacPhail	1	0·0197	12
	2	0·0129	16
	3	0·0132	24
	4	0·0091	40

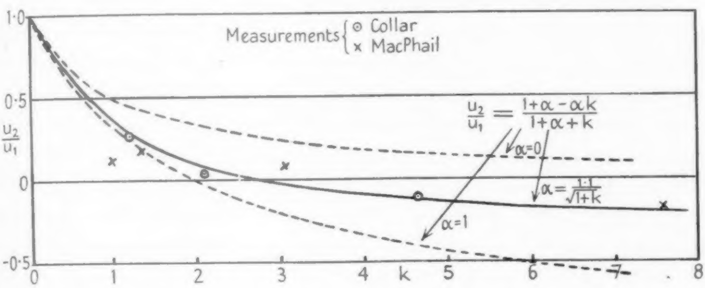

FIG. 3. Effect of gauze on a steady longitudinal disturbance.

disturbance diminished by a factor 0·35 owing to viscous decay, we have assumed that his measurements of u_2/u_1 must be divided by $\sqrt{0{\cdot}35}$ to obtain the effect of the gauze alone, the assumption being that a negligible amount of viscous decay occurs downstream from the gauze. Both Collar's and MacPhail's results show fair agreement in Fig. 3 with the theoretical ratio (2.16) if we make use of the empirical relation established by Dryden and Schubauer, viz. $\alpha = 1{\cdot}1(1+k)^{-\frac{1}{2}}$ $(k > 0{\cdot}7)$. Also shown in the figure are the curves describing the reduction in the special cases $\alpha = 0$ and $\alpha = 1$, neither of which fits the experimental points as well as the more general result.

The important practical point that small longitudinal disturbances are entirely removed by a gauze having a particular value of k appears to be supported by the experiments. This optimum value of k is given by

$$k = 1+1/\alpha,$$

i.e. $k = 2{\cdot}76$, if the gauze satisfies Dryden and Schubauer's empirical relation between α and k. Lateral disturbances are not removed by such a gauze, of course, so that the choice of the most effective gauze for

the reduction of a general steady disturbance must involve a consideration of the relative amounts of energy in the lateral and longitudinal disturbances.

PART III

Effect of gauze on turbulence

1. Outline of method

The method used in Part II of this paper to investigate the effect of a gauze or mesh on small steady disturbances in a uniform stream can be adapted to suit the case of unsteady disturbances. It will be necessary to assume that the turbulence far upstream of the gauze is homogeneous and has a root mean square velocity fluctuation which is small compared with the velocity of the uniform stream. As in Part II, the gauze will be assumed to be placed at right angles to the stream direction, and to be characterized by a resistance coefficient k and a side-force parameter α for incident streamlines of any (small) azimuthal angle. The treatment is essentially kinematical; that is to say, we take no account of change of the turbulence due to viscous or dynamical forces (other than those exerted by the gauze). The procedure is thus more accurate when the relative intensity of the turbulence is small, since the effect of the gauze depends only on the turbulence pattern and not on the speed of the uniform stream which carries it along. An attempt to solve the problem on roughly similar lines has previously been made by one of us (**3**). However, this attempt was in error inasmuch as it ignored the effect of side-force exerted by the gauze, and, moreover, the analysis was not wholly free from approximation. The analysis given below overcomes the first and improves the second of these defects.

With the assumption of small relative intensity of the turbulence, the effect of the gauze is *linear*, as in the case of a steady disturbance. Superposed velocity patterns will therefore experience independent modifications due to the gauze; we take the hint and express the turbulent flow pattern as a Fourier integral of (spatially) periodic distributions of velocity. Similarly the velocities induced by the presence of the gauze can be expressed as a Fourier integral of periodic variations of velocity. We use the conditions that the lateral components of the velocity at each point of the gauze are diminished discontinuously to a fraction α of their value, that the local longitudinal velocity is continuous at the gauze, and that the local pressure-drop across the gauze is determined by the local longitudinal velocity and by the resistance coefficient k. These conditions are sufficient to relate the amplitudes of similar periodic disturbances in the turbulence far upstream and far downstream from the gauze. The integra-

tion to determine the total intensity of turbulence far downstream from the gauze requires a knowledge of the three-dimensional energy spectrum of the upstream turbulence, although an approximation to this function can be made when the upstream turbulence is isotropic. Since the energy spectrum in isotropic turbulence can vary (possibly within fairly narrow limits only), the effect of a gauze also varies with the conditions.

2. Representation of the velocity field

Choose y- and z-axes in the plane of the gauze, with the positive x-axis pointing downstream. Far upstream and far downstream the velocity components of the disturbance are u_1, v_1, w_1 and u_2, v_2, w_2 respectively. Far from the gauze the only change in the velocity field with time is a translation downstream so that these six components are functions of $\theta(=x-Ut)$, y, and z. Now if the disturbance velocity is sufficiently small compared with U, vorticity is carried along by the uniform stream without change, except through the gauze. It follows that the velocity field in the neighbourhood of the gauze has components

$$u_1+\frac{\partial\phi_1}{\partial x},\qquad v_1+\frac{\partial\phi_1}{\partial y},\qquad w_1+\frac{\partial\phi_1}{\partial z}\quad\text{for}\quad x<0$$

and components

$$u_2+\frac{\partial\phi_2}{\partial x},\qquad v_2+\frac{\partial\phi_2}{\partial y},\qquad w_2+\frac{\partial\phi_2}{\partial z}\quad\text{for}\quad x>0.$$

Here ϕ_1 and ϕ_2 are potential functions (of x, y, z, and t) which must tend to constant values as x approaches $-\infty$ and $+\infty$ respectively.

We represent the distribution of disturbance velocity far upstream from the gauze in the form of a triple Fourier integral over all values of the wave-number components l, m, n; thus

$$u_1=\iiint_{-\infty}^{\infty} A_1(l,m,n)e^{i(l\theta+my+nz)}\,dl dm dn,\tag{3.1}$$

where $A_1(l,m,n)$ and $A_1(-l,-m,-n)$ must be complex conjugates in order to make u_1 real. Likewise the components v_1 and w_1 are determined by functions $B_1(l,m,n)$ and $C_1(l,m,n)$, and the condition of incompressibility requires

$$lA_1+mB_1+nC_1=0.\tag{3.2}$$

In the same way, the components u_2, v_2, w_2 of the disturbance velocity far downstream may be written as Fourier integrals like (3.1) and the corresponding transform functions A_2, B_2, C_2 are related by

$$lA_2+mB_2+nC_2=0.\tag{3.3}$$

The representation (3.1) is not rigorously possible when the turbulence field is infinite in extent and spatially homogeneous in the statistical sense,

for the functions A_1, etc., are then infinite. However, we shall be interested in ratios (like A_2/A_1) only and the divergence of the functions may be safely ignored. The analysis remains unchanged if we think of the velocity field as large, but not infinite, and the difficulty does not then arise.

It will be seen in the next sub-section that the equations connecting the disturbance velocities at different positions relative to the gauze are linear and homogeneous, as was found for the steady disturbance. There will therefore be no modulation of the Fourier components, and we can discuss one particular wave-number in isolation. The effect of gauze on a given field of turbulence is thus known when the effect on the triply periodic disturbance

$$(u_1, v_1, w_1) = (A_1, B_1, C_1)e^{i(l\theta+my+nz)}\,dldmdn \tag{3.4}$$

is known. Far downstream from the gauze, this disturbance will be converted to

$$(u_2, v_2, w_2) = (A_2, B_2, C_2)e^{i(l\theta+my+nz)}\,dldmdn, \tag{3.5}$$

and the problem is to determine the functions A_2, B_2, and C_2 in terms of the known functions A_1, B_1, and C_1. The relevant parts of the potential functions ϕ_1 and ϕ_2 have the same periodic character in t, y, and z, so that corresponding to (3.4) and (3.5) we put

$$\phi_1 = P_1(l, m, n)e^{\sigma x+i(-lUt+my+nz)}\,dldmdn, \tag{3.6}$$

$$\phi_2 = P_2(l, m, n)e^{-\sigma x+i(-lUt+my+nz)}\,dldmdn, \tag{3.7}$$

where $\sigma^2 = m^2+n^2$; the dependence of ϕ_1 and ϕ_2 on x is obtained from Laplace's equation and the boundary conditions at $x = -\infty$ and $+\infty$ respectively.

The characteristics of the turbulence which are of most immediate importance are the spatial means of the squares of the component fluctuations, e.g. $\overline{u_1^2}$. Now the average value of u_1^2 over a large cube of side $2D$ is

$$\frac{1}{8D^3}\iiint_{-D}^{D} u_1^2\,d\theta dydz$$

$$= \frac{1}{D^3}\iiint_{-\infty}^{\infty}\iiint_{-\infty}^{\infty} A_1(l, m, n)A_1(l', m', n')\times$$

$$\times\frac{\sin(l+l')D}{l+l'}\,\frac{\sin(m+m')D}{m+m'}\,\frac{\sin(n+n')D}{n+n'}\,dldmdndl'dm'dn'$$

$$= \frac{1}{D^3}\iiint_{-\infty}^{\infty} A_1(l, m, n)\left\{\iiint_{-\infty}^{\infty} A_1(L-l, M-m, N-n)\times\right.$$

$$\left.\times\frac{\sin LD}{L}\,\frac{\sin MD}{M}\,\frac{\sin ND}{N}\,dLdMdN\right\}dldmdn,$$

where $L = l+l'$, $M = m+m'$, $N = n+n'$. Thus when D is sufficiently large

$$\overline{u_1^2} = \frac{\pi^3}{D^3}\iiint\limits_{-\infty}^{\infty} A_1(l,m,n)A_1(-l,-m,-n)\,dldmdn$$

$$= \frac{\pi^3}{D^3}\iiint\limits_{-\infty}^{\infty} |A_1(l,m,n)|^2\,dldmdn. \tag{3.8}$$

Hence if we define an energy spectral density $F_1(l,m,n)$ such that $F_1(l,m,n)\,dldmdn$ is the contribution to $\overline{u_1^2}$ from wave-numbers in the range (l,m,n) to $(l+dl, m+dm, n+dn)$, then

$$F_1(l,m,n) = \frac{\pi^3}{D^3}|A_1|^2. \tag{3.9}$$

Likewise G_1, H_1 and F_2, G_2, H_2 are proportional to $|B_1|^2$, $|C_1|^2$ and $|A_2|^2$, $|B_2|^2$, $|C_2|^2$ respectively. The mean energy of the turbulence per unit mass of the fluid far upstream from the gauze is

$$\tfrac{1}{2}(\overline{u_1^2}+\overline{v_1^2}+\overline{w_1^2}) = \tfrac{1}{2}\iiint\limits_{-\infty}^{\infty}(F_1+G_1+H_1)\,dldmdn,$$

with a similar expression for the energy of the turbulence far downstream.

3. Conditions at the gauze

The conditions to be satisfied at $x = 0$ enable us to relate the velocity fields on either side of the gauze. The first condition is that the lateral velocities on the downstream side of the gauze are a fraction α of their value on the upstream side. Thus

$$\left(v_2+\frac{\partial\phi_2}{\partial y}\right)_{x=0} = \alpha\left(v_1+\frac{\partial\phi_1}{\partial y}\right)_0,$$

$$\left(w_2+\frac{\partial\phi_2}{\partial z}\right)_0 = \alpha\left(w_1+\frac{\partial\phi_1}{\partial z}\right)_0,$$

and for the single Fourier component described by (3.4), (3.5), (3.6), and (3.7),

$$B_2+imP_2 = \alpha(B_1+imP_1), \tag{3.10}$$

$$C_2+inP_2 = \alpha(C_1+inP_1). \tag{3.11}$$

The second condition is that the velocity normal to the gauze is the same on either side, i.e.

$$\left(u_2+\frac{\partial\phi_2}{\partial x}\right)_0 = \left(u_1+\frac{\partial\phi_1}{\partial x}\right)_0,$$

and for the typical Fourier component

$$A_2-\sigma P_2 = A_1+\sigma P_1. \tag{3.12}$$

Finally, there is the condition that the instantaneous local pressure-drop across the gauze depends on the local velocity. Consistent with our basic assumptions, the equations of lateral motion can be written

$$\left(\frac{\partial}{\partial t}+U\frac{\partial}{\partial x}\right)(v,w) = -\frac{1}{\rho}\left(\frac{\partial}{\partial y},\frac{\partial}{\partial z}\right)p,$$

so that if Δ represents the change in any quantity at the gauze,

$$\Delta\left(\frac{\partial}{\partial t}+U\frac{\partial}{\partial x}\right)(v,w) = -\frac{1}{\rho}\left(\frac{\partial}{\partial y},\frac{\partial}{\partial z}\right)\Delta p = Uk\left(\frac{\partial}{\partial y},\frac{\partial}{\partial z}\right)(u)_{x=0}. \quad (3.13)$$

There is no change in v_1, w_1, v_2, or w_2 following the mean motion, so that only the induced potential flow contributes to the left side. For the typical Fourier component, (3.13) leads to two identical equations of the form

$$l(F_2-F_1)-i\sigma(F_2+F_1) = ik(A_1+\sigma P_1). \quad (3.14)$$

In addition to the four independent equations (3.10), (3.11), (3.12), and (3.14), there are the continuity equations (3.2) and (3.3). Thus, if A_1, B_1, and C_1 are regarded as known, there are available five equations to determine the functions A_2, B_2, C_2, P_1, P_2 specifying the disturbance far downstream and in the neighbourhood of the gauze.

4. Solution of the equations

From (3.10) and (3.11), and the continuity equations (3.2) and (3.3), we find

$$i\sigma^2P_2-lA_2 = \alpha(i\sigma^2P_1-lA_1). \quad (3.15)$$

P_1, P_2, and A_2 can now be found from this equation and (3.12) and (3.14).

$$P_1 = \frac{A_1}{\sigma}\,\frac{\alpha\beta-\beta-ik}{2\beta+i(1+\alpha+k)}, \quad (3.16)$$

$$P_2 = \frac{A_1}{\sigma}\,\frac{(\beta+i)(\alpha\beta-\beta+i\alpha k)}{(\beta-i)[2\beta+i(1+\alpha+k)]}, \quad (3.17)$$

$$A_2 = A_1\frac{(\beta+i)[2\alpha\beta+i(\alpha k-\alpha-1)]}{(\beta-i)[2\beta+i(1+\alpha+k)]}, \quad (3.18)$$

where β has been written for $l(m^2+n^2)^{-\frac{1}{2}}$. Hence

$$\frac{F_2(l,m,n)}{F_1(l,m,n)} = \frac{|A_2|^2}{|A_1|^2} = \frac{4\alpha^2\beta^2+(1+\alpha-\alpha k)^2}{4\beta^2+(1+\alpha+k)^2} \quad (3.19)$$

$$= I(\beta), \quad \text{say.}$$

Thus, as a result of the passage through the gauze, the contribution to the mean square of the turbulent fluctuation parallel to the main flow from Fourier components with wave-numbers in a small range about (l,m,n) is reduced by the factor $I(\beta)$. This factor increases monotonically from

$\left(\dfrac{1+\alpha-\alpha k}{1+\alpha+k}\right)^2$ at $\beta = 0$ to α^2 at $\beta = \infty$ (for wire gauzes), and is always less than unity. The case $\beta = 0$ (i.e. $l = 0$) corresponds to a velocity disturbance which has no variation in the x-direction, and the result (2.18) obtained in Part II is recovered from (3.19) in this case.

The reduction ratio for the total intensity of the longitudinal fluctuation, arising from all Fourier components, is thus given by

$$\mu = \frac{\overline{u_2^2}}{\overline{u_1^2}} = \frac{\iiint\limits_{-\infty}^{\infty} F_2(l,m,n)\,dldmdn}{\iiint\limits_{-\infty}^{\infty} F_1(l,m,n)\,dldmdn} = \frac{\iiint\limits_{-\infty}^{\infty} I(\beta)F_1\,dldmdn}{\iiint\limits_{-\infty}^{\infty} F_1\,dldmdn}, \tag{3.20}$$

and μ is entirely specified by the spectrum of the upstream turbulence and the gauze characteristics k and α. Numerical results will, of course, need some assumption about the upstream turbulence, but before proceeding further with (3.20) we shall consider the effect of the gauze on the lateral components of the turbulence.

From equations (3.10) and (3.11)

$$nB_2 - mC_2 = \alpha(nB_1 - mC_1).$$

Multiplying this equation by its complex conjugate and making use of the continuity equations (3.2) and (3.3), we find

$$\sigma^2(|B_2|^2+|C_2|^2)-l^2|A_2|^2 = \alpha^2[\sigma^2(|B_1|^2+|C_1|^2)-l^2|A_1|^2], \tag{3.21}$$

so that the energy of the lateral motion of the typical Fourier component is reduced in the ratio

$$\frac{|B_2|^2+|C_2|^2}{|B_1|^2+|C_1|^2} = \alpha^2+\beta^2\frac{|A_1|^2}{|B_1|^2+|C_1|^2}[I(\beta)-\alpha^2].$$

In terms of the spectral densities this becomes

$$\frac{G_2+H_2}{G_1+H_1} = \alpha^2+\beta^2\frac{F_1}{G_1+H_1}[I(\beta)-\alpha^2]. \tag{3.22}$$

The reduction ratio for the energy of the lateral motion of all Fourier components is thus

$$\nu = \frac{\overline{v_2^2}+\overline{w_2^2}}{\overline{v_1^2}+\overline{w_1^2}} = \frac{\iiint\limits_{-\infty}^{\infty} (G_2+H_2)\,dldmdn}{\iiint\limits_{-\infty}^{\infty} (G_1+H_1)\,dldmdn} = \alpha^2 + \frac{\iiint\limits_{-\infty}^{\infty} \beta^2(I-\alpha^2)F_1\,dldmdn}{\iiint\limits_{-\infty}^{\infty} (G_1+H_1)\,dldmdn}.$$

But $$\beta^2[I(\beta)-\alpha^2] = \tfrac{1}{4}(1+\alpha-\alpha k)^2-\tfrac{1}{4}(1+\alpha+k)^2 I(\beta), \tag{3.23}$$

so that $$\nu = \alpha^2+\tfrac{1}{4}[(1+\alpha-\alpha k)^2-(1+\alpha+k)^2\mu]\{\overline{u_1^2}/(\overline{v_1^2}+\overline{w_1^2})\}. \tag{3.24}$$

The expression (3.23) is negative for all values of β so that ν is always less than α^2; ν can be determined when μ is known, and we must therefore return to (3.20).

5. Special case of isotropic turbulence

The essential need, if we are to make practical use of (3.20) and (3.24), is for information about the dependence of F_1 on l, m, and n in the turbulence far upstream from the gauze. We need to know how the contribution to $\overline{u_1^2}$ made by a single Fourier component varies with its vector wave-number (l, m, n). This three-dimensional spectrum function has not hitherto appeared in turbulence literature (**7**) and we know of no direct experimental data. Some guess-work will therefore be necessary, and in order to put ourselves on familiar ground we shall assume that the turbulence far upstream of the gauze is isotropic; this special case also has considerable practical significance. Even in this simple case there is no unique form for the energy spectrum, which will depend upon the origin of the isotropic turbulence in question. Prediction of the exact effect of the gauze would require a knowledge of the particular properties of the oncoming turbulence, so that (3.20) and (3.24) represent the limit of our exact analysis. However, it seems probable from experimental evidence that there are definite limits to the variation of the structure of isotropic turbulence under different conditions, and we can seek an approximate expression for the effect of gauze on all types of isotropic turbulence.

The postulate we have chosen to make in order to obtain a working estimate of the effect of the gauze on isotropic turbulence is that

$$F_1(l, m, n) = \overline{u_1^2}\,\frac{C\sigma^2}{(l^2+\sigma^2+\gamma^2)^3}, \tag{3.25}$$

where C and γ are constants. This expression satisfies all the formal conditions imposed by isotropy and incompressibility of the fluid (**7**). Moreover, the contribution to $\overline{u_1^2}$ from periodic fluctuations with wave-number components in the direction of the x-axis which lie between l and $l+dl$ is

$$dl\int_{-\infty}^{\infty}\int_{-\infty}^{\infty} F_1(l, m, n)\, dm dn = \overline{u_1^2}\,\frac{\pi C}{2(l^2+\gamma^2)}\,dl. \tag{3.26}$$

This function of l is the ordinary one-dimensional longitudinal spectrum function used in the literature, and the special form (3.26) is the form found by Dryden (**8**) to be in fair agreement with experiment for several sets of conditions. The constants C and γ can be chosen to give the

correct total energy and one length parameter of the turbulence such as the integral scale, but they will be found not to occur in the expressions for μ and ν.

The postulate (3.25) now enables the expression (3.20) for μ to be evaluated. Transforming l, m, n to spherical polar coordinates r, θ, ψ such that

$$l = r\cos\psi, \qquad m^2+n^2 = \sigma^2 = r^2\sin^2\psi,$$

(3.20) becomes

$$\mu = \frac{\displaystyle\int_0^\infty\int_0^\pi \frac{4\alpha^2\cos^2\psi+(1+\alpha-\alpha k)^2\sin^2\psi}{4\cos^2\psi+(1+\alpha+k)^2\sin^2\psi}\,\frac{Cr^2\sin^2\psi}{(r^2+\gamma^2)^3}\,r^2\sin\psi\,d\psi dr}{\displaystyle\int_0^\infty\int_0^\pi \frac{Cr^2\sin^2\psi}{(r^2+\gamma^2)^3}\,r^2\sin\psi\,d\psi dr}.$$

The integrations with respect to r can be carried out immediately, giving

$$\mu = \frac{3}{2}\int_0^{\frac{1}{2}\pi} \frac{4\alpha^2\cos^2\psi+(1+\alpha-\alpha k)^2\sin^2\psi}{4\cos^2\psi+(1+\alpha+k)^2\sin^2\psi}\sin^3\psi\,d\psi. \tag{3.27}$$

Changing the variable of integration to χ ($=\cos\psi$) and writing

$$\xi^2 = \frac{(1+\alpha-\alpha k)^2}{(1+\alpha-\alpha k)^2-4\alpha^2}, \qquad \eta^2 = \frac{(1+\alpha+k)^2}{(1+\alpha+k)^2-4},$$

we have

$$\mu = \frac{3}{2}\,\frac{(1+\alpha-\alpha k)^2-4\alpha^2}{(1+\alpha+k)^2-4}\int_0^1 \left(\frac{\chi^2-\xi^2}{\chi^2-\eta^2}\right)(1-\chi^2)\,d\chi$$

$$= \frac{(1+\alpha-\alpha k)^2+2\alpha^2}{(1+\alpha+k)^2-4}+\frac{(1+\alpha-\alpha k)^2-4\alpha^2}{(1+\alpha+k)^2-4}\,\tfrac{3}{2}(1-\eta^2)\left(1+\frac{\eta^2-\xi^2}{2\eta}.\log\frac{\eta-1}{\eta+1}\right). \tag{3.28}$$

This can be evaluated directly when the values of k and α for the gauze are known. The reduction ratio for the lateral intensity is then given by (3.24), which becomes, when the upstream turbulence is isotropic,

$$\nu = \alpha^2+\tfrac{1}{8}[(1+\alpha-\alpha k)^2-(1+\alpha+k)^2\mu]. \tag{3.29}$$

The effect of gauze on the total energy of the turbulence is to reduce it in the ratio $\frac{1}{3}(\mu+2\nu)$.

6. Numerical results

It has already been pointed out that the measurements of α and k for woven round-wire gauze made by Dryden and Schubauer (see Appendix) indicate that these quantities are uniquely related, and that, for k not less than about 0·7,

$$\alpha = 1{\cdot}1(1+k)^{-\frac{1}{2}}. \tag{3.30}$$

On the assumption that this relation holds accurately, the turbulence-reducing properties of a gauze are specified by k alone. The reductions in longitudinal and lateral intensities of the type of isotropic turbulence specified by the three-dimensional energy spectrum function (3.25) have been worked out for several values of k with the aid of (3.28), (3.29), and (3.30) and are shown in Table 3 and Fig. 4. The variations of μ and ν with k have many features analogous to those for the steady disturbances discussed in Part II.

It is worth noticing that the theoretical reduction factors are not very

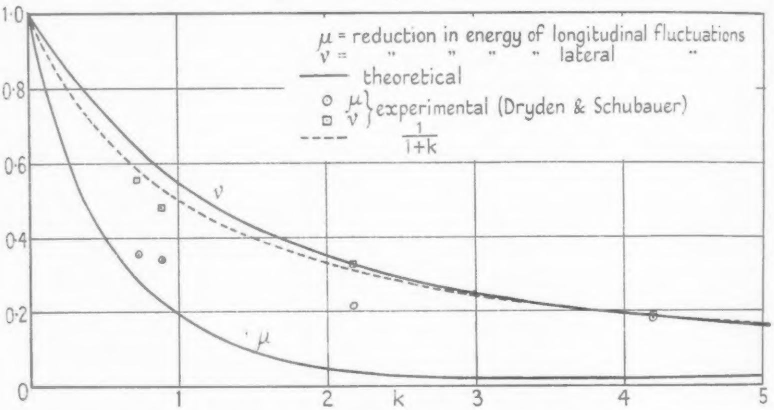

FIG. 4. Effect of gauze on isotropic turbulence.

different from those valid for a simplified type of upstream turbulence in which the longitudinal motion has no variation in the direction of the stream. It was seen in Part II of this paper that the effect of the gauze on such a disturbance is to reduce the longitudinal and lateral disturbances independently, the reduction ratios being

$$\mu = \{(1+\alpha-\alpha k)/(1+\alpha+k)\}^2, \qquad \nu = \alpha^2. \tag{3.31}$$

These expressions are nowhere different from the theoretical values by more than about 0·07, while the corresponding value of the energy reduction factor $\frac{1}{3}(\mu+2\nu)$ does not depart from theoretical value by more than 0·03. Numerical values of the expressions (3.31) are included in Table 3. The closeness of the figures is probably to be attributed to the fact that the longitudinal intensity of real turbulence is already considerably reduced by the time it reaches the gauze, and the longitudinal disturbance exercises comparatively little influence on the lateral disturbance in the neighbourhood of the gauze.

The only published measurements of the effect of wire gauze on turbulence are those made by Dryden and Schubauer (**4**). They give the values

TABLE 3

Effect of gauze on isotropic turbulence

Gauze: k	1	2	3	4	5	9	15
Gauze: α^2	0·605	0·403	0·302	0·242	0·202	0·121	0·076
Theoretical: Longitudinal intensity: μ	0·194	0·046	0·020	0·019	0·022	0·031	0·031
Theoretical: Lateral intensity: ν	0·543	0·345	0·251	0·199	0·166	0·101	0·064
Theoretical: Total energy: $\frac{1}{3}(\mu+2\nu)$	0·427	0·245	0·174	0·139	0·118	0·078	0·053
Theoretical: Longitudinal scale: $L_k/L_{k=0}$	0·670	0·222	0·025	0·398	0·690	0·954	0·988
Simplified model of turbulence: $\left(\frac{1+\alpha-\alpha k}{1+\alpha+k}\right)^2$	0·130	0·010	0·0004	0·007	0·015	0·031	0·031
Simplified model of turbulence: $\frac{2}{3}\alpha^2+\frac{1}{3}\left(\frac{1+\alpha-\alpha k}{1+\alpha+k}\right)^2$	0·447	0·272	0·201	0·164	0·140	0·091	0·061
Empirical (Dryden & Schubauer) $1/(1+k)$	0·5	0·333	0·25	0·2	0·167	0·1	0·063

of μ and ν for four different values of k, as shown in Fig. 4. Their conclusion from the measurements is that the energy of turbulence is reduced in the ratio $1/(1+k)$ and it is implied that the energy contributions from the component fluctuations are each reduced in this ratio. This is opposed to our own result that the lateral and longitudinal intensities of turbulence have different values behind the gauze, and indeed the experimental points shown in Fig. 4 are not inconsistent with our result in this respect. The measurements of ν are in quite good agreement with the theoretical values, although the measured reduction in longitudinal fluctuation is much less than the theory predicts. The conditions under which the measurements were made suggest two possible reasons for this discrepancy. The root mean squares of the three components of turbulence were measured in the working-section of a wind-tunnel, both in the absence and in the presence of a gauze of known resistance in the settling-chamber of the tunnel. The effect of a contraction is known to be greater on the longitudinal fluctuation and it is not unlikely that this effect is different for the different types of turbulence passing through it. In the second place, the considerable distance between the gauze and the measuring point would allow appreciable decay of the turbulence, and since there is a general tendency to isotropy during decay, the longitudinal intensity would be relatively increased. It is Dryden and Schubauer's intention to make further measurements of the effect of gauze on isotropic turbulence in a manner which avoids these difficulties.

7. Nature of the turbulence downstream from the gauze

The preceding analysis has shown that the gauze reduces the lateral and longitudinal intensities by different amounts. However, rotational symmetry about the x-axis of the turbulence is preserved through the gauze so

that if the turbulence far ahead of the gauze is isotropic it will be axisymmetric downstream from the gauze (**3**). One consequence of this is that the usual decay laws known to be valid for isotropic turbulence will not necessarily apply accurately to the turbulence downstream from the gauze.

The three-dimensional energy spectrum functions for the downstream turbulence follow immediately from (3.19) and (3.22). If $F_1(l,m,n)$ is the density in wave-number space of contributions to the mean square of turbulent velocities parallel to the x-axis in the turbulence far ahead of the gauze, the spectral densities of fluctuations parallel to the (x,y,z)-axes far downstream are F_2, G_2, and H_2, where

$$F_2(l,m,n) = I(\beta)F_1(l,m,n), \tag{3.32}$$

$$\begin{aligned} G_2(l,m,n)+H_2(l,m,n) &= \alpha^2[G_1(l,m,n)+H_1(l,m,n)]+\beta^2(I-\alpha^2)F_1(l,m,n) \\ &= \alpha^2[F_1(m,n,l)+F_1(n,l,m)]+\beta^2(I-\alpha^2)F_1(l,m,n). \end{aligned} \tag{3.33}$$

Most of the useful statistical characteristics of the turbulence can be obtained from these spectrum functions.†

A quantity of great practical significance is the spectrum of the variation of the longitudinal fluctuation along a line in the direction of the x-axis; far downstream it is given by

$$\int\limits_{-\infty}^{\infty}\int\limits_{-\infty}^{\infty} F_1(l,m,n)\frac{4\alpha^2l^2+(1+\alpha-\alpha k)^2\rho^2}{4l^2+(1+\alpha+k)^2\rho^2}\,dmdn. \tag{3.34}$$

Given a knowledge of $F_1(l,m,n)$, it is then possible to predict the effect of the gauze on any of the parameters describing the longitudinal correlation between longitudinal velocities. For instance, the square of the radius of curvature at the origin of the correlation function is changed according to the ratio

$$\left(\frac{\lambda_k}{\lambda_{k=0}}\right)^{-2} = \frac{\iiint\limits_{-\infty}^{\infty} F_1(l,m,n)I(\beta)l^2\,dldmdn}{\mu\iiint\limits_{-\infty}^{\infty} F_1(l,m,n)l^2\,dldmdn}. \tag{3.35}$$

Since $I(\beta)$ has its minimum value when l is small, comparison with (3.20) indicates that λ^2 is reduced on passing through the gauze. The parameter λ has not the same direct connexion with energy dissipation as in isotropic turbulence, so that it is not possible to deduce that the fractional rate of decay of energy is increased. Indeed, forming the spectrum of the longitudinal fluctuation along a line in the direction of the y-axis shows that

† In order to determine G_2 and H_2 separately we should have to consider the relation between the phases of different Fourier components in the upstream turbulence.

the change in the corresponding parameter (λ', say) is given by

$$\left(\frac{\lambda'_k}{\lambda'_{k=0}}\right)^{-2} = \frac{\iiint_{-\infty}^{\infty} F_1(l,m,n)I(\beta)m^2\,dldmdn}{\mu\iiint_{-\infty}^{\infty} F_1(l,m,n)m^2\,dldmdn}, \tag{3.36}$$

and the same reasoning indicates that λ'^2 is increased by the gauze.

An interesting result is that the change in the ordinary longitudinal integral scale L does not depend on the function $F_1(l,m,n)$ and is thus identical for all types of turbulence. L is proportional to the value of the energy spectrum function (3.34) at $l = 0$, divided by $\overline{u^2}$, so that

$$\frac{L_k}{L_{k=0}} = \frac{\overline{u_1^2}}{\overline{u_2^2}}\frac{(1+\alpha-\alpha k)^2}{(1+\alpha+k)^2} = \frac{(1+\alpha-\alpha k)^2}{\mu(1+\alpha+k)^2}. \tag{3.37}$$

Values of this factor are shown in Table 3; it is unity when k is zero or very large and has a minimum of zero at $(1+\alpha-\alpha k) = 0$, i.e. when $k = 2{\cdot}76$, according to Dryden and Schubauer's experimental relation between α and k. This vanishing of the scale is a direct consequence of the result established in Part II that a disturbance to the longitudinal velocity which has no variation in the x-direction is entirely removed by a gauze for which $(1+\alpha-\alpha k) = 0$. Evidently the effect of gauze on the longitudinal double-velocity correlation is to make it negative over a considerable range of the distance between the two points.

Since the three-dimensional energy spectrum downstream from a gauze can be predicted when the upstream spectrum is known, it follows that the effect of a succession of gauzes of the same or different resistance can be predicted. Equation (3.19) holds for each gauze, so that the reduction in the longitudinal intensity of (initially) isotropic turbulence owing to r successive gauzes having the same resistance is

$$\mu_r = \frac{\iiint_{-\infty}^{\infty} I^r(\beta)F_1(l,m,n)\,dldmdn}{\iiint_{-\infty}^{\infty} F_1(l,m,n)\,dldmdn}. \tag{3.38}$$

Equation (3.22) shows that the reduction in lateral intensity due to r successive gauzes is related to that due to $r-1$ gauzes by

$$\begin{aligned}\nu_r &= \alpha^2\nu_{r-1} + \frac{\iiint_{-\infty}^{\infty} \beta^2 I^{r-1}(I-\alpha^2)F_1(l,m,n)\,dldmdn}{2\iiint_{-\infty}^{\infty} F_1(l,m,n)\,dldmdn} \\ &= \alpha^2\nu_{r-1} - \tfrac{1}{8}(1+\alpha+k)^2\mu_r + \tfrac{1}{8}(1+\alpha-\alpha k)^2\mu_{r-1}.\end{aligned} \tag{3.39}$$

Numerical values of μ_r and ν_r for $r = 2$, 3, etc., can be calculated on the assumption that (3.25) describes the spectrum function $F_1(l, m, n)$ and they indicate, in general, that each added gauze (of the same k-value) produces a slightly smaller additional reduction in the intensity of turbulence. As the number of gauzes is increased, the turbulence tends to become a wholly lateral motion and the value of ν_r/ν_{r-1} tends to α^2. The value of μ_r/μ_{r-1} increases with r, but its value is not very important since μ is very small for $r > 1$ and $k > 1$. The energy reduction factor for each gauze in addition to the first gauze will thus be $\frac{2}{3}\alpha^2$ approximately. However, these theoretical results should be used with caution since we have taken no account of the dynamical tendency to isotropy in turbulence whose intensity is not vanishingly small. There will undoubtedly be some transfer of energy from the lateral to the longitudinal motion in the region downstream from each gauze, and this will be greater the greater the departure from isotropy.

APPENDIX

NATIONAL BUREAU OF STANDARDS MEASUREMENTS OF LATERAL FORCE ON GAUZES OF ROUND WIRES

(*Communicated by* H. L. DRYDEN *and* G. B. SCHUBAUER)

A preliminary version of the preceding paper was made available to H. L. Dryden and G. B. Schubauer of the National Bureau of Standards, who had published some information on the effect of damping screens in reducing wind-tunnel turbulence (*Journal of the Aeronautical Sciences*, **14**, No. 4, April 1947). Preparations were being made to proceed with additional and more direct measurements of the effect of damping screens on isotropic turbulence at the National Bureau of Standards. In view of the apparent importance of knowledge of the lateral force on such screens, W. Spangenberg of the Bureau staff undertook the measurement of the lateral force on screens made of round wire.

The method adopted was based on the formulae given some years ago by Taylor for the relation between the deflexion of an air stream impinging on a screen at an angle and the lateral force. The measurements were made at the end of a 12-in.-square duct discharging into free air, the end of the duct being cut off successively at various angles θ and various screens being placed over the end of the duct. Precautions were taken to secure a uniform velocity distribution upstream from the screen with thin boundary layers. The direction of flow was measured by fine silk fibres at ten stations about 1 in. apart in the central region of the stream and along a line perpendicular to the flow. In some cases measurements were made upstream of the screen as well as downstream. The angles were read to the nearest $\frac{1}{4}$ degree by a protractor, using a mirror to avoid parallax. The mean deviation for ten stations varied from 0·2 to 0·6 degree, differing from screen to screen, but fairly consistent for each screen.

The results of observations of ϕ and k_θ are shown in summary form in Table 4.

TABLE 4

Summary of values of ϕ and k_θ from faired curves

		60-*mesh*		54-*mesh*		40-*mesh*		24-*mesh*	
$\theta°$	*U ft./sec.*	ϕ	k_θ	ϕ	k_θ	ϕ	k_θ	ϕ	k_θ
10	15	4·2	4·58	6·8	2·28	6·9	1·60	8·4	0·80
	25	4·6	3·72	7·4	1·85	7·0	1·39	8·5	0·69
	35	5·0	3·40	7·1	1·65	7·1	1·25	8·5	0·64
15	15	6·4	4·65	9·1	2·31	9·5	1·65	12·8	0·90
	25	7·3	3·78	9·8	1·86	10·1	1·43	13·0	0·76
	35	7·8	3·44	10·0	1·66	10·5	1·31	13·0	0·72
30	15	13·4	3·61	18·1	1·92	20·5	1·42	24·6	0·75
	25	14·4	2·94	19·9	1·56	21·7	1·20	25·5	0·63
	35	15·0	2·64	20·5	1·39	22·2	1·09	25·9	0·58
45	15	21·4	2·58	28·6	1·33	32·4	1·05	37·8	0·51
	25	22·9	2·08	31·1	1·08	33·4	0·84	39·5	0·44
	35	23·7	1·84	32·8	0·99	35·3	0·74	40·6	0·41

F_θ/θ is determined from the formula

$$\frac{F_\theta}{\theta} = \frac{2\sin(\theta-\phi)\cos\theta}{\theta\cos\phi}.$$

k_θ is defined by the relation

$$p_1 - p_2 = k_\theta \cdot \tfrac{1}{2}\rho U^2.$$

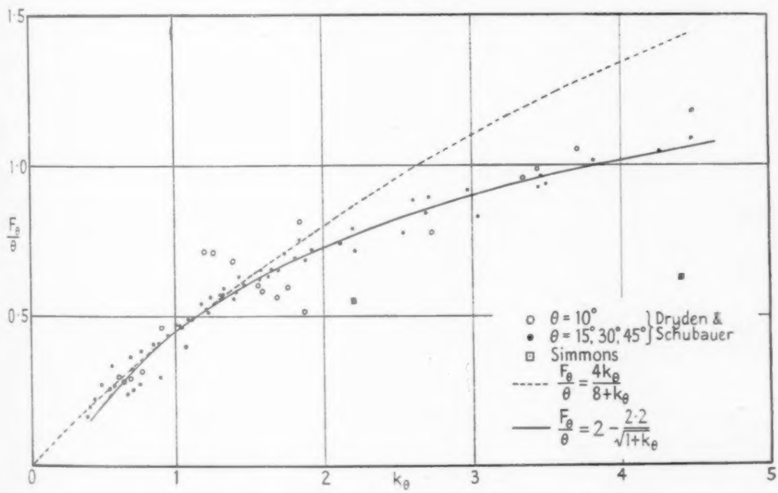

FIG. 5. Experimental values of F_θ/θ against k_θ.

There is clearly variation of ϕ with the speed (and consequently with k_θ) for a constant value of θ. However, there is a fairly definite relation between F_θ/θ and k_θ independent of the speed or mesh of the screen as shown in Fig. 5.

It is possible to account for this relationship by a crude theory. Suppose the

screen to have n wires per foot. Let D be the drag of a foot length of the wire forming one side of the square mesh and suppose it to be independent of the angle between the axis of the cylindrical wire and the wind direction. If the direction of flow at the screen is assumed to be equal to θ and the velocity at the screen is U, then

$$F_\theta \cdot \tfrac{1}{2}\rho U^2 = nD\sin\theta,$$

$$k_\theta \cdot \tfrac{1}{2}\rho U^2 = nD\cos\theta + nD.$$

Hence
$$F_\theta = \frac{k_\theta \sin\theta}{1+\cos\theta}.$$

But the direction of flow at the screen will probably be intermediate between θ and ϕ, analogous to the induced angle of attack on a cascade of airfoils producing lift. As an approximation, assume that the induced deflexion at the screen is equal to one-half the final deflexion $(\theta-\phi)$; i.e. replace θ in the first-order theory by $\theta-\frac{1}{2}(\theta-\phi)$. Thus, designating $\theta-\phi$ by 2δ, we have the pair of equations

$$F_\theta = \frac{2\cos\theta}{\cos(\theta-2\delta)}\sin 2\delta,$$

$$F_\theta = \frac{k_\theta \sin(\theta-\delta)}{1+\cos(\theta-\delta)}.$$

On elimination of δ, we obtain a relation between F_θ and k_θ depending slightly on θ. Typical values are given in Table 5.

TABLE 5

Theoretical relation between F_θ and k_θ

	ϕ	F_θ	F_θ/θ	k_θ
$\theta = 15^\circ$	5	·337	1·287	3·85
	7	·271	1·035	2·80
	9	·204	0·780	1·94
	11	·137	·524	1·21
	13	·069	·265	·57
$\theta = 30^\circ$	10	·601	1·149	3·41
	14	·492	·940	2·53
	18	·379	·723	1·78
	22	·260	·497	1·13
	26	·124	·257	·54
$\theta = 45^\circ$	13	·771	·981	2·97
	17	·694	·884	2·50
	21	·616	·784	2·08
	25	·534	·679	1·69
	29	·446	·568	1·33
	33	·351	·446	·99
	37	·247	·314	·66
	41	·131	·166	·33

If θ and ϕ are small, the two equations reduce to

$$F_\theta = 4\delta,$$

$$F_\theta = \tfrac{1}{2}k_\theta(\theta-\delta),$$

whence
$$\frac{F_\theta}{\theta} = \frac{4k_\theta}{8+k_\theta}.$$

This simple equation fits the experimental data very closely for $k_\theta < 1{\cdot}4$. The departure at larger values of k_θ is not surprising in view of the probable interactions between the individual wires.

Details of these measurements will be published by the staff of the National Bureau of Standards in conjunction with further data on the effect of screens on isotropic turbulence.

REFERENCES

1. L. PRANDTL, *The Attainment of a Steady Air Stream in Wind Tunnels*, translated as N.A.C.A. (U.S.A) Tech. Mem. 726 (1933).
2. A. R. COLLAR, *The Effect of a Gauze on the Velocity Distribution in a Uniform Duct*, Brit. Aero. Res. Coun., Rep. and Mem. 1867 (1939).
3. G. K. BATCHELOR, *On the Concept and Properties of the Idealized Hydrodynamic Resistance*, Australian Council for Aeronautics, Rep. A.C.A. 13 (1945).
4. H. L. DRYDEN and G. B. SCHUBAUER, 'The use of damping screens for the reduction of wind tunnel turbulence': *Journ. Aero. Sci.* **14** (1947), 221–8.
5. L. F. G. SIMMONS and C. F. COWDREY, 'Measurements of the aerodynamic forces acting on porous screens' (to be published).
6. D. C. MACPHAIL, *Experiments on turning Vanes at an Expansion*, Brit. Aero. Res. Coun., Rep. and Mem. 1876 (1939).
7. G. K. BATCHELOR, 'The role of big eddies in homogeneous turbulence', *Proc. Roy. Soc.* (in the press).
8. H. L. DRYDEN, 'A review of the statistical theory of turbulence': *Quart. of Appl. Math.* **1** (1943), 7–42.

THEORY OF A LOOP REVOLVING IN AIR, WITH OBSERVATIONS ON THE SKIN-FRICTION

By C. C. L. GREGORY

(*University of London Observatory, Mill Hill Park, N.W.*7)

[Received 22 December 1947]

SUMMARY

An investigation is made of the dynamics of a flexible loop, driven by a small pulley at a constant speed, for the case when the speed is sufficient to cause the loop to become air-borne. It does this when the air-friction is greater than the weight of the loop. The shape and position of the loop may be calculated for values of the ratio, 2α, of air-friction to weight and the angle, ϕ^*, that the tangent to the ascending portion of the loop at the pulley makes with the horizontal. This angle may be controlled by means of a second pulley so arranged as to press the loop against the driven pulley. If $\alpha = 1$, theory predicts a point of the loop at which its radius of curvature becomes zero. For values of α between $\frac{1}{2}$ and 1 the motion is stable, and the precise value of α may be found from the photographed shape of the loop. As the result of some trials, values of α have been obtained which have given a value of the air-friction drag coefficient of the right order of magnitude.

Introduction

It has long been known to engineers that a belt when driven at a high speed will occasionally be seen to stand up in the air in the form of a loop. This may happen when a shaft breaks, or when a belt slips off a driven pulley at the end of a shaft. The dynamics of such a revolving loop does not appear to have received previous consideration, nor does the more general problem of an endless flexible cord subjected to external forces which do not all pass through a fixed point.

The author's attention was drawn to this problem at the Admiralty when examining a proposal to use such a loop as a means of defence against aircraft. At that time no very precise values of the air-friction at a moving surface were available, and it occurred to the author that the revolving loop, found to be valueless for the purpose proposed, might prove useful as a means of obtaining this information. Accordingly, the theory of the revolving loop has now been rewritten. Some tests of the suitability of the loop for measurement of surface air-friction were made at the University of London Observatory in February 1947 when astronomical observations were interrupted by bad weather.

Part I. Theory of the revolving loop

Let the arc APO (Fig. 1) be the locus of any point, P, of a uniform, flexible, inextensible string of weight mg per unit length, which is moving

with constant tangential velocity V. Suppose the string is subject to the following external forces:

(i) its weight acting vertically downwards,

(ii) a constant tangential retarding force $2\alpha mg\,\delta s$ on every element of length δs,

(iii) a constant tension, T_0, at O, where the tangent to the string is horizontal,

(iv) a constant tension, T^*, at A, the tangent at A making an angle ϕ^* with the horizontal.

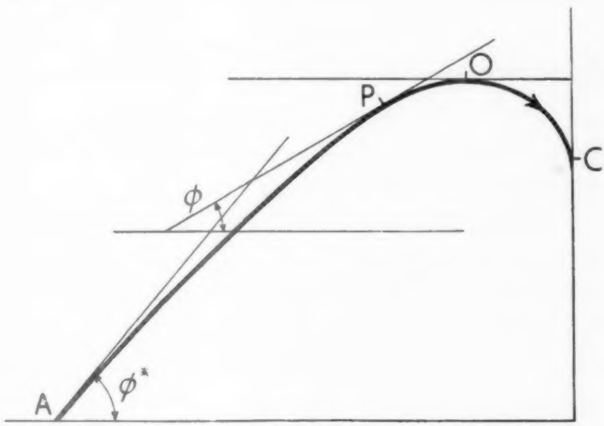

FIG. 1.

For uniform motion the forces (i) to (iv) must balance the centripetal force $(mV^2\,\delta s)/R$, where R is the radius of curvature at P. If T is the tension at P, and the tangent at P makes an angle ϕ with the horizontal, then

$$\delta T = -mg(2\alpha+\sin\phi)\,\delta s,$$

$$T\,\delta\phi = mg\left(\frac{V^2}{gR}-\cos\phi\right)\delta s,$$

where the motion is in the direction APO, and s is measured from O along the curve of the string to P. The differential equations to be solved are thus

$$\left.\begin{aligned} \frac{dT}{ds} &= -mg(2\alpha+\sin\phi), && (a)\\ mV^2-T &= mgR\cos\phi, && (b)\\ \text{where}\qquad R &= \frac{ds}{d\phi}. && (c) \end{aligned}\right\} \qquad (1)$$

From 1(b) and 1(c),

$$\frac{dT}{ds} = -mg\frac{dR}{ds}\cos\phi + mg\sin\phi,$$

so that, by 1(a),
$$\frac{dR}{ds}\cos\phi = 2(\alpha+\sin\phi),$$

or,
$$\frac{dR}{R} = 2(\alpha\sec\phi+\tan\phi)\,d\phi.$$

Hence, we obtain $\quad R = k\{\tan(\frac{1}{4}\pi+\frac{1}{2}\phi)\}^{2\alpha}\sec^2\phi,$

where k is a constant of integration, and by 1(b),

$$mV^2-T = mgk\{\tan(\tfrac{1}{4}\pi+\tfrac{1}{2}\phi)\}^{2\alpha}\sec\phi.$$

Consideration of the conditions at $\phi = 0$ leads finally to the expression

$$mV^2-T = (mV^2-T_0)\{\tan(\tfrac{1}{4}\pi+\tfrac{1}{2}\phi)\}^{2\alpha}\sec\phi. \tag{2}$$

Since change of sign of α corresponds to reversal of the direction of V, the above equation, when written in the form

$$mV^2-T = (mV^2-T_0)\{\tan(\tfrac{1}{4}\pi+\tfrac{1}{2}\phi)\}^{-2\alpha}\sec\phi,$$

represents, for negative values of ϕ, the descending branch of the curve from O to the point C, where the tangent is vertical.

Writing t for $\tan(\frac{1}{4}\pi+\frac{1}{2}\phi)$ and K for $(V^2/g-T_0/mg)$, (2) becomes

$$mV^2-T = \tfrac{1}{2}Kmg(t^{2\alpha+1}+t^{2\alpha-1}). \tag{3}$$

Since $T > T_0$ at C, it follows that

$$2\alpha > 1. \tag{4}$$

We also have, from (1)

$$R = K\{\tan(\tfrac{1}{4}\pi+\tfrac{1}{2}\phi)\}^{2\alpha}\sec^2\phi = \tfrac{1}{4}K(t^{2\alpha-2}+2t^{2\alpha}+t^{2\alpha+2}), \tag{5}$$

and since $\quad ds/dt = R\,d\phi/dt = \frac{1}{2}K(t^{2\alpha-2}+t^{2\alpha}),$

it follows that
$$s = \tfrac{1}{2}K[t^{2\alpha-1}/(2\alpha-1)+t^{2\alpha+1}/(2\alpha+1)]. \tag{6}$$

Taking axes through C, x to the left and y downwards, the coordinates of P are

$$x = \tfrac{1}{2}Kt^{2\alpha}/\alpha, \qquad y = \tfrac{1}{2}K[t^{2\alpha+1}/(2\alpha+1)-t^{2\alpha-1}/(2\alpha-1)]. \tag{7}$$

We consider now the equations of motion of an element $\delta s'$ of a similar string at the point P' and moving with the same velocity, V, the tangent at C being vertical and the tension at C being mV^2 (Fig. 2). These equations are

$$\left.\begin{aligned} \delta T' &= -mg(2\alpha-\sin\phi')\,\delta s', \\ T'\,\delta\phi' &= mg\left(\frac{V^2}{gR'}+\cos\phi'\right)\delta s'. \end{aligned}\right\} \tag{8}$$

Using a similar method to that given above we obtain

$$T'-mV^2 = \tfrac{1}{2}K'mg(t'^{2\alpha+1}+t'^{2\alpha-1}), \tag{9}$$

where ϕ' is the angle which the tangent at P' makes with the horizontal,

$$K' = (T^{*\prime}-mV^2)/\tfrac{1}{2}mg(t^{*\prime 2\alpha+1}+t^{*\prime 2\alpha-1}).$$

$$t' = \tan(\tfrac{1}{4}\pi-\tfrac{1}{2}\phi'), \qquad t^{*\prime} = \tan(\tfrac{1}{4}\pi-\tfrac{1}{2}\phi^{*\prime}).$$

$T^{*\prime}$ and $\phi^{*\prime}$ are, respectively, the string tension and the angle of the tangent at a point, B, at which the constant driving force, $T^{*\prime}$, is applied

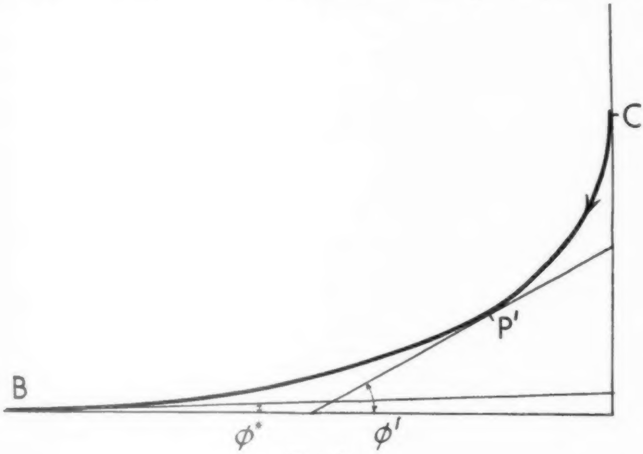

FIG. 2.

to the string. Accordingly, P' lies on a curve similar to the portion, OC, of the curve in Fig. 1, except that it is inverted and the scale is increased by the factor K'/K.

We may now suppose that the two portions of string form one continuous loop $COPAP'C$, by joining the curves P and P' at C and making B coincide with A. [In practice this may be done, approximately, by using a large loop constrained to bend around a small driving pulley at A.] Equating the x-coordinates of A and B, we have

$$K'/K = (t^*/t^{*\prime})^{2\alpha}, \tag{10}$$

where t^* is the value of t at A. Equating the y-coordinates of A and B, and using (10), we obtain

$$t^*t^{*\prime} = (2\alpha+1)/(2\alpha-1); \tag{11}$$

also, $$S' = \text{arc}\, CP'A = \tfrac{1}{2}K'\left[\frac{t^{*\prime 2\alpha+1}}{2\alpha+1}+\frac{t^{*\prime 2\alpha-1}}{2\alpha-1}\right] \tag{12}$$

and, from (6), $$S = \text{arc}\, COPA = \tfrac{1}{2}K\left[\frac{t^{*2\alpha+1}}{2\alpha+1}+\frac{t^{*2\alpha-1}}{2\alpha-1}\right]. \tag{13}$$

Equations (10) to (13) give

$$S = S', \quad \text{or} \quad \text{arc}\, COPA = \text{arc}\, CP'A. \tag{14}$$

From (9),

$$\begin{aligned} T^{*\prime} - mV^2 &= \tfrac{1}{2}K'mg(t^{*\prime}+t^{*\prime -1})t^{*\prime 2\alpha} \\ &= \tfrac{1}{2}Kmg[(2\alpha-1)t^{*2\alpha+1}/(2\alpha+1)+(2\alpha+1)t^{*2\alpha-1}/(2\alpha-1)] \end{aligned}$$

and from (3), $$mV^2 - T^* = \tfrac{1}{2}Kmg(t^*+t^{*-1})t^{*2\alpha},$$

whence $$T^{*\prime} - T^* = 4\alpha mgS, \tag{15}$$

and also

$$\left.\begin{aligned} T^{*\prime}+T^* &= 2mV^2 - K[t^*/(2\alpha+1)-t^{*-1}/(2\alpha-1)]t^{*2\alpha}g \\ &= 2mV^2 - 2y^*mg, \end{aligned}\right\} \tag{16}$$

where x^*, y^* are the coordinates of A. Accordingly,

$$T^{*\prime} = mV^2 + 2\alpha mgS - mgy^* \tag{17}$$

and $$T^* = mV^2 - 2\alpha mgS - mgy^*. \tag{18}$$

Also, if x', y' be the coordinates of P',

$$x' = \tfrac{1}{2}K't'^{2\alpha}/\alpha, \tag{19}$$

$$y' = \tfrac{1}{2}K'\left[\frac{t'^{2\alpha-1}}{2\alpha-1} - \frac{t'^{2\alpha+1}}{2\alpha+1}\right]. \tag{20}$$

The area of the loop is given by

$$\begin{aligned} \Delta &= \int_O^A y'\,dx' - \int_O^A y\,dx \\ &= \tfrac{1}{2}K'^2\left[\int_0^{t^{*\prime}} \frac{t'^{4\alpha-2}}{2\alpha-1}\,dt - \int_0^{t^{*\prime}} \frac{t'^{4\alpha}}{2\alpha+1}\,dt\right] - \tfrac{1}{2}K^2\left[\int_0^{t^*} \frac{t^{4\alpha}}{2\alpha+1}\,dt - \int_0^{t^*} \frac{t^{4\alpha-2}}{2\alpha-1}\,dt\right] \\ &= \frac{K^2t^{*4\alpha}}{4}\left[\frac{t^*}{(2\alpha+1)(4\alpha-1)} - \frac{t^{*-1}}{(2\alpha-1)(4\alpha+1)} - \frac{t^*}{(2\alpha+1)(4\alpha+1)} + \right. \\ &\qquad\qquad \left. + \frac{t^{*-1}}{(2\alpha-1)(4\alpha-1)}\right] \\ &= \frac{2\alpha Sx^*}{16\alpha^2-1}. \end{aligned} \tag{21}$$

The left-handed couple about A, required to balance the weight of S and S' together (considered as a rigid, stationary loop held at the point A), is given by

$$\begin{aligned} G &= mg\left[\int_O^A (x^*-x)\,ds + \int_O^A (x^*-x')\,ds'\right] \\ &= 2mgx^*S - mg\int_O^A x\,ds - mg\int_O^A x'\,ds'. \end{aligned}$$

Since

$$x = Kt^{2\alpha}/2\alpha,\ x' = K't'^{2\alpha}/2\alpha,\ ds = \tfrac{1}{2}K(t^{2\alpha}+t^{2\alpha-2})dt,\ ds' = \tfrac{1}{2}K'(t'^{2\alpha}+t'^{2\alpha-2})dt,$$

it follows from (21) that

$$G = \frac{16\alpha^2}{16\alpha^2-1} mgSx^* = 4\alpha mg\Delta. \tag{22}$$

Here G is the left-handed couple about A, arising from air skin-friction when the loop is rotating with constant speed V. Air-friction will exactly balance gravity, and the loop becomes airborne provided $\alpha > \frac{1}{2}$, as required by (4).

In order to determine whether the radius of curvature, R, of the loop always remains finite, we have, from (5)

$$dR/dt = \tfrac{1}{2}K[(\alpha+1)t^{2\alpha+1}+2\alpha t^{2\alpha-1}+(\alpha-1)t^{2\alpha-3}]$$

$$= 0 \quad \text{when} \quad t^2 = 0 \text{ (when } 2\alpha > 3\text{)},\ -1, \text{ or } \frac{1-\alpha}{1+\alpha}.$$

$t^2 = \dfrac{1-\alpha}{1+\alpha}$ gives values of ϕ from $-30°$ to $-90°$ for values of α from $\frac{1}{2}$ to 1 respectively. The corresponding values of R, given by

$$R_{\min} = K(1-\alpha)^{\alpha-1}(1+\alpha)^{-\alpha-1},$$

are finite for $\alpha < 1$. For $\alpha \geqslant 1$, $R_{\min} = 0$ at C, where $-\phi = \frac{1}{2}\pi$. [In an actual case some distortion of the loop occurs when $\alpha > 1$, since no material loop is infinitely flexible; the rotational effect of air-friction, in this case, causes the top of the loop to bend back somewhat.]

From (21) it will be seen that, when V (and consequently α) is constant, the area of the loop, Δ, varies as x^*; the locus of A when C is supposed fixed may be found as follows.

Let the two tangents at A meet the vertical through C in E and D (Fig. 3), then

$$AE = x^* \sec\phi^* = Kt^{*2\alpha}(t^*+t^{*-1})/4\alpha$$

$$= (mV^2-T^*)/2\alpha mg = (S+y^*)/2\alpha,$$

from (18), $$AD = x^* \sec\phi^{*\prime}$$

$$= Kt^{*2\alpha}\left[\frac{2\alpha+1}{2\alpha-1}t^{*-1}+\frac{2\alpha-1}{2\alpha+1}t^*\right]\Big/4\alpha.$$

Thus $$AE+AD = Kt^{*2\alpha}[(2\alpha+1)^{-1}t^*+(2\alpha-1)^{-1}t^{*-1}]$$

$$= 2S = \text{constant},$$

$$AD = S-y^*/2\alpha,$$

$$CE = x^*\tan\phi^*-y^* = S/2\alpha,$$

and $$CD = y^*-x^*\tan\phi^{*\prime} = S/2\alpha = CE,$$

hence the locus of A is the ellipse

$$y^{*2}+\frac{4\alpha^2}{4\alpha^2-1}x^{*2} = S^2, \tag{23}$$

D and E being the foci, C the centre, and S and $S(4\alpha^2-1)^{\frac{1}{2}}/2\alpha$ the semi-axes.

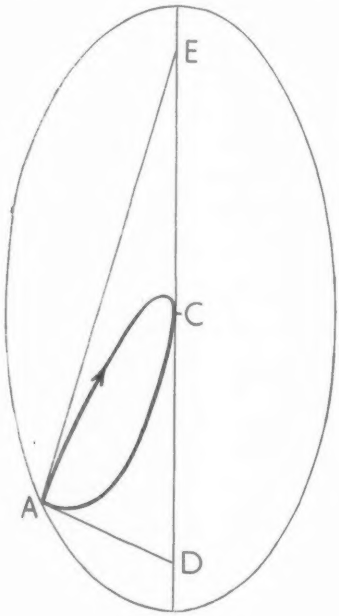

FIG. 3.

Part II. The airborne loop in practice, and the determination of skin-friction at various speeds

The determination of air-resistance to a surface, when in uniform motion relative to still air parallel to the surface, has always proved difficult from an experimental point of view on account of end-effects of the material body which provides the moving surface. An endless cord or belt of uniform cross-section driven by a pair of wheels mounted on fixed parallel axes, and made to revolve at a constant known speed would, indeed, overcome the difficulty of 'end effects', but other difficulties would arise. Only at very low speeds would such a driven belt be free from 'flutter' unless it were stretched very tight, in which case the presence of eddy currents might be concealed. Another difficulty with such an arrangement would be the accurate determination of the rather small additional force required to drive the belt against air resistance, over and above that

required to overcome the friction and air resistance of the driving wheels and other moving parts of the apparatus.

When a belt is driven by a single small wheel or pulley, however, these difficulties do not arise, the motion of the 'loop' being observably steady so long as the speed is such that the value of α lies between $\frac{1}{2}$ and 1. The precise value of α can be found from the curvature of the loop in the

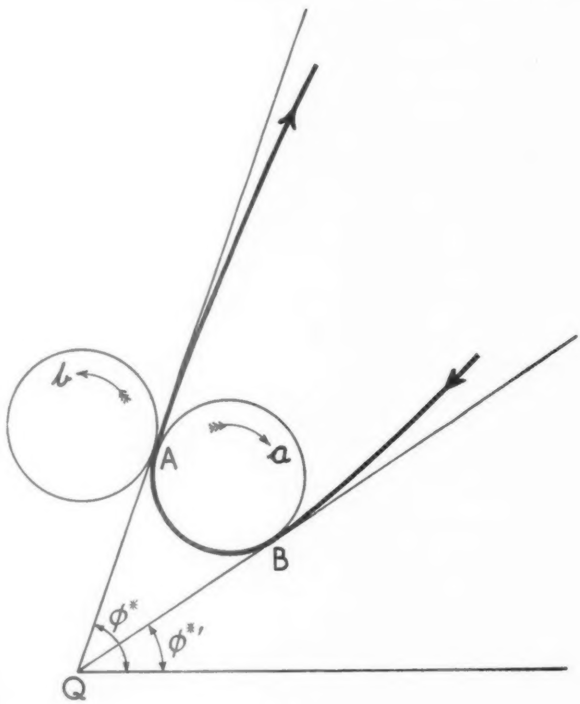

FIG. 4.

vicinity of the point C (Fig. 1), no measurement of force being required. Both the shape of the loop (giving α) and its rotational speed, V, may be determined by a cinematograph camera working at a known speed, a short length of the (white) loop being blackened so as to be visible.

From the foregoing theoretical discussion the necessary and sufficient conditions for the maintenance of an air-borne loop in a steady state can readily be seen.

Let a (Fig. 4) be a cylindrical pulley wheel driven at a constant peripheral speed, V, by an electric motor, say. Around a is placed the loop of

length $2S$ and weight $2Smg$. A loose pulley, b, on an axle parallel to that of a, keeps the loop in contact with a at A.

Let QA be the common tangent of a and b at A, and let QA make an angle ϕ^* with the plane of the horizon. On first starting the motor, the part of the loop in the vicinity of A is projected along this tangent QA with velocity V, and, if air resistance is neglected, would attain a vertical height equal to $V^2/2g$. Taking air-resistance into account, V must be sufficiently great to make T^* greater than zero in (18).

Once the loop is airborne, the whole family of possible curves given by (23) for all positions of A in Fig. 3, and subject to the restriction $\phi^* > 90°$, may be obtained by rotating the line of centres of a and b, and thus altering ϕ^*. However large V may be, the loop will fall as soon as $\phi^* = 90°$, as may be seen from (2).

Should it be possible to measure with accuracy the constant couple which must be applied to a to maintain the loop at any (sufficient) speed, α would at once be obtained from (15), the mass ($2Smg$) of the loop being readily measured. This value of α could then be compared with that derived from the radius of curvature of the loop at C, as mentioned in the second paragraph.

It is worth noting that measurements of surface air-friction over a considerable range of speed can be made by employing loops of very different cross-section, V being greatest (for $\alpha = 0{\cdot}6$, say) when the cross-section is circular. If the cross-section be rectangular, of thickness a and breadth b much greater than a, then

$$\alpha mg = cV_1^2(a+b),$$

where c is assumed constant.

If r be the radius of the circular section of a loop of similar material such that $\pi r^2 = ab$, the ratio of the speed, V_2, which it must have to give the same α, to V_1 is given by

$$V_2/V_1 = \frac{\pi^{\frac{1}{4}} r^{\frac{1}{2}}}{(a+b)^{\frac{1}{2}}} = (\pi b/a)^{\frac{1}{4}} \text{ (approx.)}$$

With $b/a = 800$, the ratio of the speeds is about seven.

A few trials were made at the University of London Observatory in February 1947. Loops from 7 to 20 feet in length were maintained in the air by an electric motor driving pulleys of 0·298 and 0·255 ft. diameter respectively at about 50 r.p.s. The loops were made from strips of chronograph paper 0·0833 ft. wide and 0·00031 ft. thick, m being 0·0012 lb./ft. α was found to vary from about 0·5 to 0·7 with speeds of about 40 and 46 ft./sec. and was obtained from photographs of the loop by measuring R_{min}. It was found that the loop could be kept steady for any length of time so

long as it was subjected to a slight draught of air perpendicularly to its plane. This was probably necessary in order to prevent circulatory air currents forming and so reducing the air-speed of the loop. When driven at constant speed in still air the loop was observed slowly to drop a little and then more quickly recover its original height, this 'hunting' continuing in a somewhat irregular manner.

Regarding the accepted value of the skin-friction drag coefficient K_f, the value suggested by M.A.P. for a steel wire is between 0·003 and 0·0015.

Assuming $$K_f \rho V^2(a+b) = \alpha m,$$

where $\rho = 0{\cdot}00238$, $a = 0{\cdot}00031$, $b = 0{\cdot}0833$, and $m = 0{\cdot}0012$, we deduce that
$$K_f = \alpha/0{\cdot}166V^2,$$

whence, (i) for $\alpha = 0{\cdot}5$ and $V^2 = 1600$, we obtain $K_f = 0{\cdot}0019$,

and (ii) for $\alpha = 0{\cdot}7$ and $V^2 = 2100$, we obtain $K_f = 0{\cdot}0020$.

THE PLASTIC YIELDING OF NOTCHED BARS UNDER TENSION

By R. HILL (*Cavendish Laboratory, Cambridge*)

[Received 3 February 1948]

SUMMARY

The state of stress in the core of a notched bar is analysed at the moment when pronounced plastic yielding begins. The theory is two-dimensional and an ideal plastic-rigid material is assumed. Following a general analysis of the problem, the magnitude of the constraint factor is calculated for a deep notch with a semi-circular root. The correct approach to problems of plane plastic strain is discussed, and is further illustrated by a re-examination of the classical work of Prandtl on indentation (which is closely related in principle with the notched bar problem).

1. General considerations

THE paper is concerned with the state of stress in the core of a notched bar under an applied load sufficient to cause plastic flow. It is known that the fairly well-defined bend in the load-extension relation for a notched bar corresponds to a mean stress in the core that is greater than the yield stress in a tensile test of an unnotched specimen. The investigation will be directed particularly to a calculation of the magnitude of this effect in relation to the shape of the notch. The problem will be treated as one of plane strain, so that the specimen is a wide rectangular block, symmetrically notched through the thickness on two sides. The notch is shown in Fig. 1, the plane of the paper representing a plane of flow. Let it be supposed that the applied load at the ends of the specimen is statically equivalent to a tension along the central longitudinal axis. It is also supposed that a distribution of stress, suitable to ensure plane strain, is applied to the two lateral surfaces of the block which are parallel to the planes of flow. The specimen is assumed so long that the state of stress in the neighbourhood of the notch is, to any desired approximation, independent of the precise distribution of the end load. It is further assumed that the notch is of sufficient depth to ensure that the plastic region is localized in and around the core (this will be discussed more carefully later).

If the curvature of the notch is greatest at the root, the yield limit is first attained at that point. As the applied end-load is further increased, the plastic region can be expected to spread in the manner shown in Fig. 1. If the constant maximum shear-stress criterion of Tresca is adopted (the work-hardening being supposed zero), the problem of calculating the

stress components in the plane is statically determined (the stress normal to the plane is the intermediate stress). While part of the core is still elastic, the strains are small enough for the changes in the external surfaces to be neglected. The stress boundary conditions, known *a priori*, are then sufficient to determine the distribution of stress (in the plane) without

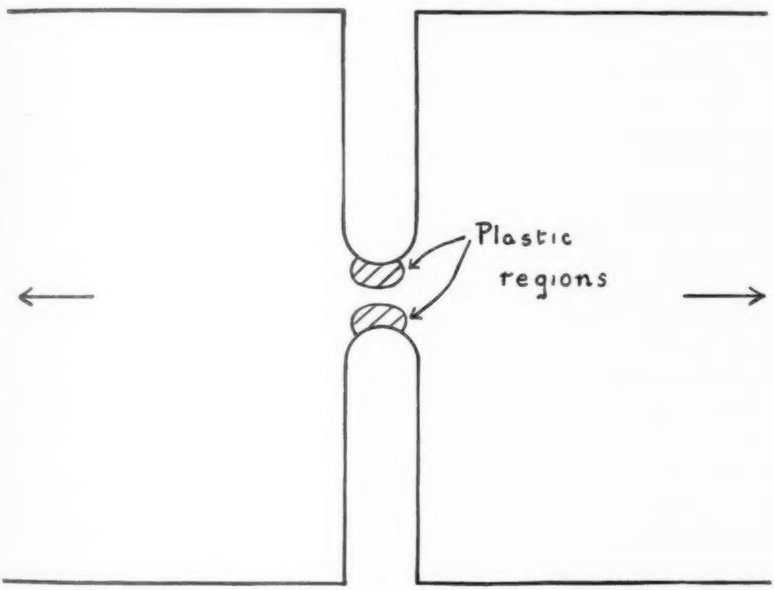

Fig. 1. The notched tensile specimen. A typical plane of flow.

reference to the velocities of flow.† Since the elastic compatibility equation does not involve elastic constants (there being no body forces), the entire distribution (in the plane) is independent of the elastic constants. In the elastic region the stress normal to the planes of motion is equal to $\nu \times$ the sum of the other two principal stresses (where ν is Poisson's ratio); in the plastic region it can only be found by following the history of the deformation, using Reuss's equations.‡ The plastic-elastic boundary is a curve along which the maximum shear stress is constant (not a slip-line). It seems that the stress can only be universally calculated by numerical methods. The relaxation technique has been applied by Southwell and Allen (**14**) in determining the plastic and elastic stress in a

† Strictly, the velocity distribution at each moment should be examined to see whether the plastic work done on each element is positive; otherwise unloading takes place.

‡ These may most conveniently be found in ref. (**3**).

notched bar with a shallow notch, but no calculation appears to have been made for the deep notch considered here.

In the absence of such a calculation we can proceed further by introducing the assumption of a plastic-rigid material, which is rigid up to a well-defined yield point and does not work-harden. This does not affect the stress distribution in the plane, nor the shape of the plastic region, corresponding to a given end-load. In the plastic region the stress normal to the plane is now equal to the mean of the principal stresses in the plane; hence there is a discontinuity in the stress normal to the plane (unless $\nu = \frac{1}{2}$) along the line of separation between rigid material and material undergoing deformation. So long as part of the core is not plastic no displacement of the ends of the specimen is possible. However, even when the plastic region has spread right across the core it still does not necessarily follow that deformation is possible, since the incipiently plastic material may be rigidly constrained by the adjacent bulk of non-plastic material. To state this more precisely it is necessary to introduce the equations of Saint-Venant governing the flow velocities in the plastic region. These are simply (i) that the volume change is zero, and (ii) that the principal axes of the rate of strain coincide with the principal axes of stress. The characteristics of the velocity equations are the slip-lines (curves whose directions coincide with the directions of maximum shear stress). A little consideration shows that no extension of the specimen is therefore possible until the plastic region has spread sufficiently far to include the entire slip-lines OS, OS' from the centre O to the free surface (Fig. 2).† This is the mathematical expression of the reason normally offered to account for the raising of the apparent yield stress by a notch: namely, the constraint on the possible deformation of plastic material exerted by the adjacent bulk of elastic material. At the moment when extension first occurs, the plastic boundary must touch OS, OS' as in (a); or must pass either through S and S' as in (b), or through O as in (c). It does not seem possible to say which configuration actually occurs without the full solution; however, this is not necessary for the present purpose.‡

Since both velocity components are known on the plastic boundary in terms of the (unit) speed of extension, the velocity solution is uniquely determined in regions SOB, $S'OB'$ by virtue of the properties of characteristics. Hence the material within SOB, $S'OB'$, though plastic, moves as a rigid body attached to the non-plastic material. The velocity solution

† The initial assumption of a sufficiently deep notch is used here; with shallow notches the plastic region will be quite different.

‡ It appears from calculations of Southwell and Allen that (b) is probably the actual configuration (private communication). The calculations have so far been carried out for shallow notches only, and for an intermediate range of loads.

within SOS' is uniquely determined by the known velocity components normal to the slip-lines SO, $S'O$. It can be found, if required, by the application of Riemann's method (see Geiringer, **1**). Across SO, $S'O$ there is a discontinuity in the tangential component of velocity (constant saltus $\sqrt{2}$). Such discontinuities in tangential velocity across slip-lines are of

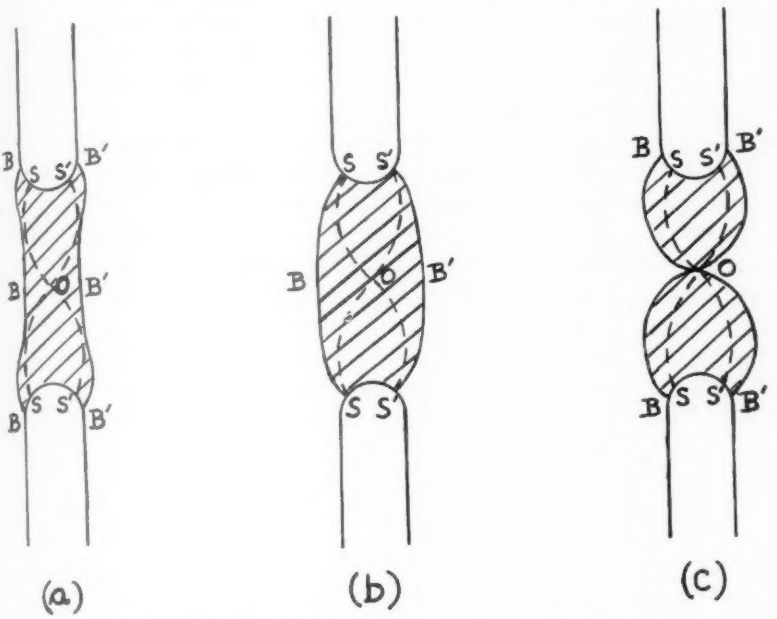

FIG. 2. The three possible modes of development of the plastic region.

frequent occurrence in plane-strain deformation of a plastic-rigid material which does not work-harden. They represent an extreme case of the analytic possibility of arbitrarily prescribing the normal components of velocity along two intersecting slip-lines of a given field. The discontinuity, be it noted, is only momentary in each element crossing the slip-line. Such an element abruptly changes its direction of motion, and undergoes a finite instantaneous change of strain. In a real metal the discontinuity would be diffused, partly by elastic strain-increments and partly by work-hardening, into a region where the rate of shear is large. The closer the approximation effected by the plastic-rigid material, the narrower will this region be. Also, in a real metal, regions BOS and $B'OS'$ would not be rigid, but would be undergoing plastic strains of the same order as elastic strains.

We now examine how the load can be calculated at the moment when extension begins. Since the slip-lines are also characteristics of the stress equations in the plastic region (Hencky, **2**), the slip-line field and stresses within SOS' are uniquely determined by the shape of the stress-free surface SS'.† Furthermore, they are independent of the notch depth provided this is sufficiently large; the plastic boundary will of course vary with notch depth. The load and distribution of stress across the narrowest section can thus be found at the beginning of the extension without a precise knowledge of the shape of the plastic region or of the elastic stress distribution. It is clear that this fortunate possibility is due to the coincidence in pairs of the characteristics for the stresses and velocities. The possibility would not necessarily occur for a material yielding according to Mohr's criterion (**9**). The four characteristics are then distinct. The stress characteristics are in the directions corresponding to the points of contact of a Mohr circle of stress with the yield envelope (Mandel, **7** and **8**); the velocity characteristics are still the slip-lines. It must be emphasized, too, that the assumed manner of the spreading of the plastic region for a deep notch, while almost certainly correct, has yet to be confirmed by a full solution. Similar methods cannot be used for shallow notches, since the general shape of the plastic region can scarcely be surmised in advance. For this reason the present considerations are limited to notches which are deep in comparison with the core diameter.

A calculation of the variation of the load with increasing extension is outside the scope of the present investigation. It is merely necessary to remark that, since the core width decreases during the deformation, the load needed to maintain flow depends only on the changing contour of the notch. Hence the load-extension curve for the plastic-rigid material has a sharp corner at the beginning of extension. In a real metal with a sharp yield point and a small rate of hardening, this 'corner' is rounded off by the influence of elastic strains, but is sufficiently well defined to allow an approximate estimate of the constraint factor. Plastic strains of elastic order occur, of course, before the corner is reached, following the initiation of plasticity at the root of the notch for a much smaller load. When the metal work-hardens rapidly, any basis of comparison between notched and unnotched specimens must be somewhat arbitrary in view of the completely rounded load-extension curves and the non-uniformity of the deformation. However, the constraining effect of the notch is still apparent from the general raising of the load-extension curve.

In the above discussion the problem was simplified by the use of Tresca's

† The stresses are also uniquely determined in terms of the notch contour within a part, at least, of regions BOS, $B'OS'$.

yield criterion. If the Huber-Mises criterion is used, certain differences must be noted. For the plastic-rigid material the yield criterion reduces to Tresca's with a modified yield stress $2Y/\sqrt{3}$, since the stress normal to the plane is equal to the mean of the other two principal stresses. The slip-line field within SOS' is therefore unchanged, and all stresses there are simply multiplied by the factor $2/\sqrt{3}$. The plastic boundary is, however, different unless $\nu = \frac{1}{2}$, since the yield criterion now involves the stress normal to the plane and this is discontinuous across the plastic boundary. Hence the stress component acting normally to a plane element perpendicular to the boundary is also discontinuous unless $\nu = \frac{1}{2}$. For the same reason the stress distribution in the plane before extension begins is not everywhere independent of elastic constants as before, but depends on the value of ν. With a general plastic-elastic material the stress problem is no longer statically determined, since the stress normal to the plane in the plastic region depends on the previous strain-history. The stress distribution in the plane should nevertheless be closely approximated by that for the plastic-rigid material.

2. Notch with a semicircular root

Suppose the notch is parallel-sided with a semicircular root, centre C and radius r (Fig. 3, showing half of specimen only). The slip-lines in the field SOS' defined by the stress-free semicircular surface are logarithmic spirals; the trajectories of principal stress are the normals to the surface and concentric circular arcs. If $2R$ is the width of the narrowest section, the angle $SCS' = 2\theta$ (Fig. 3a) is given by the relation

$$\frac{R}{r} = e^{\theta} - 1 \quad (0 < \theta \leqslant \tfrac{1}{2}\pi). \tag{1}$$

This slip-line field is valid in the range

$$0 < \frac{R}{r} \leqslant e^{\frac{1}{2}\pi} - 1 = 3{\cdot}81 \text{ approx.} \tag{2}$$

For larger values of R/r the field is shown in Fig. 3b. The regions SQR and $S'Q'R'$, containing straight slip-lines, are uniquely defined (in type, but not extent) by the parallel free sides of the notch. Region RTR' is defined, as before, by the semicircular surface, and $CT = e^{\frac{1}{2}\pi}r$. Regions $PQRT$ and $P'Q'R'T$ are then uniquely determined by the base slip-lines RQ, RT, and $R'Q'$, $R'T$. The normals to TR, TR', respectively, constitute one family of slip-lines, the other being the orthogonal trajectories of these normals. Furthermore, TP, QR, TP', $Q'R'$ are all equal. Finally, region $TPP'O$ with straight slip-lines is uniquely defined by the base lines TP and TP'. The rigid part of the plastic region lying outside SOS', at present unknown, is not indicated in the figures.

The stress can now be calculated by integration of Hencky's well-known equations

$$\left.\begin{aligned} dp+2k\,d\phi &= 0 \quad \text{on an } \alpha\text{-line,} \\ dp-2k\,d\phi &= 0 \quad \text{on a } \beta\text{-line,} \end{aligned}\right\} \tag{3}$$

where p is the mean compressive stress in the plane (i.e. $-\frac{1}{2}(\sigma_1+\sigma_2)$, where

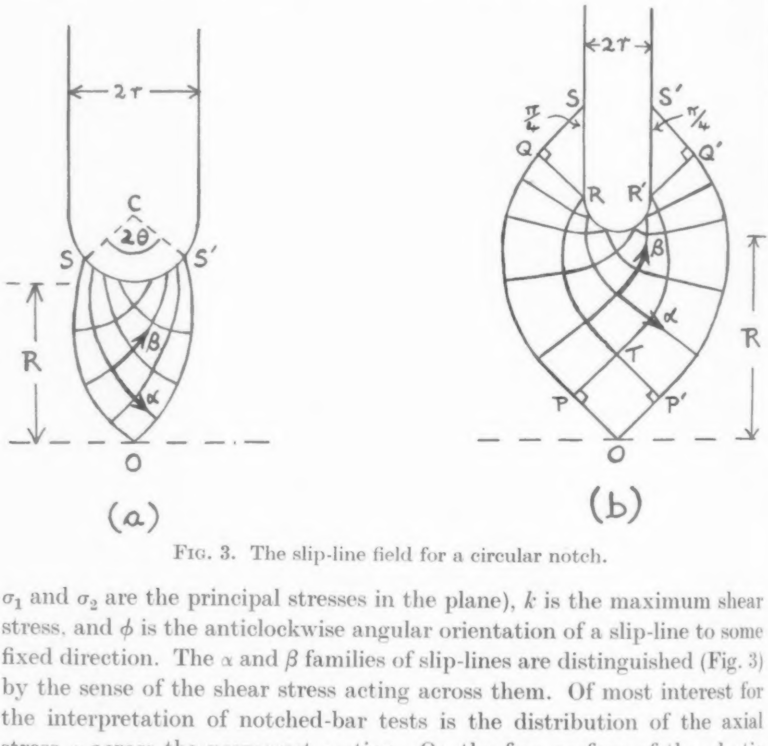

FIG. 3. The slip-line field for a circular notch.

σ_1 and σ_2 are the principal stresses in the plane), k is the maximum shear stress, and ϕ is the anticlockwise angular orientation of a slip-line to some fixed direction. The α and β families of slip-lines are distinguished (Fig. 3) by the sense of the shear stress acting across them. Of most interest for the interpretation of notched-bar tests is the distribution of the axial stress σ across the narrowest section. On the free surface of the plastic region $p = -k$, and so, in the configuration of Fig. 3a, σ is distributed according to the formula

$$\frac{\sigma}{2k} = 1+\log\left(1+\frac{x}{r}\right) \quad (0 \leqslant x \leqslant R), \tag{4}$$

where x is distance measured from the root. Hence σ rises steadily from the value $2k$ at the surface. Plastic flow has thus dissipated the stress concentration present when the material is still elastic. The transverse stress in the neck is always $\sigma-2k$, and is a tension. By integration the load is

$$L = 2R\bar{\sigma} = 4kR\left(1+\frac{r}{R}\right)\log\left(1+\frac{R}{r}\right) \quad \left(\frac{R}{r} \leqslant e^{\frac{1}{2}\pi}-1\right), \tag{5}$$

where $\bar{\sigma}$ is the mean value of the axial stress, and $\bar{\sigma}/2k$ is, by definition, the constraint factor measured in notched-bar tests. This factor rises steadily from the value unity with increasing R/r. In Fig. 3*b* the axial stress is distributed up to T according to equation (4). Along TO, σ is constant and equal to $2k(1+\frac{1}{2}\pi)$. It is clear that this will always be the stress sufficiently far from the root, whatever the shape of the notch, provided it has parallel sides and is not re-entrant. The constraint factor is

$$\frac{\bar{\sigma}}{2k} = 1+\tfrac{1}{2}\pi-\frac{r}{R}(e^{\frac{1}{2}\pi}-1-\tfrac{1}{2}\pi). \tag{6}$$

The maximum constraint factor obtainable with a parallel-sided notch is thus $1+\frac{1}{2}\pi$, or about 2·57. This is close to the value found experimentally for cylindrical notched bars, when the material has a sharp yield point. Thus Orowan, Nye, and Cairns (**11**) report a maximum constraint factor 2·6 for annealed mild steel. The significance of this in relation to Kuntze's so-called 'cohesive strength' has been discussed by Orowan (**10**). When the notch is not parallel-sided but wedge-shaped (the sides being tangential to the circular root), the modification of the above solution is obvious. If 2α is the wedge angle, the maximum constraint factor is $1+\frac{1}{2}\pi-\alpha$, corresponding to vanishingly small root radius.

Certain properties of the velocity solution are worth noting for the field of Fig. 3*b*. If u, v are the velocity components along the α, β slip-lines respectively, Geiringer's equations (**1**) are

$$\left.\begin{array}{ll} du-v\,d\phi = 0 & \text{along an } \alpha \text{ slip-line,} \\ dv+u\,d\phi = 0 & \text{along a } \beta \text{ slip-line.} \end{array}\right\} \tag{7}$$

If the speed of the extension is U, the material within $OPP'T$ moves as a rigid body with speed U in the direction $\overrightarrow{TO}$. In the right-hand half of the field (say) the velocity component u is constant on each α-line within $P'Q'R'T$. Hence since v is constant on TP' (and equal to $-U/\sqrt{2}$), v is also constant on each α-line. In particular v is equal to $-3U/\sqrt{2}$ on $Q'R'$. The material within $Q'R'S'$ moves, therefore, as a rigid body with component speeds U, $2U$, parallel and perpendicular to the side $S'R'$. The effect of the plastic deformation is thus towards the formation of a key-hole at the bottom of the notch. The velocity within TRR' can be determined by applying Riemann's formula.

Van Iterson (**6**) has independently proposed various slip-line fields in the neighbourhood of wedge-shaped notches when the root radius is vanishingly small, but without discriminating between deep and shallow notches. He did not discuss the inter-relation of the solutions in the plastic and elastic regions, and was evidently unaware of the need to consider the associated velocity solution in deciding when extension is first possible.

3. Relation to the problem of indentation with a flat punch

When the strains are so small that changes in external surfaces can be neglected, the problem of the indenting of a semi-infinite mass by a flat rigid punch is clearly identical (apart from changes of sign) with that of a notched tensile specimen when the notch is infinitely deep and sharp. The boundary conditions on the punch face RR' (Fig. 4), namely, zero

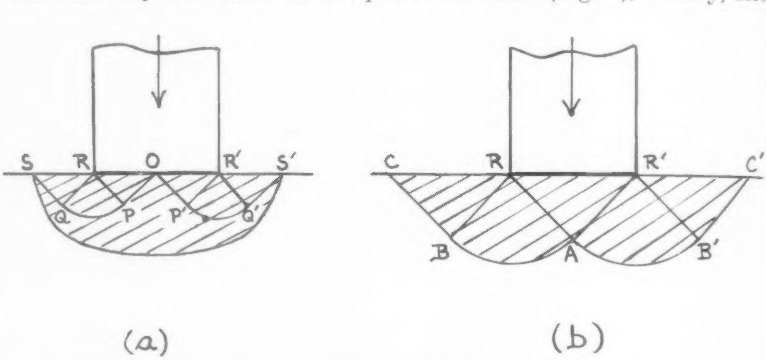

FIG. 4. Comparison of present solution (*a*) with Prandtl's solution (*b*) for the indentation problem.

shear stress and constant normal velocity, are just those on the narrowest section of the core in the notched bar. Again, the surface of the mass not touching the punch is stress-free, as are the sides of the notch. This indentation problem, now classical in the development of plastic theory, was first considered in 1920 in a highly original paper by Prandtl (**12**). Although Prandtl's work preceded by three years the general equations of the slip-line field obtained by Hencky, he recognized the hyperbolic character of the stress equations and derived the two special fields needed in the solution. However, Prandtl seems not to have fully appreciated the nature of the problem and the underlying assumptions, with the result that his solution is not entirely accurate in detail. It has not been corrected by later writers. It is necessary, therefore, to re-examine the problem carefully in the light of the previous discussion.

A smooth flat punch is pressed into the plane surface of a semi-infinite mass of plastic-rigid material (Fig. 4*a*). Indentation cannot begin until the plastic region has spread sufficiently far to include the entire slip-lines $OPQS$ and $OP'Q'S'$ from the centre O of the punch face.† The curved plastic boundary SS' can be expected to be of the form indicated in Fig. 4, which seems the most likely of the three possibilities of Fig. 2.

† At any earlier stage the slip-lines through the extreme points S and S' of the incipiently plastic surface do not meet on the punch face.

It would be interesting to have this checked by detailed calculations. The slip-line field within $OPQSR$ is uniquely determined by the shape of the free surface and the stress conditions along it. In the left-hand half of the diagram, for example, the slip-lines in OPR and QRS are straight lines meeting the surface in 45°, while in PQR they are radii from the corner and circular arcs. The pressure at the beginning of indentation is uniform and equal to $2k(1+\frac{1}{2}\pi)$. There is a tangential velocity discontinuity across $OPQS$ (and $OP'Q'S'$); the plastic material on one side is still held rigidly by the non-plastic material, while on the other it moves with constant speed $\sqrt{2}\,U$ along the slip-lines of the same family as $OPQS$ (U = speed of the punch). In a real plastic-elastic material with a sharp yield point, irrecoverable indentation occurs at the first application of load, due to plastic flow around the corners of the punch. However, the load-penetration curve should have a fairly well-defined bend, the penetration prior to this being restricted by the constraint of elastic material. When the material work-hardens rapidly and does not possess a sharp yield point, it is observed that the displaced material does not flow sideways towards a raised lip, but is accommodated by the compressibility of the whole mass. It seems that rapid hardening causes the plastic region to spread downwards rather than sideways. A balance is, as it were, struck between (i) flow out to the surface with hardening accompanying the associated severe strains, and (ii) a downward displacement requiring relatively small plastic strains and hardening, but against the constraint of surrounding elastic material.

We can now compare the present solution with Prandtl's. Prandtl made no mention of the rigid part of the plastic region, and seems not to have realized the significance of the fact that the plastic boundary can only be determined by a calculation of the stresses in both plastic and elastic regions. He was also apparently not aware of the condition determining the start of indentation: namely, that the plastic region should just include the slip-lines $OPQS$, $OP'Q'S'$ from the centre O of the punch face to the free surface. Nor was he apparently aware of the reason for this, namely, that the slip-lines are characteristics of the velocity equations. In Prandtl's solution (Fig. 4 *b*) the extreme slip-lines $CBAR'$, $C'B'AR$ pass, not through the centre of the face, but through the corners. If the present argument be correct, plastic flow has not spread so far before indentation begins; the velocity is, in fact, indeterminate in the configuration of Fig. 4 *b*. Prandtl arbitrarily assumed the region RAR' to move downwards as a rigid body attached to the punch. The indentation pressure corresponding to this slip-line field is, however, still $2k(1+\frac{1}{2}\pi)$. These objections to Prandtl's solution have not been noted by other

writers. It should be mentioned that it may be difficult to distinguish in an experiment the moment corresponding to the present solution, not only because of the influence of elastic strains, but also because the numerical work of Southwell and Allen for shallow notches shows that the plastic region develops very rapidly at this stage.

Prandtl also considered the problem when yielding depends on hydrostatic pressure, and took an arbitrary yield envelope in accordance with Mohr's suggestion. His solution for this case is open to a further objection. Following Mohr's formulation of his yield criterion (**9**), Prandtl assumed that, after yielding, the deformation consisted of simple shears in the direction of the so-called surfaces of sliding. These correspond to the points of contact of a Mohr circle with the envelope and are, as has been mentioned, the characteristic directions for the stress equations. In view of Mohr's formulation it was natural for Prandtl to take the plastic boundary and the streamlines to be surfaces of sliding. However, for an isotropic material the principal axes of stress and strain-rate must coincide (elastic strains being neglected). This condition is sufficient to determine the velocity solution for an incompressible material in plane strain, once the stress distribution is known. Mohr's deformation hypothesis cannot thus be universally valid. In the present problem the plastic region when indentation begins must, as before, have spread sufficiently far to include the two slip-lines from the face centre to the free surfaces, since the slip-lines are still the characteristics of the velocity equations. The region where plastic deformation is taking place is bounded by these two slip-lines and not, as Prandtl assumed, by the stress characteristics. The fortunate situation whereby the indentation pressure can be surmised without a full solution no longer exists. The part of the plastic region uniquely defined by the free surface does not, necessarily, now extend over the entire face of the punch. The indentation pressure cannot then be found without a calculation of the stress distribution in the plastic and elastic regions. For this reason also, Prandtl's solution for a general material cannot be correct. It has been applied primarily in soil mechanics, where the ubiquitous surface of sliding is substituted for a general law of deformation.

4. Conclusions

A main aim of the present paper has been to clarify the approach to plane strain problems in plasticity, and to formulate the assumptions explicitly. Not only the first writers on the subject, but also the most recent writers (e.g. Sokolovsky, **13**, and van Iterson, **6**) have suggested slip-line fields for various problems quite arbitrarily and with no adequate

discussion of their plausibility. In some cases elementary considerations suffice to prove them wrong, but in others only detailed numerical calculations can decide. In many problems, it is true, the slip-line field in the region of plastically deforming material may be surmised without a full solution for the stresses in both elastic and plastic regions. This is particularly so in steady-state problems,† even more than in non-steady-state problems such as the one considered here. In a steady-state problem it has only to be assumed that the rigid material outside the region of plastically deforming material is capable of supporting the applied stresses on its perimeter, corresponding to the proposed slip-line field (which must of course be compatible with the velocity boundary conditions). General considerations may suffice to show whether the assumption is likely to be correct. In a non-steady-state problem it has to be supposed that the proposed slip-line field is actually developed during the prior loading; this automatically includes the assumption that the still-rigid material can sustain the calculated forces on its perimeter at the moment under consideration. The difference in degree of the assumptions corresponds, in fact, to the extra independent variable characterizing non-steady-state problems: that of time, or progress of the deformation.

It is easy to suggest apparently plausible slip-line fields for a notched bar under a bending couple, or for a tensile specimen with a deep rectangular notch, or even for shallow notches of arbitrary shape, but the assumption that such fields will actually be developed is too risky. This is particularly so when, as the work of Southwell and Allen shows in the case of a shallow wedge-shaped notch, the actual plastic region develops in a direction which could hardly have been surmised in advance. For many problems, then, detailed numerical calculations constitute the only safe basis. The successful application of relaxation methods to the simpler types of boundary-value problems is a valuable beginning.

Acknowledgement

The slip-line field for a circular notch was first described in a report by the present writer for the Armament Research Department in 1946. I wish to express by thanks to the Chief Scientific Officer, Ministry of Supply, for permission to publish the material in the report.

† See, for example, the discussion by the present writer of the problems of extrusion (**4**) and drawing (**5**).

REFERENCES

1. H. Pollaczek-Geiringer, *International Congress for Applied Mechanics*, 2 (1930), 185.
2. H. Hencky, *Zeits. f. ang. Math. u. Mech.* **3** (1923), 241.
3. R. Hill, *Quart. J. Mech. and Applied Math.* **1** (1948), 18.
4. ——, *Journal of the Iron and Steel Institute*, **158** (1948), 177.
5. R. Hill and S. J. Tupper, ibid. **159** (1948), 353.
6. F. K. Th. van Iterson, *Plasticity in Engineering* (Blackie, 1947).
7. J. Mandel, *Équilibres par tranches planes des solides* (Louis-Jean, Paris, 1942).
8. ——, *International Congress for Applied Mechanics*, Paris, 1946.
9. O. Mohr, *Zeits. f. d. Ver. deutsch. Ing.* **44** (1900).
10. E. Orowan, *Institute of Engineers and Ship-builders in Scotland*, 1945.
11. ——, J. F. Nye, and W. J. Cairns. (To be published.)
12. L. Prandtl, *Nachr. Ges. Wiss. Göttingen*, 1920, 74.
13. W. W. Sokolovsky, *Theory of Plasticity* (Moscow, 1946).
14. R. V. Southwell and N. G. Allen. (To be published.)

THE DISTRIBUTION OF STRESS IN THE NEIGHBOURHOOD OF A CRACK

By T. J. WILLMORE

(*Department of Mathematics, Durham Colleges, University of Durham*)

[Received 31 March 1948]

SUMMARY

In this paper we determine by complex variable methods the distribution of stress in the neighbourhood of a two-dimensional Griffith crack when the pressure varies along the crack. The analysis is extended to deal with problems involving cracks in aeolotropic materials possessing two directions of elastic symmetry. The paper concludes with an investigation of the stress distribution in the neighbourhood of two collinear cracks of equal length, and formulae are found giving the shape of the cracks and the critical tensile stress normal to the cracks which will produce rupture. It is shown that the influence of one crack on the other is very small provided that the distance between the cracks exceeds the length of each crack.

The methods of this paper can also be used to solve the problem of the indentation of the plane boundary of an isotropic or aeolotropic material by a single punch of any shape, or by a flat-ended double punch.

1. THE theory of cracks in a two-dimensional elastic material was first developed by Griffith (**1**). Recently Sneddon (**2**) gave an alternative treatment of a crack opened by a *uniform* internal pressure, by using Westergaard's complex stress function (**3**). In a recent paper (**4**) Sneddon and Elliot show how to solve the problem when the pressure varies along the crack, by an elegant but rather complicated method involving the solution of a pair of dual integral equations, and the authors state that the complex stress function corresponding to a variable internal pressure is apparently unknown.

In the first part of this paper we give a simpler solution by complex variable methods and obtain stress functions corresponding to a variable distribution of pressure. In the second part we show how the analysis may be extended to deal with problems involving cracks in aeolotropic materials possessing two directions of elastic symmetry. In the last part we investigate the stress distribution in the neighbourhood of two collinear cracks of equal length, the case of an infinite number of cracks having been solved by Westergaard (**3**). Formulae are found giving the shape of the cracks and the critical tensile stress normal to the cracks which will produce rupture. It is shown that the influence of one crack on the other is very small, provided that the distance between the cracks exceeds the length of each crack. The theory is illustrated by drawing curves of

maximum shearing stress in the neighbourhood of the cracks when they are separated by a distance equal to two-ninths of the length of each crack. It is shown that the presence of one crack considerably increases the stresses near the other only in the immediate vicinity of the ends of the crack.

2. In this section we consider the effect of a single plane crack in an isotropic material which is in a state of plane strain. The crack may be represented by a cut from $z = c$ to $z = -c$, where c is real. The transformation

$$z = c\cos\zeta \quad (\zeta = \xi + i\eta) \tag{1}$$

transforms the region outside the cut into the semi-infinite strip $\eta > 0$, $0 \geqslant \xi \geqslant -2\pi$ in the ζ-plane, the line $\eta = 0$ corresponding to the boundary of the cut and $\eta \to \infty$ corresponding to the point at infinity in the z-plane. The transformation inverse to (1) is

$$e^{i\zeta} = \{z - (z^2 - c^2)^{\frac{1}{2}}\}/c, \tag{2}$$

where the sign of the square root is suitably chosen.

When an isotropic solid is in a state of plane strain the distribution of stress has been represented in compact form with the help of complex variable analysis by Muschelisvili (**5**) and others. Among the possible equivalent representations, for the present paper we write the displacement and stresses as the real parts of

$$\left.\begin{aligned} 2\mu u &= (3-4\sigma)g(z) - f'(z) - \bar{z}g'(z), \\ 2\mu v &= -i(3-4\sigma)g(z) - i\{f'(z) + \bar{z}g'(z)\}, \\ \widehat{xx} &= -f''(z) - \bar{z}g''(z) + 2g'(z), \\ \widehat{yy} &= f''(z) + \bar{z}g''(z) + 2g'(z), \\ \widehat{xy} &= -if''(z) - i\bar{z}g''(z), \end{aligned}\right\} \tag{3}$$

where σ is Poisson's ratio, μ is the modulus of rigidity, and f and g are chosen to give single-valued stresses and displacements which vanish at infinity. The corresponding formulae in generalized plane stress are found by replacing σ by $\sigma/(1+\sigma)$, keeping μ unaltered.

The integrated effect of the stress components $(\widehat{\eta x}, \widehat{\eta y})$ round part of a curve $\eta =$ constant which surrounds the crack is given by the change in value of

$$\int_0^s (\widehat{\eta y} + i\widehat{\eta x})\,ds = -[f'(z) + \bar{z}g'(z) + \bar{g}(\bar{z})] = -\int (\widehat{\eta\eta} + i\widehat{\xi\eta})\,d\bar{z}, \tag{4}$$

as z traces out the curve. In particular, this relation holds on the crack $\eta = 0$.

We shall consider the case when there is no shearing force along the

crack, i.e. $\widehat{\xi\eta} = 0$ when z is real, but the analysis may easily be extended to apply when shearing force is present. We shall also restrict our attention to those distributions of pressure which form a self-equilibrating system. These conditions can be satisfied by taking

$$f'(z) = g(z) - zg'(z). \tag{5}$$

The stresses and displacements are then given by the real parts of

$$\left.\begin{aligned} 2\mu u &= (2-4\sigma)g(z)+(z-\bar{z})g'(z), \\ 2\mu v &= -4i(1-\sigma)g(z)+i(z-\bar{z})g'(z), \\ \widehat{xx} &= 2g'(z)+(z-\bar{z})g''(z), \\ \widehat{yy} &= 2g'(z)-(z-\bar{z})g''(z), \\ \widehat{xy} &= i(z-\bar{z})g''(z). \end{aligned}\right\} \tag{6}$$

The maximum shearing stress τ may be found from the relation

$$\tau = \tfrac{1}{2}|\widehat{xx}-\widehat{yy}+2i\widehat{xy}|, \tag{7}$$

and, on using (6), this becomes

$$\tau^2 = 4y^2 g''(z).\bar{g}''(\bar{z}). \tag{8}$$

On the crack when $\eta = 0$, equation (4) reduces to

$$g(z)+\bar{g}(z) = -c\int \widehat{\eta\eta}\sin\zeta\, d\zeta. \tag{9}$$

From equation (9) we find suitable complex stress functions giving single-valued stresses and displacements which vanish at infinity. Corresponding to a uniform distribution of pressure $\widehat{\eta\eta} = -p_0$, we obtain

$$g(z) = -\tfrac{1}{2}p_0\{z-(z^2-c^2)^{\frac{1}{2}}\}, \tag{10}$$

which agrees with Westergaard's solution used by Sneddon. With $\widehat{\eta\eta} = -p_1\cos\zeta$ the corresponding solution is

$$g(z) = -\frac{p_1}{8c}\{z-(z^2-c^2)^{\frac{1}{2}}\}^2, \tag{11}$$

and with $\widehat{\eta\eta} = -p_n\cos n\zeta$ $(n \geqslant 2)$ the solution is

$$g(z) = \frac{cp_n}{4}\left[\frac{1}{n-1}\left\{\frac{z-(z^2-c^2)^{\frac{1}{2}}}{c}\right\}^{n-1} - \frac{1}{n+1}\left\{\frac{z-(z^2-c^2)^{\frac{1}{2}}}{c}\right\}^{n+1}\right]. \tag{12}$$

When $\widehat{\eta\eta} = -q_n\sin n\zeta$ $(n \geqslant 2)$ the stress function is

$$g(z) = -\frac{icq_n}{4}\left[\frac{1}{n-1}\left\{\frac{z-(z^2-c^2)^{\frac{1}{2}}}{c}\right\}^{n-1} - \frac{1}{n+1}\left\{\frac{z-(z^2-c^2)^{\frac{1}{2}}}{c}\right\}^{n+1}\right]. \tag{13}$$

The value $\widehat{\eta\eta} = -q_1\sin\zeta$ is not considered as the corresponding stress system is not self-equilibrating. By superposition of the solutions (10)–(13), we obtain the resulting displacement and stresses associated with

a general variable distribution of normal pressure along the length of the crack. The energy of the crack and the criterion for rupture may be calculated as in Sneddon's paper (**2**).

3. Generalized plane stress problems in aeolotropic materials with two directions of elastic symmetry have been considered by Green and others. We shall use the notation of one of Green's papers (**6**), suitably modified for application to problems involving plane strain; and we shall consider only the case when the crack is parallel to one of the directions of symmetry.

The crack is represented by a cut from $z = c$ to $z = -c$, where c is real. Then if $z_1 = x+i\lambda_1 y$, $z_2 = x+i\lambda_2 y$, the displacements and stresses corresponding to plane strain are given by the real parts of

$$\left.\begin{aligned} u &= -(a\lambda_1^2+b)f'(z_1)-(a\lambda_2^2+b)g'(z_2), \\ v &= -i(b\lambda_1+d\lambda_1^{-1})f'(z_1)-i(b\lambda_2+d\lambda_2^{-1})g'(z_2), \\ \widehat{xx} &= -\lambda_1^2 f''(z_1)-\lambda_2^2 g''(z_2), \\ \widehat{yy} &= f''(z_1)+g''(z_2), \\ \widehat{xy} &= -i\lambda_1 f''(z_1)-i\lambda_2 g''(z_2), \end{aligned}\right\} \tag{14}$$

where f and g are chosen to give single-valued displacements and stresses which vanish at infinity. The constants a, b, d, λ_1, λ_2 are related to the elastic constants s_{ij} by the equations

$$\left.\begin{aligned} a &= \frac{s_{11}s_{33}-s_{13}^2}{s_{33}}, & \lambda_1^2\lambda_2^2 &= \frac{s_{22}s_{33}-s_{23}^2}{s_{11}s_{33}-s_{13}^2}, \\ b &= \frac{s_{13}s_{23}-s_{12}s_{33}}{s_{33}}, & \frac{1}{\lambda_1^2}+\frac{1}{\lambda_2^2} &= \frac{s_{33}s_{66}-2s_{13}s_{23}+2s_{12}s_{33}}{s_{22}s_{33}-s_{23}^2}. \\ d &= \frac{s_{22}s_{33}-s_{23}^2}{s_{33}}, \end{aligned}\right\} \tag{15}$$

For generalized plane stress the corresponding results may be obtained from Green's paper (**6**).

We shall restrict ourselves to the case when there is no shearing force along the crack, and the applied forces are self-equilibrating. These conditions can then be satisfied by taking

$$\lambda_1 f(z)+\lambda_2 g(z) = 0. \tag{16}$$

The displacements and stresses then become the real parts of

$$\left.\begin{aligned} u &= -(a\lambda_1^2+b)f'(z_1)+(a\lambda_2^2+b)\lambda_1\lambda_2^{-1}f'(z_2), \\ v &= -i(b\lambda_1+d\lambda_1^{-1})f'(z_1)+i(b\lambda_2+d\lambda_2^{-1})\lambda_1\lambda_2^{-1}f'(z_2), \\ \widehat{xx} &= -\lambda_1^2 f''(z_1)+\lambda_1\lambda_2 f''(z_2), \\ \widehat{yy} &= f''(z_1)-\lambda_1\lambda_2^{-1}f''(z_2), \\ \widehat{xy} &= -i\lambda_1 f''(z_1)+i\lambda_1 f''(z_2). \end{aligned}\right\} \tag{17}$$

Suitable forms for the function $f(z)$ may be deduced from the corresponding stress functions for isotropic material. In the case when the normal pressure along the crack is uniform, the appropriate stress function is given by

$$f'(z) = \frac{p\lambda_2}{\lambda_2-\lambda_1}\{z-(z^2-c^2)^{\frac{1}{2}}\}. \tag{18}$$

The displacements and stresses are then obtained from equation (17). In particular, the displacement at points on the crack is given by

$$v = pd\left(\frac{\lambda_1+\lambda_2}{\lambda_1\lambda_2}\right)(c^2-x^2)^{\frac{1}{2}}, \tag{19}$$

showing that, as in the isotropic case, the shape of the crack is elliptical. The potential energy of the crack may be shown to be

$$W = \tfrac{1}{2}\pi dp^2c^2\left(\frac{\lambda_1+\lambda_2}{\lambda_1\lambda_2}\right). \tag{20}$$

By using this expression and an argument similar to that of Sneddon (**2**), we can show that the crack will extend when the normal stress exceeds the critical value p_c, where

$$p_c = \sqrt{\left\{\frac{4T\lambda_1\lambda_2}{\pi cd(\lambda_1+\lambda_2)}\right\}}, \tag{21}$$

and T is the surface tension acting round the crack. Our formula (21) reduces to Sneddon's formula (2.3.4) when the material becomes isotropic.

4. In this section we find the distribution of stress in the neighbourhood of two equal collinear cracks in an isotropic material, when a uniform pressure acts normally along each crack and there is no shearing force. The complex stress function found in § 2 for a single crack under uniform pressure could also have been obtained by considering the following boundary problem for the half-plane $y \geqslant 0$. When z is real, we must satisfy

(a) $\widehat{yy} = -p \quad (|x| \leqslant c),$

$\quad v = 0 \quad (|x| \geqslant c),$

(b) $\widehat{xy} = 0$ for all x.

The stresses and displacements given by (6) satisfy condition (b); and condition (a) leads to

$$\text{Real part of } 2g'(z) = -p \quad (|x| \leqslant c),$$

$$\text{Real part of }\left\{-\frac{2i(1-\sigma)}{\mu}g(z)\right\} = 0 \quad (|x| \geqslant c).$$

But these conditions correspond to the hydrodynamical problem of the uniform motion of a flat plate of width $2c$ moving normal to its plane in

a fluid at rest at infinity, and the complex potential function which represents this motion is well known.

In the same way, the problem of two collinear cracks on the x-axis from $z = k$ to $z = 1$ and from $z = -k$ to $z = -1$, is equivalent to the hydrodynamical problem of the uniform normal motion of two equal collinear flat plates through a fluid at rest at infinity. The appropriate complex potential function is given in Durand (**7**); and we deduce that a suitable expression for $g'(z)$ is given by

$$g'(z) = \tfrac{1}{2}p\left[\frac{z^2-\lambda^2}{\sqrt{\{(z^2-1)(z^2-k^2)\}}}-1\right] \quad (k<1), \tag{22}$$

where $\lambda^2 = E'/K'$, and K', E' are respectively the complete elliptic integrals of the first and second kind associated with k', the modulus complementary to k. Our choice of coordinates for the ends of the cracks involves no real loss of generality.

From (22) it follows that a suitable form for $g(z)$ is

$$g(z) = \tfrac{1}{2}p\int\limits_1^z \frac{t^2-\lambda^2}{\{(t^2-1)(t^2-k^2)\}^{\frac{1}{2}}}\,dt-\tfrac{1}{2}pz. \tag{23}$$

The substitutions $z = \mathrm{dc}(\zeta, k)$, $t = \mathrm{dc}(u, k)$ transform (23) into

$$g(z) = \tfrac{1}{2}p\{\mathrm{sn}\,\zeta\,\mathrm{dc}\,\zeta+\zeta-E(\zeta)-\lambda^2\zeta-\mathrm{dc}\,\zeta\}, \tag{24}$$

where $$E(\zeta) = \int\limits_0^\zeta \mathrm{dn}^2\,u\,du,$$

and the elliptic functions are referred to modulus k. It is convenient to make the further substitution $\zeta = i\tau$, when equation (24) gives for points x on the crack,

$$g(x) = \tfrac{1}{2}ip\{E(\tau, k')-\lambda^2\tau+ix\}, \tag{25}$$

where $$x = \mathrm{dn}(\tau, k'). \tag{26}$$

It follows from (6) and (25) that displacements at points along the crack are given by the relation

$$v = \frac{(1-\sigma)p}{\mu}\{E(\tau, k')-\lambda^2\tau\}. \tag{27}$$

The elliptic function in (26) and the incomplete elliptic integral in (27) have been tabulated (**8**, **9**), so that the shape of the cracks can easily be obtained with little numerical computation. The energy of both cracks is given by the formula

$$L = \frac{2(1-\sigma)p^2}{\mu}\int\limits_0^{K'} \{E(\tau, k')-\lambda^2\tau\}k'^2\,\mathrm{sn}(\tau, k')\mathrm{cn}(\tau, k')\,d\tau,$$

which after some calculation becomes

$$L = \frac{\pi(1-\sigma)p^2}{\mu}\{1-\lambda^2-\tfrac{1}{2}k'^2\}. \tag{28}$$

As a useful check we may verify that as the distance between the cracks tends to zero, the above expression becomes identical with the energy of a single crack of length 2 units.

The theory of the Griffith crack considers the stress distribution when the crack is opened by the application of an average tension p to the surface of the body, and the surface of the crack is assumed free from stress. This condition may be obtained by superposing on the stress function (23) a second function giving a uniform tension perpendicular to the cracks. The presence of the two cracks then lowers the potential energy of the body by an amount L. But the cracks have a surface energy

$$U = 4(1-k)T, \tag{29}$$

where T is the surface tension of the material. Thus the resultant loss of potential energy due to the presence of the cracks is

$$L-U = \frac{\pi(1-\sigma)p^2}{\mu}\{1-\lambda^2-\tfrac{1}{2}k'^2\}-4(1-k)T.$$

The condition $(\partial/\partial k)(L-U) = 0$ holds when the two cracks are just on the point of extending inwards. This leads to the result that the material will rupture if the tension exceeds the critical value p_c, where

$$p_c = \left(\frac{K'k'k^{\frac{1}{2}}}{E'-K'k^2}\right)\sqrt{\left\{\frac{4T\mu}{\pi(1-\sigma)}\right\}}. \tag{30}$$

The corresponding critical value for a single crack of length $(1-k)$ is given by

$$p'_c = \frac{1}{\sqrt{(1-k)}}\sqrt{\left\{\frac{4T\mu}{\pi(1-\sigma)}\right\}}. \tag{31}$$

The value of the ratio p_c/p'_c is a measure of the amount by which the body is weakened by the presence of the second crack. The variation of this value with the ratio

$$r = \frac{\text{distance between cracks}}{\text{length of crack}}$$

is shown in Fig. 1, from which it can be seen that if the cracks are separated by a distance comparable with the length of each crack, then the effect of the second crack is very small.

The maximum shearing stress may be shown from equations (8) and

(22) to be given by the relation

$$\frac{\tau}{p} = \frac{(1+k^2-2\lambda^2)y(x^2+y^2)^{\frac{1}{2}}\{x^2+(y+\beta)^2\}^{\frac{1}{2}}\{x^2+(y-\beta)^2\}^{\frac{1}{2}}}{\{(x+1)^2+y^2\}^{\frac{3}{4}}\{(x-1)^2+y^2\}^{\frac{3}{4}}\{(x+k)^2+y^2\}^{\frac{3}{4}}\{(x-k)^2+y^2\}^{\frac{3}{4}}}, \tag{32}$$

where

$$\beta^2 = \frac{\lambda^2+k^2\lambda^2-2k^2}{1+k^2-2\lambda^2}. \tag{33}$$

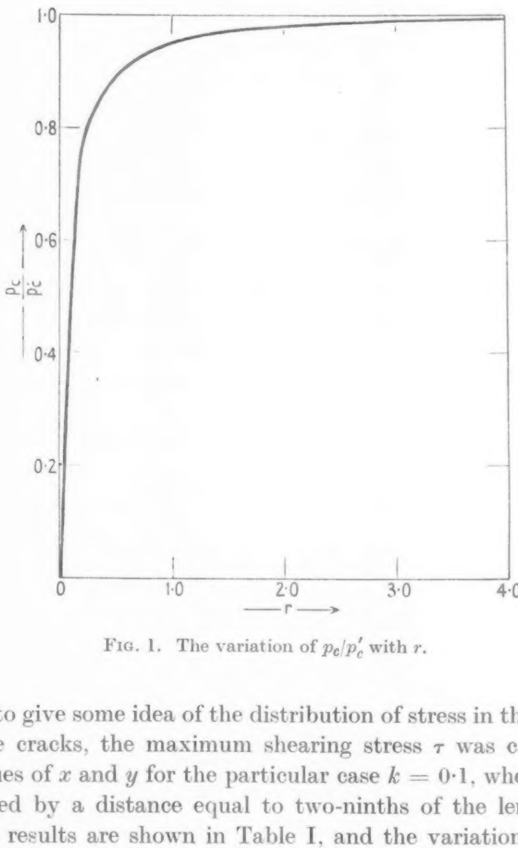

FIG. 1. The variation of p_c/p_c' with r.

In order to give some idea of the distribution of stress in the neighbourhood of the cracks, the maximum shearing stress τ was calculated for several values of x and y for the particular case $k = 0{\cdot}1$, when the cracks are separated by a distance equal to two-ninths of the length of each crack. The results are shown in Table I, and the variation of τ with x and y is shown graphically in Fig. 2, where on account of the symmetry of the problem only one-half of the configuration is shown. For purposes of comparison corresponding curves for a single crack are shown in Fig. 3, these being drawn from results given in Sneddon's paper (**2**). It can be seen that the presence of the second crack does increase appreciably the stresses near the ends of the crack, particularly the inner end, but the

TABLE I

Variation of τ/p with x and y.

y/c \ x/c	0·0	0·1	0·2	0·3	0·4	0·5	0·6	0·7	0·8
0·2	·469	1·134	·653	·351	·244	·205	·202	·231	·316
0·4	·859	·833	·664	·485	·383	·339	·335	·369	·445
0·6	·616	·596	·536	·463	·410	·384	·384	·407	·447
0·8	·410	·407	·398	·383	·371	·367	·373	·387	·403
1·2	·148	·161	·190	·222	·250	·270	·285	·296	·299

y/c \ x/c	0·9	1·0	1·1	1·2	1·3	1·4	1·6	1·8	2·0
0·2	·539	·852	·400	·173	·091	·055	·026	·014	·009
0·4	·558	·587	·420	·250	·152	·098	·048	·028	·018
0·6	·481	·461	·370	·262	·180	·125	·067	·040	·026
0·8	·406	·379	·320	·249	·187	·139	·074	·049	·033
1·2	·292	·272	·243	·208	·172	·140	·092	·062	·043

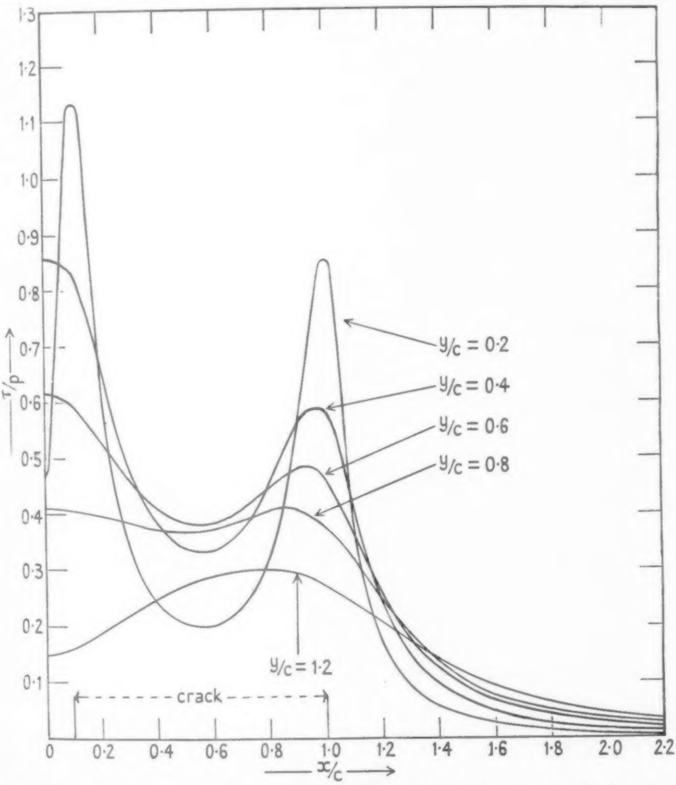

FIG. 2. The variation of the maximum shearing stress τ with x and y (double crack).

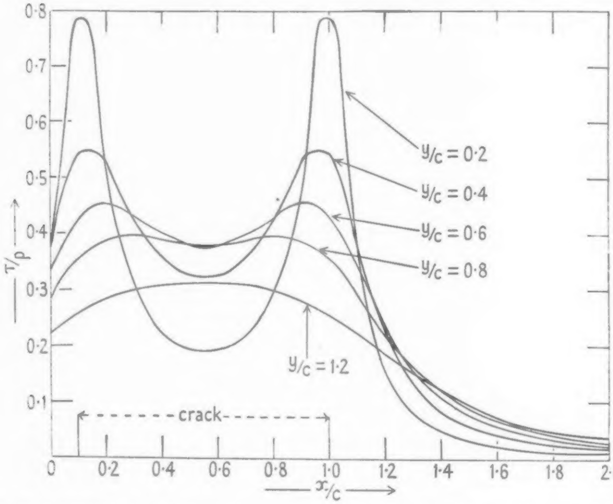

FIG. 3. The variation of the maximum shearing stress τ with x and y (single crack).

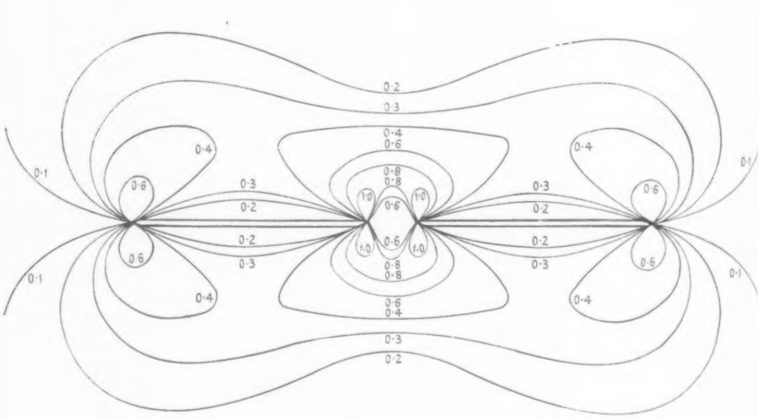

FIG. 4. The isochromatic lines in the vicinity of the double crack.

general character of the curves is preserved. A convenient method of showing the variation of τ consists of plotting the contours of equal maximum shearing stress, i.e. constructing the family of curves $\tau/p = \alpha$, where α is a parameter. These curves, which are the isochromatic lines of photo-elasticity, are shown in Fig. 4.

The shape of the crack is shown in Fig. 5 which also shows, for purposes

of comparison, the elliptical shape of a single crack of the same length under the same internal pressure. It can be seen that the presence of the second crack makes only a slight change in shape.

The analysis of this section could be extended by the methods of § 3

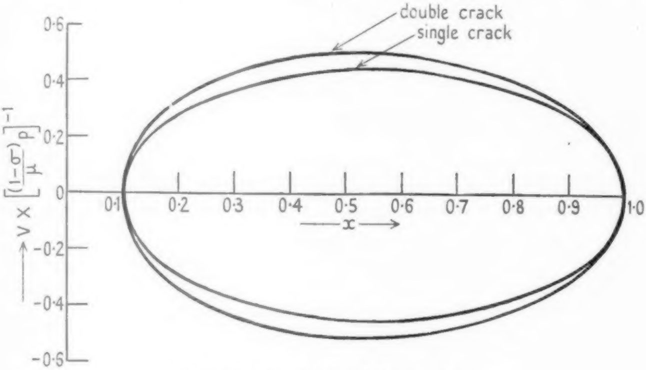

FIG. 5. The shape of the cracks.

to obtain the stress distribution near a double crack in an aeolotropic material with two directions of elastic symmetry. The methods of this paper could also be used to find the stress distribution due to the indentation of the plane boundary of an isotropic or aeolotropic material by a single punch of any shape, or by a flat-ended double punch.

I wish to thank Dr. A. E. Green for acquainting me with the problems of this paper, and for many helpful suggestions. I also thank my wife for preparing the diagrams.

REFERENCES

1. A. A. GRIFFITH, *Phil. Trans.* A, **221** (1920), 163.
2. I. N. SNEDDON, *Proc. Roy. Soc.* A, **187** (1946), 229.
3. H. M. WESTERGAARD, *J. Appl. Mech.* **6** (1939), A 49.
4. I. N. SNEDDON and H. A. ELLIOT, *Quart. of Appl. Math.* **4** (1946), 262.
5. MUSCHELISVILI, *Z. angew. Math. Mech.* **13** (1933), 264.
6. A. E. GREEN, *Proc. Cambridge Phil. Soc.* **41** (1945), 224.
7. DURAND, *Aerodynamic Theory* (J. Springer, 1935), vol. ii, p. 83.
8. L. M. MILNE-THOMSON, *Die elliptischen Funktionen von Jacobi* (J. Springer, 1931).
9. A. M. LEGENDRE, *Tables of Complete and Incomplete Elliptic Integrals* (Cambridge, 1934).

THE FORMATION OF CLOSED WAKES IN FLUID MOTIONS

By D. N. DE G. ALLEN (*Imperial College, London*)

[Received 7 January 1948]

SUMMARY

Southwell and Vaisey (**1**) (1946) have applied relaxation methods to obtain a variety of solutions to problems of two-dimensional (steady) motion in an inviscid fluid. These are concerned with the determination of 'free' streamlines, and include one type of solution which is believed to be new, in that examples have been found of a flow which exhibits a junction of two 'free' streamlines. At such a junction the wake boundary must be cuspidal, and a remark of Sir Geoffrey Taylor about the existence of such cusps has stimulated this investigation. It was undertaken with the aim of finding a solution of cuspidal type by 'orthodox' mathematical analysis, i.e. by an extension of the classical method (using conformal transformation) which was employed by Helmholtz, Kirchhoff, and Rayleigh.

1. THE method of determination of 'free' stream boundaries, in the two-dimensional steady motion of an inviscid fluid, by the use of conformal transformation is described by Lamb (**2**) (1932), who gives a number of illustrative examples. We write

$$z = x+iy, \qquad w = \phi+i\psi, \tag{1}$$

where ϕ is the velocity-potential and ψ the stream-function of the flow. Then

$$dw/dz = \partial\phi/\partial x - i\,.\,\partial\phi/\partial y = -u+iv,$$

u, v being the components of velocity at a point in the axial x-, y-directions. Let q denote the resultant velocity at a point and θ its inclination to the axis of x. Then

$$u = q\cos\theta, \qquad v = q\sin\theta,$$

and we have

$$-\frac{dz}{dw} = \frac{1}{u-iv} = \frac{1}{q}e^{i\theta} = \zeta, \text{ say;}$$

and

$$\log\zeta = \log(1/q)+i\theta. \tag{2}$$

Now $\log\zeta$ and w are both functions of the complex variable z. If then the complete boundary of the flow can be specified both in the planes of w and of $\log\zeta$, and if a relation can be found whereby the regions so bounded in these planes can be conformally transformed into each other, we shall have obtained an equation of the form

$$F(\log\zeta, w) = 0. \tag{3}$$

On a free streamline the real part of $\log\zeta$, i.e. $\log(1/q)$, has a known constant value, since the pressure is constant and therefore also the velocity, $q = a$,

say. Also on a free streamline the imaginary part of w, i.e. $i\psi$, has a known constant value, and the velocity-potential satisfies the relation

$$\partial\phi/\partial s = -a, \tag{4}$$

where s is arc-length measured along the free streamline. Integration of (4) along a free stream boundary, with a suitably chosen origin for s, gives

$$\phi = -as. \tag{5}$$

Thus (3) reduces along a free streamline to a relation between θ and s; it is the intrinsic equation to that boundary, which is therefore at once defined.

The appropriate form of equation (3) is found by introducing an intermediate function t between $\log\zeta$ and w; the corresponding regions in the planes of $\log\zeta$ and w are in turn transformed into a half-plane in the plane of t, by relations of the form

$$f(\log\zeta, t) = 0, \qquad g(w, t) = 0, \tag{6}$$

and t can then be eliminated between the equations (6) to obtain (3). Or, sufficiently, we may regard (6) as giving the transformation between $\log\zeta$ and w in parametric form.

2. It is convenient to take units of length and time so that the value of the velocity along a free boundary 'open' to the atmosphere is 1. Along the boundary of a 'closed' wake, of the type described by Southwell and Vaisey (**1**), the velocity q has some other constant value, a, less than 1, and $q = 0$ at a stagnation point. In examples previously treated by this method, by Helmholtz (**3**) (1868), Kirchhoff (**4**) (1869), and Rayleigh (**5**) (1876), all free streamlines are 'open' to the atmosphere, and so a single constant value can be given to q along all parts of the stream boundary which are free. In the example treated here the boundary of the stream comprises both an 'open' and a 'closed' free streamline, so that different constant values must be given to q along different parts of the stream boundary which are free.

3. Complete specification of the fluid boundary, both in the planes of $\log\zeta$ and of w, is possible when every part of the bounding streamlines is either free or fixed and straight; a fixed but curved boundary introduces complications. In the plane of $\log\zeta$ a fixed and straight boundary (since θ is then constant) becomes a line parallel to the real axis, whilst a free boundary (since $\log(1/q)$ is then constant) becomes a line parallel to the imaginary axis. In the plane of w, the stream-function ψ is constant along each bounding streamline, which therefore becomes a line parallel to the real axis.

4. The example to which we apply this method of solution is illustrated in Fig. 1. The axes Ox and Oy represent two fixed straight boundaries; fluid flows in a stream of finite breadth from the direction I far upstream and in contact with the fixed boundary Oy. The direction of flow is turned

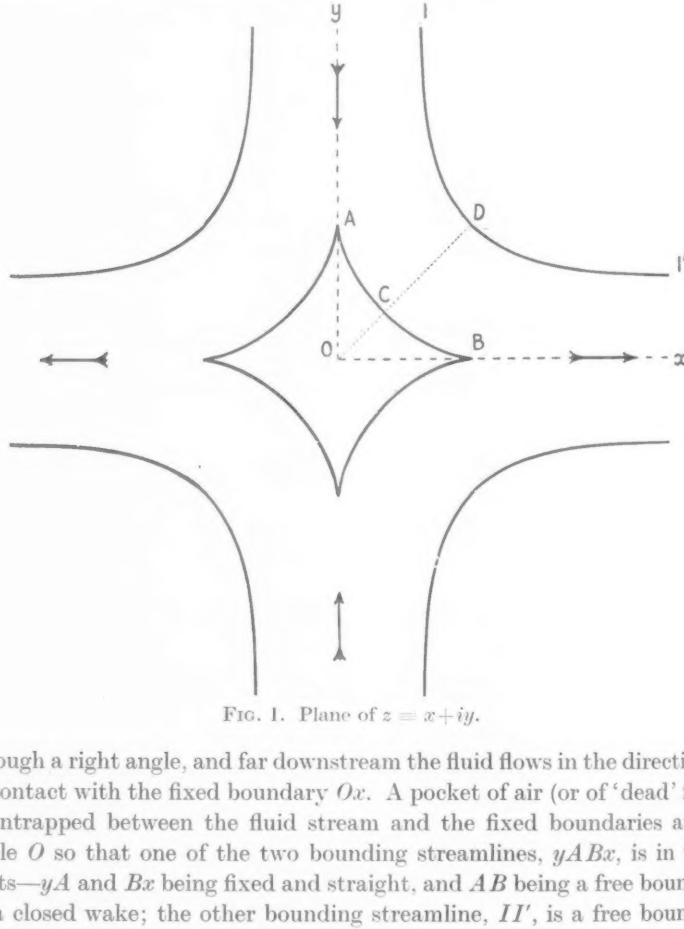

FIG. 1. Plane of $z = x+iy$.

through a right angle, and far downstream the fluid flows in the direction I' in contact with the fixed boundary Ox. A pocket of air (or of 'dead' fluid) is entrapped between the fluid stream and the fixed boundaries at the angle O so that one of the two bounding streamlines, $yABx$, is in three parts—yA and Bx being fixed and straight, and AB being a free boundary of a closed wake; the other bounding streamline, II', is a free boundary open to the atmosphere. Far upstream towards I and far downstream towards I' the uniform velocity of flow is given by $q = 1$ which is also the velocity at all points of II'. On the closed boundary AB, the constant velocity is given by $q = a < 1$. We take d to denote the uniform width of the flow both far up- and downstream, so that if the stream-function ψ is given the value 0 along II', then along $yABx$ we have $\psi = d$.

5. The boundary of the region of the flow in the plane of $\log \zeta$ is shown in Fig. 2; the fixed and straight boundaries IA and BI' become parts of the lines $\theta = -\pi/2$ and $\theta = 0$, while the free boundaries AB and II' become parts of the lines $\log(1/q) = \log(1/a)$ and $\log(1/q) = 0$. The first

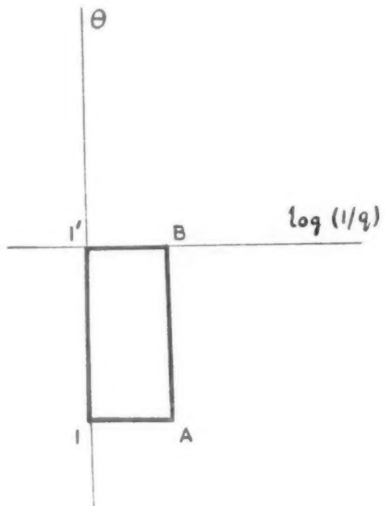

FIG. 2. Plane of $\log \zeta = \log(1/q) + i\theta$.

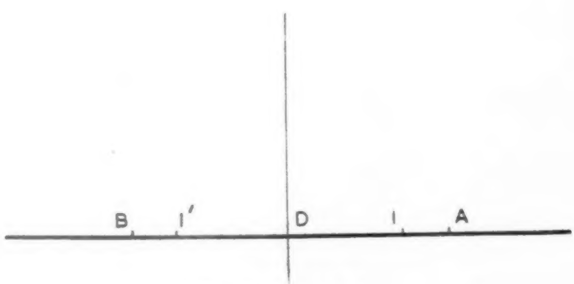

FIG. 3. Plane of t.

conformal transformation to be found is that which transforms the rectangular region $IABI'$ in the plane of $\log \zeta$ into the half-plane above the real axis in the plane of the intermediate variable t (Fig. 3). The rectangular boundary in the plane of $\log \zeta$ is transformed into the real axis in the plane of t. The values $t = -1$ and $t = +1$ may be assigned to the points I' and I respectively, and then $t = \mp(1/k)$ at B and A, where k has a

value (<1) dependent on that of a. The transformation of the rectangle into the half-plane is given by the Schwarz-Christoffel formula in the form

$$\log\zeta = \alpha \int_0^t \frac{dt}{\sqrt{\{(1-t^2)(1-k^2t^2)\}}} + \beta. \tag{7}$$

The constants α and β are determined by the conditions that, at I, $\log\zeta = -i\pi/2$ when $t = 1$, and, at I', $\log\zeta = 0$ when $t = -1$; therefore, from (7),

$$\left.\begin{aligned} -i\pi/2 &= \alpha K+\beta \\ \text{and} \qquad 0 &= -\alpha K+\beta \end{aligned}\right\}, \tag{8}$$

where
$$K = \int_0^1 \frac{dt}{\sqrt{\{(1-t^2)(1-k^2t^2)\}}}. \tag{9}$$

$4K$ is the real period of Jacobi's elliptic function $\operatorname{sn}(u, k)$ and the imaginary period of this function is $2iK'$, where

$$K' = \int_1^{1/k} \frac{dt}{\sqrt{\{(t^2-1)(1-k^2t^2)\}}}. \tag{10}$$

Solving equations (8) for α and β and substituting in equation (7) we find that

$$\frac{4Ki}{\pi}\log\zeta = K + \int_0^t \frac{dt}{\sqrt{\{(1-t^2)(1-k^2t^2)\}}}$$

or
$$t = \operatorname{sn}\left(\frac{4Ki}{\pi}\log\zeta - K\right). \tag{11}$$

6. The second conformal transformation to be found is that which transforms the plane of t into the plane of w. The region of flow in the plane of w becomes an infinite strip between the lines $\psi = 0$ and $\psi = d$ and is shown in Fig. 4. The velocity-potential is conveniently given the value 0 on the line of symmetry CD and hence, using equation (5), we see that the origins from which the arc-distances s are measured along the two free streamlines are the points C and D (Fig. 1). The infinite strip is a rectangle with two vertices at I and two vertices at I' so that the transformation between w and t is again given by the Schwarz-Christoffel formula:

$$\begin{aligned} w &= 2\gamma \int \frac{dt}{(1-t)(1+t)} + \delta \\ &= \gamma \log\left(\frac{1+t}{1-t}\right) + \delta. \end{aligned} \tag{12}$$

The constants γ and δ are determined by the conditions that at C, $w = id$ when $t = \infty$, and at D, $w = 0$ when $t = 0$; therefore, from (12)

$$id = i\pi\gamma+\delta,$$

and

$$0 = \delta,$$

so that equation (12) becomes

$$w = (d/\pi)\log\left(\frac{1+t}{1-t}\right). \tag{13}$$

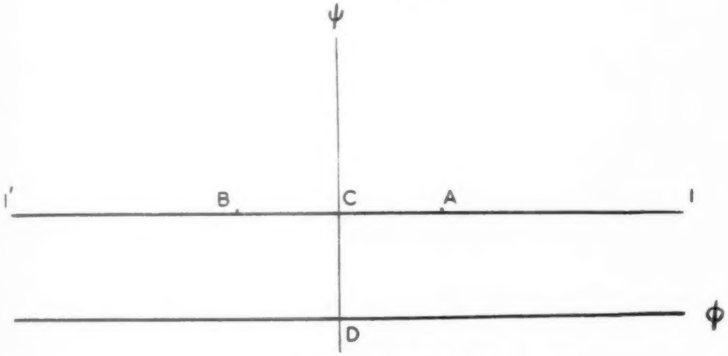

FIG. 4. Plane of $w = \phi+i\psi$.

7. The complete transformation between $\log\zeta$ and w is given by the equations (11) and (13) taken in conjunction. To find the equation of the closed free boundary AB we substitute in these equations the conditions

$$\left.\begin{aligned} \log\zeta &= \log(1/a)+i\theta \\ \text{and}\qquad w &= -as+id \end{aligned}\right\} \tag{14}$$

obtained from equation (5) and § 4. Thus, along AB,

$$t = \operatorname{sn}\left(-K+\frac{4Ki}{\pi}\log\frac{1}{a}-\frac{4K\theta}{\pi}\right) \tag{15}$$

and

$$s = \frac{d}{\pi a}\log\left(\frac{1-t}{1+t}\right)+\frac{id}{a}. \tag{16}$$

But it is known (Fig. 3) that t is real along AB, and, therefore, in (15) it follows that

$$\frac{4K}{\pi}\log\frac{1}{a} = K', \tag{17}$$

whence (15) becomes

$$\begin{aligned} t &= \operatorname{sn}(-K+iK'-4K\theta/\pi) \\ &= -\operatorname{sn}(K+iK'+4K\theta/\pi) \\ &= -\frac{1}{k}\frac{\operatorname{dn}(4K\theta/\pi)}{\operatorname{cn}(4K\theta/\pi)}. \end{aligned} \tag{18}$$

Equations (16) and (18) form the intrinsic equation to the closed boundary AB in parametric form; elimination of t and differentiation yields

$$\frac{ds}{d\theta} = -\frac{8Kdk}{\pi^2 a}\,\mathrm{sn}\left(\frac{4K\theta}{\pi}\right). \tag{19}$$

8. In a similar way the equations which hold on the open boundary II' may be found. There we have

$$\left.\begin{aligned} \log\zeta &= i\theta \\ \text{and} \qquad w &= -s \end{aligned}\right\} \tag{20}$$

in place of (14), so that

$$t = -\mathrm{sn}(K+4K\theta/\pi) \tag{21}$$

and

$$s = \frac{d}{\pi}\log\left(\frac{1-t}{1+t}\right), \tag{22}$$

replace (18) and (16) and

$$\frac{ds}{d\theta} = -\frac{8dK}{\pi^2}\,\frac{1}{\mathrm{sn}(4K\theta/\pi)} \tag{23}$$

replaces (19).

9. The boundaries of the flow (in the plane of z) have been computed for two particular values of a. The first case is that in which $a = 0$ and the closed boundary AB reduces to a stagnation point at O (Fig. 1). We have then that

$$k = 0, \qquad K = \pi/2, \qquad K' = \infty, \tag{24}$$

and the equation (23) to the open boundary II' becomes

$$ds/d\theta = -(4d/\pi)\mathrm{cosec}\,2\theta;$$

therefore

$$dx/d\theta = -(2d/\pi)\mathrm{cosec}\,\theta$$

and

$$dy/d\theta = -(2d/\pi)\sec\theta,$$

and, on integration,

$$\left.\begin{aligned} x &= d-(2d/\pi)\log\tan(-\theta/2) \\ y &= d-(2d/\pi)\log\tan(\theta/2+\pi/4) \end{aligned}\right\}. \tag{25}$$

Fig. 5 shows the shape of the boundaries in this flow of a fluid stream round a right-angled corner. The result presumably is not new, but no previous reference has been found.

10. The second computed example is one in which a has a typical non-zero value. To lighten the arithmetic k is assigned the value $1/\sqrt{2}$ so that

$$\left.\begin{aligned} a &= 0{\cdot}45593 \\ K = K' &= 1{\cdot}85407 \end{aligned}\right\}. \tag{26}$$

Along AB we have, from (19),

$$\left.\begin{aligned} \frac{dx}{d\theta} &= -\frac{8Kdk}{\pi^2 a}\,\mathrm{sn}\left(\frac{4K\theta}{\pi}\right)\cos\theta \\ \text{and}\qquad \frac{dy}{d\theta} &= -\frac{8Kdk}{\pi^2 a}\,\mathrm{sn}\left(\frac{4K\theta}{\pi}\right)\sin\theta \end{aligned}\right\}, \tag{27}$$

and along II', from (23),

$$\left.\begin{aligned} \frac{dx}{d\theta} &= -\frac{8Kd}{\pi^2}\,\frac{\cos\theta}{\mathrm{sn}(4K\theta/\pi)} \\ \text{and}\qquad \frac{dy}{d\theta} &= -\frac{8Kd}{\pi^2}\,\frac{\sin\theta}{\mathrm{sn}(4K\theta/\pi)} \end{aligned}\right\}. \tag{28}$$

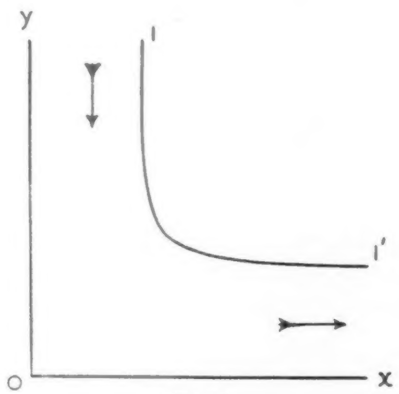

FIG. 5.

On the free boundaries values of x and y are found by numerical integration of (27) and (28). In Fig. 1 the flow is shown reflected in the axes Ox, Oy; in this way it becomes a flow, with no fixed boundaries, of two equal and opposite streams each of which, on meeting, bifurcate into parts which pair with one another, departing in opposite directions at right angles to the original direction, and including a four-cusped wake at the junction.

REFERENCES

1. R. V. SOUTHWELL and G. VAISEY, *Phil. Trans.* A, **240** (1946), 117.
2. H. LAMB, *Hydrodynamics*, 6th ed. (Cambridge, 1932).
3. H. v. HELMHOLTZ, *Berl. Monatsber.* 23 April, 1868; *Phil. Mag.* Nov. 1868.
4. G. KIRCHHOFF, *J. reine angew. Math.* **70** (1869), 289.
5. LORD RAYLEIGH, *Collected Papers*, **1** (1876), 287, 297.

RECURRENCE RELATIONS FOR CROSS-PRODUCTS OF BESSEL FUNCTIONS

By E. T. GOODWIN (*Mathematics Division, National Physical Laboratory*)

[Received 10 February 1948; revised 21 July 1948]

THE solutions of some electromagnetic problems contain cross-products of Bessel functions, frequently of complex argument. It is most convenient to compute these from the recurrence relations which they can be shown to satisfy and which are detailed in this note. The notation used is that of Watson's standard treatise.

If

$$\left.\begin{aligned} p_n &= J_n(x)Y_n(y)-J_n(y)Y_n(x) \\ q_n &= J_n(x)Y'_n(y)-J'_n(y)Y_n(x) \\ r_n &= J'_n(x)Y_n(y)-J_n(y)Y'_n(x) \\ s_n &= J'_n(x)Y'_n(y)-J'_n(y)Y'_n(x) \end{aligned}\right\}, \tag{1a}$$

where dashes denote derivatives; then

$$\left.\begin{aligned} p_{n+1}-p_{n-1} &= -\frac{2n}{x}q_n-\frac{2n}{y}r_n \\ q_{n+1}+r_n &= \frac{n}{x}p_n-\frac{n+1}{y}p_{n+1} \\ r_{n+1}+q_n &= \frac{n}{y}p_n-\frac{n+1}{x}p_{n+1} \\ s_n &= \tfrac{1}{2}p_{n+1}+\tfrac{1}{2}p_{n-1}-\frac{n^2}{xy}p_n \\ p_n s_n-q_n r_n &= \frac{4}{\pi^2 xy} \end{aligned}\right\}. \tag{1b}$$

The last relation is analogous to the Wronskian and affords a powerful check on the values of p, q, r, s as they are calculated.

Similarly, if

$$\left.\begin{aligned} f_n &= J_n(x)Y_n(y)-J_n(y)Y_n(x) \\ g_n &= J_n(x)Y_{n+1}(y)-J_{n+1}(y)Y_n(x) \\ h_n &= J_{n+1}(x)Y_n(y)-J_n(y)Y_{n+1}(x) \end{aligned}\right\}, \tag{2a}$$

then

$$\left.\begin{aligned} f_{n+1}-f_{n-1} &= -\frac{4n^2}{xy}f_n+\frac{2n}{x}g_n+\frac{2n}{y}h_n \\ g_{n+1}+h_n &= \frac{2(n+1)}{y}f_{n+1} \\ h_{n+1}+g_n &= \frac{2(n+1)}{x}f_{n+1} \\ f_n f_{n+1}-g_n h_n &= \frac{4}{\pi^2 xy} \end{aligned}\right\}. \tag{2b}$$

The first of these relations may be expressed in either of the simpler forms

$$f_{n+1}-f_{n-1} = \frac{2n}{x}g_n-\frac{2n}{y}g_{n-1} = \frac{2n}{y}h_n-\frac{2n}{x}h_{n-1}.$$

Similar relations for the functions I, K are as follows:

If

$$\left.\begin{aligned} p_n &= I_n(x)K_n(y)-I_n(y)K_n(x) \\ q_n &= I_n(x)K_n'(y)-I_n'(y)K_n(x) \\ r_n &= I_n'(x)K_n(y)-I_n(y)K_n'(x) \\ s_n &= I_n'(x)K_n'(y)-I_n'(y)K_n'(x) \end{aligned}\right\}, \tag{3a}$$

then

$$\left.\begin{aligned} p_{n+1}-p_{n-1} &= \frac{2n}{x}q_n+\frac{2n}{y}r_n \\ q_{n+1}+r_n &= \frac{n}{x}p_n-\frac{n+1}{y}p_{n+1} \\ r_{n+1}+q_n &= \frac{n}{y}p_n-\frac{n+1}{x}p_{n+1} \\ s_n &= -\tfrac{1}{2}p_{n+1}-\tfrac{1}{2}p_{n-1}-\frac{n^2}{xy}p_n \\ p_n s_n-q_n r_n &= \frac{1}{xy} \end{aligned}\right\}. \tag{3b}$$

In this case the cross-products g, h analogous to $(2a)$ which are of interest contain positive signs. Thus, if

$$\left.\begin{aligned} f_n &= I_n(x)K_n(y)-I_n(y)K_n(x) \\ g_n &= I_n(x)K_{n+1}(y)+I_{n+1}(y)K_n(x) \\ h_n &= I_{n+1}(x)K_n(y)+I_n(y)K_{n+1}(x) \end{aligned}\right\}, \tag{4a}$$

then

$$\left.\begin{aligned} f_{n+1}-f_{n-1} &= \frac{4n^2}{xy}f_n-\frac{2n}{x}g_n+\frac{2n}{y}h_n \\ g_{n+1}-h_n &= \frac{2(n+1)}{y}f_{n+1} \\ h_{n+1}-g_n &= -\frac{2(n+1)}{x}f_{n+1} \\ f_n f_{n+1}-g_n h_n &= -\frac{1}{xy} \end{aligned}\right\}. \tag{4b}$$

For the spherical Bessel functions, if j_n, y_n are defined by

$$j_n(x) = \sqrt{\left(\frac{\pi}{2x}\right)}J_{n+\frac{1}{2}}(x), \qquad y_n(x) = \sqrt{\left(\frac{\pi}{2x}\right)}Y_{n+\frac{1}{2}}(x),$$

and if

$$\left.\begin{aligned} p_n &= j_n(x)y_n(y)-j_n(y)y_n(x) \\ q_n &= j_n(x)y_n'(y)-j_n'(y)y_n(x) \\ r_n &= j_n'(x)y_n(y)-j_n(y)y_n'(x) \\ s_n &= j_n'(x)y_n'(y)-j_n'(y)y_n'(x) \end{aligned}\right\}, \tag{5a}$$

then

$$\left.\begin{aligned} p_{n+1}-p_{n-1} &= -(2n+1)\left(\frac{1}{x}q_n+\frac{1}{y}r_n+\frac{1}{xy}p_n\right) \\ q_{n+1}+r_n &= \frac{n}{x}p_n-\frac{n+2}{y}p_{n+1} \\ r_{n+1}+q_n &= \frac{n}{y}p_n-\frac{n+2}{x}p_{n+1} \\ s_n &= \frac{n+1}{2n+1}p_{n+1}+\frac{n}{2n+1}p_{n-1}-\frac{n(n+1)}{xy}p_n \\ p_n s_n-q_n r_n &= \frac{1}{x^2y^2} \end{aligned}\right\}. \tag{5b}$$

In scattering problems the cross-products arising naturally are not those of $j_n(x)$, $y_n(x)$ but those of $xj_n(x)$, $xy_n(x)$ and their derivatives. In this case, if

$$\left.\begin{aligned} p_n &= [xj_n(x)]\,[yy_n(y)]\;-[yj_n(y)]\,[xy_n(x)] \\ q_n &= [xj_n(x)]\,[yy_n(y)]'-[yj_n(y)]'[xy_n(x)] \\ r_n &= [xj_n(x)]'[yy_n(y)]\;-[yj_n(y)]\,[xy_n(x)]' \\ s_n &= [xj_n(x)]'[yy_n(y)]'-[yj_n(y)]'[xy_n(x)]' \end{aligned}\right\}, \tag{6a}$$

then

$$\left.\begin{aligned} p_{n+1}-p_{n-1} &= -(2n+1)\left(\frac{1}{x}q_n+\frac{1}{y}r_n-\frac{1}{xy}p_n\right) \\ q_{n+1}+r_n &= (n+1)\left(\frac{1}{x}p_n-\frac{1}{y}p_{n+1}\right) \\ r_{n+1}+q_n &= (n+1)\left(\frac{1}{y}p_n-\frac{1}{x}p_{n+1}\right) \\ s_n &= \frac{n}{2n+1}p_{n+1}+\frac{n+1}{2n+1}p_{n-1}-\frac{n(n+1)}{xy}p_n \\ p_n s_n-q_n r_n &= 1 \end{aligned}\right\}. \tag{6b}$$

Finally it may be noted that similar expressions can no doubt be produced for the cross-products of any functions which themselves satisfy similar recurrence relations.

The work described above has been carried out as part of the research programme of the National Physical Laboratory, and this paper is published by permission of the Director of the Laboratory.

SUPERSONIC FLOW PAST SLENDER POINTED BODIES†

By G. N. WARD

(*Department of Mathematics, The University, Manchester*)

[Received 6 January 1948]

SUMMARY

By assuming irrotational inviscid flow of a perfect gas moving past slender pointed bodies at supersonic speeds, the limiting values of the aerodynamic force coefficients as the thickness tends to zero are determined for bodies of general cross-section. The expression for the drag coefficient at zero incidence is the same as that for a body of revolution when expressed in terms of the cross-sectional area at any point. The lateral force coefficients and the extra drag coefficient at incidence depend only on the shape of the base section.

The general results are applied to the problem of a body of revolution carrying wings of small aspect ratio, and the interference between the body and the wings is determined; this leads to a particularly simple expression for the lift in terms of the lift of the wing alone and that of the body alone which, it is suggested, may apply approximately to any wing system on a body of revolution.

1. Introduction

THE isentropic flow of a perfect inviscid compressible fluid past slender pointed bodies of general cross-section at supersonic speeds will be treated by an approximate method based on the well-known linearized equation of motion. The body, either pointed at both ends or with a flat base, will be taken to be of unit length (no loss of generality is incurred, since if we wish to treat a body of length l, we have only to scale up all the lengths involved by a factor l) and of maximum thickness t. Since we are considering only slender bodies, t must be small compared with unity; the angle which any tangent plane to the body boundary makes with the undisturbed stream direction must be small and $O(t)$, and the rate of change of this angle along the direction of the body must also be small and $O(t)$. One further condition on the shape of the body is required in general: this concerns the radius of curvature of any section of the boundary of the body by a plane perpendicular to the stream direction. If d is the maximum diameter of the section, then the curvature must be $O(1/d)$ for all points where the section is convex outwards: there is no restriction at points where the section is concave outwards. This last condition is not always necessary for bodies at zero incidence, but is always required if we wish to calculate the flow at incidence within a known approximation. These conditions ensure that the extra velocity

† Abstract read to the Seventh International Congress of Applied Mechanics, London, 1948.

due to the disturbance caused in the uniform stream by the presence of the body is everywhere small compared with the velocity of the main stream.

Some interesting body shapes are excluded by the above curvature condition, and it may be relaxed under certain conditions, but in these cases the degree of approximation of the solutions becomes difficult to estimate. Examples of such bodies are treated near the end of the paper.

2. The solution of the equation of motion

Consider the isentropic flow of a perfect inviscid compressible fluid. We shall take Ox, Oy, Os to be rectangular Cartesian coordinate axes forming a right-handed system, the undisturbed stream at infinity to be parallel to the s-axis flowing in the direction of increasing s with velocity U, and c_1 to be the velocity of sound in the undisturbed stream. It may be shown that the general velocity components parallel to the coordinate axes are given by

$$u_x = U\frac{\partial\phi}{\partial x}, \qquad u_y = U\frac{\partial\phi}{\partial y}, \qquad u_s = U\left(1+\frac{\partial\phi}{\partial s}\right), \tag{1}$$

where the velocity potential ϕ satisfies the well-known equation of compressible flow

$$\frac{c^2}{U^2}\nabla^2\phi = \left(1+\frac{\partial\phi}{\partial s}\right)^2\frac{\partial^2\phi}{\partial s^2}+\left(\frac{\partial\phi}{\partial x}\right)^2\frac{\partial^2\phi}{\partial x^2}+\left(\frac{\partial\phi}{\partial y}\right)^2\frac{\partial^2\phi}{\partial y^2}+2\left(1+\frac{\partial\phi}{\partial s}\right)\frac{\partial\phi}{\partial x}\frac{\partial^2\phi}{\partial x\partial s}+$$
$$+2\left(1+\frac{\partial\phi}{\partial s}\right)\frac{\partial\phi}{\partial y}\frac{\partial^2\phi}{\partial y\partial s}+2\frac{\partial\phi}{\partial x}\frac{\partial\phi}{\partial y}\frac{\partial^2\phi}{\partial x\partial y}, \tag{2}$$

c being the local velocity of sound given by

$$c^2 = c_1^2-\frac{\gamma-1}{2}U^2\left[2\frac{\partial\phi}{\partial s}+\left(\frac{\partial\phi}{\partial s}\right)^2+\left(\frac{\partial\phi}{\partial x}\right)^2+\left(\frac{\partial\phi}{\partial y}\right)^2\right], \tag{3}$$

and ∇^2 being the Laplacian operator.

As a first approximation we assume that the disturbance velocity $U\nabla\phi$ is everywhere small compared with U, so that the squares and higher powers of the velocity components may be neglected. Equation (2) then becomes

$$\nabla^2\phi = M^2\frac{\partial^2\phi}{\partial s^2}, \tag{4}$$

$M = U/c_1$ being the stream Mach number. This is the linearized equation for the velocity potential. We shall be considering supersonic flow, so that $M > 1$, and we shall write $B^2 = M^2-1$.

By transforming (4) to cylindrical polar coordinates r, θ, s such that $x = r\cos\theta$, $y = r\sin\theta$, we obtain

$$\frac{\partial^2\phi}{\partial r^2}+\frac{1}{r}\frac{\partial\phi}{\partial r}+\frac{1}{r^2}\frac{\partial^2\phi}{\partial\theta^2} = B^2\frac{\partial^2\phi}{\partial s^2}. \tag{5}$$

Consider now a slender pointed body placed in the stream with its pointed nose at the origin. The disturbance caused by the body will be confined to the region behind the Mach cone $s = Br$ from the nose and so the disturbance velocities and the potential vanish for $s \leqslant 0$. Thus the Heaviside operational form of (5) for this problem is

$$\frac{\partial^2\phi}{\partial r^2}+\frac{1}{r}\frac{\partial\phi}{\partial r}+\frac{1}{r^2}\frac{\partial^2\phi}{\partial\theta^2} = B^2p^2\phi. \tag{6}$$

We require a solution of (6) representing waves travelling outwards and downstream from the body only: hence the general solution of (6) for flow past finite bodies in $s \geqslant 0$ is, assuming that the series obtained by integrating converges outside the body under consideration,

$$\phi = A_0 K_0(Bpr)+\sum_{n=1}^{\infty} A_n K_n(Bpr)\cos(n\theta+\beta_n), \tag{7}$$

where the A_n and β_n are arbitrary functions of p which must be chosen to satisfy the boundary conditions on the body; K_n are modified Bessel functions of the second kind, which for large r have the asymptotic value

$$K_n(Bpr) \sim \left(\frac{\pi}{2Bpr}\right)^{\frac{1}{2}} e^{-Bpr}, \tag{8}$$

showing that (7) represents waves travelling outwards from the axis, and along the surfaces $s-Br =$ constant at infinity.

Near the body, where r is a small quantity and $O(t)$, the dominant terms of (7) are included in

$$\phi_0 = -(\log \tfrac{1}{2}Bpr+\gamma)A_0+\tfrac{1}{2}\sum_{n=1}^{\infty}(n-1)!\left(\frac{2}{Bp}\right)^n A_n r^{-n}\cos(n\theta+\beta_n), \tag{9}$$

γ being Euler's constant here. The error is a factor $1+O(t)$.

If our slender body lies just inside a cylinder $r = R =$ constant, where R is $O(t)$, then it will become apparent later that the series obtained by interpreting (7) and (9) certainly converge for $r > R$, and ϕ_0 may be continued suitably outside the body for $r < R$ if they do not converge in this region.

By writing $z = x+iy = re^{i\theta}$, (9) may be expressed as the real part of

$$w = \phi_0+i\psi_0 = a_0\log z+b_0+\sum_{n=1}^{\infty} a_n z^{-n}, \tag{10}$$

where a_0, b_0, a_1,..., etc., are functions of s given by

$$a_0 = -A_0, \quad b_0 = -(\log\tfrac{1}{2}Bp+\gamma)A_0, \quad a_n = \tfrac{1}{2}e^{i\beta_n}(n-1)!\left(\frac{2}{Bp}\right)^n A_n \tag{11}$$

and ψ_0 is a real function of s, r, θ which is not a true stream function for the motion, but is denoted by ψ_0 because it has the properties of a stream function in a two-dimensional incompressible flow. Thus ϕ_0 is a harmonic function of r, θ approximately near the body, and the results of two-dimensional incompressible flow may be used to determine $w-b_0$ from the boundary conditions on the body, and hence b_0 from a_0, by means of the second equation of (11). The expansion for w given in (10) certainly converges for $|z| > R$ since there can be no singularities outside the body, but may have to be continued analytically for $|z| < R$. Usually, however, it is the analytic continuation of $w-b_0$ which is obtained from the boundary conditions, and a_0, a_1, etc., have to be obtained by expanding the function in the form (10).

In order to determine the accuracy of (10) or (9) as a solution of the equation of motion, it is advantageous to transform (2) and (3) to the independent variables z, $\bar{z}$, s, where $z = x+iy$, $\bar{z} = x-iy$. The equation of motion becomes

$$\frac{c^2}{U^2}\left(4\frac{\partial^2\phi}{\partial z\partial\bar{z}}+\frac{\partial^2\phi}{\partial s^2}\right) = \left(1+\frac{\partial\phi}{\partial s}\right)^2\frac{\partial^2\phi}{\partial s^2}+4\left(1+\frac{\partial\phi}{\partial s}\right)\frac{\partial}{\partial s}\left(\frac{\partial\phi}{\partial z}\frac{\partial\phi}{\partial\bar{z}}\right)+4\left(\frac{\partial\phi}{\partial z}\right)^2\frac{\partial^2\phi}{\partial\bar{z}^2}+$$
$$+4\left(\frac{\partial\phi}{\partial\bar{z}}\right)^2\frac{\partial^2\phi}{\partial z^2}+4\frac{\partial\phi}{\partial z}\frac{\partial\phi}{\partial\bar{z}}\frac{\partial^2\phi}{\partial z\partial\bar{z}}, \quad (12)$$

where
$$c^2 = c_1^2\left[1-\frac{\gamma-1}{2}M^2\left\{2\frac{\partial\phi}{\partial s}+\left(\frac{\partial\phi}{\partial s}\right)^2+4\frac{\partial\phi}{\partial z}\frac{\partial\phi}{\partial\bar{z}}\right\}\right]. \quad (13)$$

It is now necessary to assume some of the results which will be proved later: when we come to determine the coefficients in the expansion (10), it will be found that a_0 and b_0 are $O(t^2)$ and that the a_n ($n = 1, 2, 3, \ldots$) are $O(t^{n+2})$. By using these results, it will be seen from (10) that near the body where the series converges

$$\frac{\partial\phi_0}{\partial s},\ \frac{\partial^2\phi_0}{\partial s^2} \text{ are } O(t^2\log t),\ \frac{\partial\phi_0}{\partial z},\ \frac{\partial^2\phi_0}{\partial z\partial s} \text{ etc. are } O(t), \text{ and } \frac{\partial^2\phi_0}{\partial z^2} \text{ etc. are } O(1).$$

Thus near the body we may write (12) in the form

$$4\frac{\partial^2\phi}{\partial z\partial\bar{z}}-B^2\frac{\partial^2\phi}{\partial s^2} = 4M^2\left\{\frac{\partial}{\partial s}\left(\frac{\partial\phi}{\partial z}\frac{\partial\phi}{\partial\bar{z}}\right)+\left(\frac{\partial\phi}{\partial z}\right)^2\frac{\partial^2\phi}{\partial\bar{z}^2}+\left(\frac{\partial\phi}{\partial\bar{z}}\right)^2\frac{\partial^2\phi}{\partial z^2}+\frac{\partial\phi}{\partial z}\frac{\partial\phi}{\partial\bar{z}}\frac{\partial^2\phi}{\partial z\partial\bar{z}}\right\}+$$
$$+O(t^4\log^2 t). \quad (14)$$

If we now assume that

$$\phi = \phi_0+\phi_1 = \tfrac{1}{2}(w+\bar{w})+\phi_1, \quad (15)$$

where ϕ_1 and its derivatives are of sufficiently smaller order than ϕ_0 and

its corresponding derivatives so that ϕ_1 may be neglected in the right-hand side of (14), then substituting in (14) we obtain

$$4\frac{\partial^2\phi_1}{\partial z\partial\bar{z}}-B^2\frac{\partial^2\phi_1}{\partial s^2}=\frac{B^2}{2}\left(\frac{\partial^2 w}{\partial s^2}+\frac{\partial^2\bar{w}}{\partial s^2}\right)+ \\ +M^2\left\{\frac{\partial}{\partial s}\left(\frac{\partial w}{\partial z}\frac{\partial\bar{w}}{\partial\bar{z}}\right)+\frac{1}{2}\left(\frac{\partial w}{\partial z}\right)^2\frac{\partial^2\bar{w}}{\partial\bar{z}^2}+\frac{1}{2}\left(\frac{\partial\bar{w}}{\partial\bar{z}}\right)^2\frac{\partial^2 w}{\partial z^2}\right\} \\ =f(z,\bar{z},s),\quad\text{say.} \tag{16}$$

From this we have, as a particular integral, by solving in series,

$$\phi_1=\frac{1}{4}\int^{z}\int^{\bar{z}}f(z,\bar{z},s)\,dzd\bar{z}+\frac{B^2}{16}\frac{\partial^2}{\partial s^2}\int^{z}\int^{z}\int^{\bar{z}}\int^{\bar{z}}f(z,\bar{z},s)\,(dz)^2(d\bar{z})^2+\ldots \tag{17}$$

$$=\frac{B^2}{8}\frac{\partial^2}{\partial s^2}\left(\bar{z}\int^{z}w\,dz+z\int^{\bar{z}}\bar{w}\,d\bar{z}\right)+ \\ +\frac{M^2}{4}\left\{\frac{\partial}{\partial s}(w\bar{w})+\frac{1}{2}\frac{\partial\bar{w}}{\partial\bar{z}}\int^{z}\left(\frac{\partial w}{\partial z}\right)^2dz+\frac{1}{2}\frac{\partial w}{\partial z}\int^{\bar{z}}\left(\frac{\partial\bar{w}}{\partial\bar{z}}\right)^2d\bar{z}\right\}+\ldots, \tag{18}$$

from which it will be seen that

$$\begin{aligned}&\phi_1\text{ is }O(t^4\log^2 t);\\&\partial\phi_1/\partial s,\ \partial^2\phi_1/\partial s^2,\text{ etc., are }O(t^4\log^2 t);\\&\partial\phi_1/\partial z,\ \partial^2\phi_1/\partial z\partial s,\text{ etc., are }O(t^3\log t),\text{ and}\\&\partial^2\phi_1/\partial z^2,\text{ etc., are }O(t^2\log t),\end{aligned} \tag{19}$$

the terms omitted in (18) being of lower order than those shown.

Now our conditions on the shape of the body ensure that ϕ_0 and its derivatives are of the same order of magnitude on the body as they are near it, so that the order of magnitude of ϕ_1 and its derivatives on and near the body are those given above. Hence ϕ_0 gives the velocities on and near the body within a factor $1+O(t^2\log t)$.

3. The boundary condition on the body

Let the contour C be the cross-section of the boundary of the body in a plane s = const., and let C' represent the projection on the same plane of the cross-section at $s+ds$ (see Fig. 1). If ν is the outward normal and τ is the tangent to C at any point, and $d\nu$ is the distance between C and C' measured along the normal, then the boundary condition of zero velocity normal to the body is

$$\frac{\partial\phi}{\partial\nu}=\frac{d\nu}{ds}\left(1+\frac{\partial\phi}{\partial s}\right). \tag{20}$$

Now $d\nu/ds$ is $O(t)$ by definition, so that $\partial\phi/\partial\nu$ must be $O(t)$ on the body, and if the curvature of C satisfies the condition of § 1, then $\partial\phi/\partial\tau$ will also be $O(t)$ on the body. Thus $|\partial w/\partial z|$ is $O(t)$ on the body and near to it, and

so a_0, a_1, etc., in the expression (10) will be $O(t^2)$, $O(t^3)$, etc. $\partial\phi/\partial s$ will then be $O(t^2 \log t)$ and (20) becomes

$$\frac{\partial\phi}{\partial\nu} = \frac{\partial\phi_0}{\partial\nu} + \frac{\partial\phi_1}{\partial\nu} = \frac{d\nu}{ds} + O(t^3 \log t). \tag{21}$$

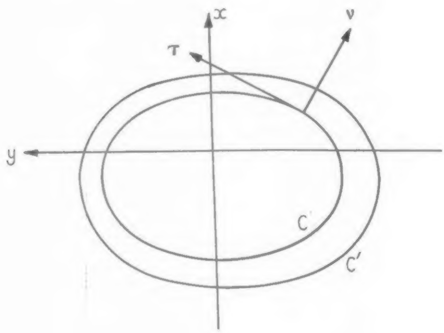

FIG. 1.

Thus, by using the results (19), it will be seen that we can determine ϕ_0 from

$$\frac{\partial\phi_0}{\partial\nu} = \frac{d\nu}{ds}, \tag{22}$$

and we shall have

$$\begin{aligned} \frac{\partial\phi}{\partial x} &= \frac{\partial\phi_0}{\partial x} + O(t^3 \log t), \\ \frac{\partial\phi}{\partial y} &= \frac{\partial\phi_0}{\partial y} + O(t^3 \log t), \\ \frac{\partial\phi}{\partial s} &= \frac{\partial\phi_0}{\partial s} + O(t^4 \log^2 t). \end{aligned} \tag{23}$$

4. Determination of the coefficients a_0 and b_0

Consider the integral $\int\limits_C \frac{\partial\phi_0}{\partial\nu}\, d\tau$. By using Gauss's theorem, since ϕ_0 satisfies

$$\frac{\partial^2\phi_0}{\partial x^2} + \frac{\partial^2\phi_0}{\partial y^2} = 0,$$

the contour C may be replaced by a circle of small radius $r_1 > R$, centre the origin of x and y, and the expression (10) may be used for ϕ_0, since it converges for $r > R$. Thus we get

$$\int\limits_C \frac{\partial\phi_0}{\partial\nu}\, d\tau = \int\limits_0^{2\pi} \left(\frac{\partial\phi_0}{\partial r}\right)_{r=r_1} r_1\, d\theta = 2\pi a_0. \tag{24}$$

Also, from the boundary condition (22), if the area enclosed by C is denoted by $S(s)$

$$\int_C \frac{\partial \phi_0}{\partial \nu}\,d\tau = \int_C \frac{d\nu}{ds}\,d\tau = S'(s). \tag{25}$$

Then, comparing (24) and (25), we have the result

$$a_0 = \frac{1}{2\pi} S'(s). \tag{26}$$

From (11), by using the product theorem to interpret the operational form, we have for b_0

$$b_0 = \frac{1}{2\pi}\left\{S'(s)\log\frac{B}{2} - \int_0^s \log(s-\sigma)S''(\sigma)\,d\sigma\right\} \tag{27}$$

since $S'(0) = 0$.

We sometimes require the derivative of b_0 with respect to s when calculating the pressure: this is

$$b_0' = \frac{1}{2\pi}\left\{S''(s)\log\frac{B}{2} - S''(0)\log s - \int_0^s \log(s-\sigma)S'''(\sigma)\,d\sigma\right\}. \tag{28}$$

5. The drag force on the body

We shall calculate the drag force from the rate of change of momentum in the s-direction through a cylinder $r = r_1$, where r_1 is small but greater than R, with plane ends at $s = 0$ and $s = 1$. Let S_1 denote the end at $s = 0$, S_2 denote the curved surface $r = r_1$, and S_3 denote the end at $s = 1$ outside the body (see Fig. 2). Then the drag force D, measured parallel to the main stream direction, is given by

$$D = \int_{S_1} (p_1 + \rho_1 U^2)\,dS_1 - \int_{S_2} \rho U^2\left(1+\frac{\partial\phi}{\partial s}\right)\frac{\partial\phi}{\partial r}\,dS_2 - \\ - \int_{S_3} \left\{p + \rho U^2\left(1+\frac{\partial\phi}{\partial s}\right)^2\right\} dS_3 - p_B\,S(1), \tag{29}$$

where p_B is the base pressure if $S(1) \neq 0$.

Conservation of mass flow through the cylinder gives

$$\int_{S_1} \rho_1 U\,dS_1 - \int_{S_2} \rho U \frac{\partial\phi}{\partial r}\,dS_2 - \int_{S_3} \rho U\left(1+\frac{\partial\phi}{\partial s}\right) dS_3 = 0. \tag{30}$$

Therefore, by multiplying (30) by U and subtracting from (29), we have

$$D = \int_{S_1} p_1\,dS_1 - \int_{S_2} \rho U^2 \frac{\partial\phi}{\partial r}\frac{\partial\phi}{\partial s}\,dS_2 - \int_{S_3} \left\{p + \rho U^2 \frac{\partial\phi}{\partial s}\left(1+\frac{\partial\phi}{\partial s}\right)\right\} dS_3 - p_B\,S(1). \tag{31}$$

From Bernoulli's equation, by using the results (23), we get

$$\frac{p-p_1}{\frac{1}{2}\rho_1 U^2} = -2\frac{\partial\phi_0}{\partial s} - \left(\frac{\partial\phi_0}{\partial r}\right)^2 - \frac{1}{r^2}\left(\frac{\partial\phi_0}{\partial\theta}\right)^2 + O(t^4\log^2 t), \tag{32}$$

and from the condition of isentropy we get

$$\rho/\rho_1 = 1+O(t^2\log t). \tag{33}$$

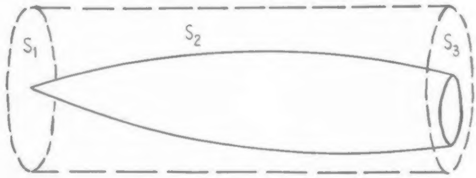

FIG. 2.

By substituting these last two results in (31), we find

$$\frac{D}{\frac{1}{2}\rho_1 U^2} = -2\int\limits_{S_2} \frac{\partial\phi_0}{\partial r}\frac{\partial\phi_0}{\partial s}\,dS_2 + \int\limits_{S_3}\left\{\left(\frac{\partial\phi_0}{\partial r}\right)^2 + \frac{1}{r^2}\left(\frac{\partial\phi_0}{\partial\theta}\right)^2\right\} dS_3 +$$

$$+\frac{p_1-p_B}{\frac{1}{2}\rho_1 U^2} S(1) + O(t^6\log^2 t). \tag{34}$$

The quantity $(p_1-p_B)/\frac{1}{2}\rho_1 U^2$ is usually called the base pressure coefficient, and is denoted by C_{pB}.

The integral over S_3 can be transformed into integrals taken round the boundaries of S_3 by using Green's theorem and we can write (34) as

$$\frac{D}{\frac{1}{2}\rho_1 U^2} = -2\int\limits_0^1\int\limits_0^{2\pi}\left(\frac{\partial\phi_0}{\partial r}\frac{\partial\phi_0}{\partial s}\right)_{r=r_1} r_1\,d\theta ds + \int\limits_0^{2\pi}\left(\phi_0\frac{\partial\phi_0}{\partial r}\right)_{r=r_1,\,s=1} r_1\,d\theta -$$

$$-\left(\int\limits_C \phi_0\frac{\partial\phi_0}{\partial\nu}\,d\tau\right)_{s=1} + C_{pB}\,S(1) + O(t^6\log^2 t). \tag{35}$$

We may now substitute the expansion for ϕ_0 in the first two integrals of (35) and we get

$$\frac{D}{\frac{1}{2}\rho_1 U^2} = 4\pi\int\limits_0^1 a_0' b_0\,ds - 2\pi(a_0 b_0)_{s=1} - \left(\int\limits_C \phi_0\frac{\partial\phi_0}{\partial\nu}\,d\tau\right)_{s=1} +$$

$$+C_{pB}\,S(1) + O(t^6\log^2 t). \tag{36}$$

By putting in the values of a_0 and b_0 found in § 4, (36) becomes

$$\frac{D}{\frac{1}{2}\rho_1 U^2} = \frac{1}{2\pi}\int_0^1\int_0^1 \log\frac{1}{|s-\sigma|} S''(s)S''(\sigma)\,d\sigma ds - \frac{S'(1)}{2\pi}\int_0^1 \log\frac{1}{1-\sigma} S''(\sigma)\,d\sigma -$$

$$-\left(\int_C \phi_0 \frac{\partial\phi_0}{\partial\nu}\,d\tau\right)_{s=1} + C_{pB}\,S(1) + O(t^6\log^2 t). \quad (37)$$

This appears to be the simplest form into which the expression for the drag force can be put for the completely general case. Two somewhat general special cases arise for which the result assumes a simpler form. These are (i), when $S(1) = 0$ and the body is pointed at both ends, and (ii), when the body is of general cylindrical form near $s = 1$ so that $S'(1) = 0$, and the generators of the cylinder are parallel to the main stream (so that we may think of the body as at zero incidence) which makes $\partial\phi_0/\partial\nu = d\nu/ds = 0$. For both of these cases, omitting the base drag term for case (ii),

$$\frac{D}{\frac{1}{2}\rho_1 U^2} = \frac{1}{2\pi}\int_0^1\int_0^1 \log\frac{1}{|s-\sigma|} S''(s)S''(\sigma)\,d\sigma ds + O(t^6\log^2 t). \quad (38)$$

This is the same result as that obtained by von Kármán (**1**) and Lighthill (**2**) for the special case of a body of revolution at zero incidence and having $S'(1) = 0$.

The extra terms in (37) occur when $S'(1) \neq 0$ or when the body is at incidence: the extra drag due to incidence comes entirely from the third integral in (37).

6. The lateral forces on the body

The lateral forces X, Y on the body in the directions of positive x and y respectively may be obtained by considering the rates of change of momentum in the x and y directions through the cylinder $r = r_1$, as before. We have then

$$\left.\begin{aligned} X &= -\int_{S_2}\left(\rho U^2\frac{\partial\phi}{\partial r}\frac{\partial\phi}{\partial x} + p\cos\theta\right)dS_2 - \int_{S_3}\rho U^2\left(1+\frac{\partial\phi}{\partial s}\right)\frac{\partial\phi}{\partial x}\,dS_3, \\ Y &= -\int_{S_2}\left(\rho U^2\frac{\partial\phi}{\partial r}\frac{\partial\phi}{\partial y} + p\sin\theta\right)dS_2 - \int_{S_3}\rho U^2\left(1+\frac{\partial\phi}{\partial s}\right)\frac{\partial\phi}{\partial y}\,dS_3. \end{aligned}\right\} \quad (39)$$

It will be found to be convenient to treat the complex combination of

X and Y, $F = X+iY$. On substituting the approximate potential and retaining only the terms $O(t^3)$, (39) becomes

$$\frac{F}{\frac{1}{2}\rho_1 U^2} = -\int\limits_{S_2}\left\{2\frac{\partial\phi_0}{\partial r}\frac{\partial\bar{w}}{\partial\bar{z}}-\left(2\frac{\partial\phi_0}{\partial s}+\frac{\partial w}{\partial z}\frac{\partial\bar{w}}{\partial\bar{z}}\right)e^{i\theta}\right\}dS_2-2\int\limits_{S_3}\frac{\partial\bar{w}}{\partial\bar{z}}\,dS_3+ +O(t^5\log^2 t). \quad (40)$$

Now

$$\int\limits_{S_3}\frac{\partial\bar{w}}{\partial\bar{z}}\,dS_3 = \int\limits_{S_3}\left(\frac{\partial\phi_0}{\partial x}+i\frac{\partial\phi_0}{\partial y}\right)dS_3 = \left\{i\int\limits_C\phi_0\,dz+\int\limits_0^{2\pi}(\phi_0)_{r=r_1}\,r_1e^{i\theta}\,d\theta\right\}_{s=1}$$

$$= \left(i\int\limits_C\phi_0\,dz\right)_{s=1}+\int\limits_0^1\int\limits_0^{2\pi}\left(\frac{\partial\phi_0}{\partial s}\right)_{r=r_1}r_1e^{i\theta}\,d\theta ds, \quad (41)$$

by applying Stokes's theorem for two dimensions; hence (40) becomes

$$\frac{F}{\frac{1}{2}\rho_1 U^2} = \left(-2i\int\limits_C\phi_0\,dz\right)_{s=1}-\int\limits_0^1\int\limits_0^{2\pi}\left(2\frac{\partial\phi_0}{\partial r}\frac{\partial\bar{w}}{\partial\bar{z}}-e^{i\theta}\frac{\partial w}{\partial z}\frac{\partial\bar{w}}{\partial\bar{z}}\right)_{r=r_1}r_1\,d\theta ds+ +O(t^5\log^2 t). \quad (42)$$

On substituting the expression (10) for w and ϕ_0, or otherwise by remembering that F must be independent of r_1 and letting $r_1\to\infty$, we find that the double integral vanishes, and we are left with

$$\frac{F}{\frac{1}{2}\rho_1 U^2} = \left(-2i\int\limits_C\phi_0\,dz\right)_{s=1}+O(t^5\log^2 t). \quad (43)$$

This expression for F can be put into a somewhat more convenient form as follows. Since $\phi_0 = w-i\psi_0$, (43) may be written

$$\frac{F}{\frac{1}{2}\rho_1 U^2} = \left(-2i\int\limits_C w\,dz-2\int\limits_C\psi_0\,dz\right)_{s=1}+O(t^5\log^2 t). \quad (44)$$

Now w is an analytic function of z in a cut z-plane, and C encloses all the singularities of w, none of which lies on C. Thus the expansion (10) converges on some arc of C and we can choose another contour C_1 on which the expansion (10) is valid and which has at least one common point z_0 with C. We make the cut in the z-plane pass through z_0 and start and end our contours C, C_1 at z_0 (on opposite sides of the cut). Then we have

$$\int\limits_C w\,dz = \int\limits_{C_1} w\,dz = \int\limits_{C_1}\left(\frac{S'(1)}{2\pi}\log z+b_0+\frac{a_1}{z}+\frac{a_2}{z^2}+\dots\right)dz$$

$$= \frac{S'(1)}{2\pi}2\pi iz_0+2\pi ia_1. \quad (45)$$

Also we have
$$\int_C \psi_0\,dz = [\psi_0 z]_C - \int_C z\frac{\partial\psi_0}{\partial\tau}\,d\tau. \tag{46}$$

Now since ϕ_0 and ψ_0 are conjugate functions
$$\frac{\partial\psi_0}{\partial\tau} = \frac{\partial\phi_0}{\partial\nu} = \frac{d\nu}{ds}, \tag{47}$$

so that
$$[\psi_0]_C = \int_C \frac{d\nu}{ds}\,d\tau = S'(s); \tag{48}$$

hence (46) becomes
$$\int_C \psi_0\,dz = S'(s)z_0 - \int_C z\frac{d\nu}{ds}\,d\tau. \tag{49}$$

The last integral has a simple geometrical interpretation: it is the rate of change (with respect to s) of the moment of area of C. If we let the coordinates of the centre of area of C be given by x_g, y_g so that
$$z_g(s) = x_g + iy_g,$$
then
$$\int_C z\frac{d\nu}{ds}\,d\tau = \frac{d}{ds}[S(s)z_g(s)] = S'(s)z_g(s)+S(s)z_g'(s). \tag{50}$$

By substituting all these results in (44) we obtain finally
$$\frac{F}{\frac{1}{2}\rho_1 U^2} = 4\pi(a_1)_{s=1}+2S'(1)z_g(1)+2S(1)z_g'(1)+O(t^5\log^2 t). \tag{51}$$

The moments of the lateral forces about the x and y axes may be calculated from this expression. If we write
$$\frac{F(s)}{\frac{1}{2}\rho_1 U^2} = 4\pi(a_1)_s+2S'(s)z_g(s)+2S(s)z_g'(s), \tag{52}$$

then the lateral force per unit length is given by $F'(s)$ and we have for the complex moment M_z
$$M_z = M_x+iM_y = i\int_0^1 sF'(s)\,ds = iF(1)-i\int_0^1 F(s)\,ds. \tag{53}$$

On substituting (52) in (53), we have, finally,
$$\frac{M_z}{\frac{1}{2}\rho_1 U^2} = 4\pi i(a_1)_{s=1}-4\pi i\int_0^1 a_1\,ds+2i[S'(1)z_g(1)+S(1)z_g'(1)-S(1)z_g(1)]+ \\ +O(t^5\log^2 t). \tag{54}$$

These results have been given in their most general form for a slender body satisfying the conditions given in § 1. We shall now go on to show how they may be applied in special cases.

7. Bodies of revolution with a flat base

Consider a body of revolution at incidence α, the incidence being applied in the (x, s)-plane. Then $z_g = -\alpha s$ and the appropriate potential w is

$$w-b_0 = \frac{S'(s)}{2\pi}\log(z-z_g)-\frac{S(s)}{\pi}\frac{z_g'}{z-z_g}, \tag{55}$$

neglecting a factor $1+O(\alpha^2)$ (since we have taken the sections to be circles whereas they are really ellipses); $w-b_0$ is composed of a term representing radial flow outwards from z_g and a term due to the cross-flow past the circular section, centre z_g. This may be expanded to give

$$w-b_0 = \frac{S'(s)}{2\pi}\log z-\frac{z_g S'(s)+2z_g' S(s)}{2\pi z}+\dots. \tag{56}$$

On the body $z-z_g = R(s)e^{i\vartheta}$, say, so that

$$w-b_0 = \frac{S'(s)}{2\pi}[\log R(s)+i\vartheta]+\alpha R(s)e^{-i\vartheta}. \tag{57}$$

Therefore

$$\phi_0 = \frac{S'(s)}{2\pi}\log\frac{BR(s)}{2}-\frac{1}{2\pi}\int\limits_0^s \log(s-\sigma)S''(\sigma)\,d\sigma+\alpha R(s)\cos\vartheta, \tag{58}$$

and from the boundary condition, or otherwise directly from (55),

$$\frac{\partial\phi_0}{\partial\nu} = R'(s)-\alpha\cos\vartheta, \tag{59}$$

so that

$$\left(\int\limits_C \phi_0\frac{\partial\phi_0}{\partial\nu}\,d\tau\right)_{s=1}$$

$$= \int\limits_0^{2\pi}\left[\left\{\frac{S'(1)}{2\pi}\log\frac{BR(1)}{2}-\frac{1}{2\pi}\int\limits_0^1 \log(1-\sigma)S''(\sigma)\,d\sigma\right\}R'(1)-\alpha^2 R(1)\cos^2\vartheta\right]\times$$

$$\times R(1)\,d\vartheta$$

$$= \frac{[S'(1)]^2}{2\pi}\log\frac{BR(1)}{2}-\frac{S'(1)}{2\pi}\int\limits_0^1 \log(1-\sigma)S''(\sigma)\,d\sigma-S(1)\alpha^2. \tag{60}$$

On putting this expression into the formula (37) for the drag, we have

$$\frac{D}{\frac{1}{2}\rho_1 U^2} = \frac{1}{2\pi}\int\limits_0^1\int\limits_0^1 \log\frac{1}{|s-\sigma|}S''(\sigma)S''(s)\,d\sigma ds-\frac{S'(1)}{\pi}\int\limits_0^1 \log\frac{1}{1-\sigma}S''(\sigma)\,d\sigma+$$

$$+\frac{1}{2\pi}[S'(1)]^2\log\frac{2}{BR(1)}+S(1)\alpha^2+O(t^6\log^2 t). \tag{61}$$

Thus the drag coefficient is given by

$$C_D = \frac{D}{\frac{1}{2}\rho_1 U^2 S(1)} = C_{D0} + \alpha^2, \tag{62}$$

where C_{D0} is the drag coefficient at zero incidence. This result was obtained by Lighthill (**3**).

The lateral force F is given from (51) and (56)

$$\frac{F}{\frac{1}{2}\rho U^2} = -4z_g' S(1) - 2z_g S'(1) + 2z_g S'(1) + 2z_g' S(1) + O(t^5 \log^2 t)$$

$$= -2z_g' S(1) = 2\alpha S(1). \tag{63}$$

Thus there is only a lifting force in the direction of positive x, and the lift coefficient is given by

$$C_L = \frac{\mathrm{Lift}(X)}{\frac{1}{2}\rho_1 U^2 S(1)} = 2\alpha + O(t^3 \log^2 t), \tag{64}$$

a result due originally to Tsien (**4**).

From (62) and (64) we see that the direction of the extra force due to incidence bisects the angle between the normals to the stream direction and the body axis in the plane of incidence.

8. Bodies with a flat base of elliptical section for which $S'(1) = 0$

Let the base of the body be an ellipse with major and minor axes of lengths $2a$, $2b$ respectively, and let the major axis make an angle β with the x-axis. The centre of the ellipse is at

$$z_g = -\alpha \quad (z_g(s) = -\alpha s)$$

(see Fig. 3). Since $S'(1) = 0$, the potential $w - b_0$ is that appropriate to an elliptic cylinder moving in an infinite fluid at rest at infinity with velocity $-\alpha$ in the x-direction.

Now $-\frac{1}{2}\int\limits_C \phi_0 \frac{\partial \phi_0}{\partial \nu}\, d\tau$ is the well-known expression for the kinetic energy of the incompressible fluid motion due to the movement of the cylinder C (for density $= 1$). For the elliptic cylinder defined above, the kinetic energy of the motion is

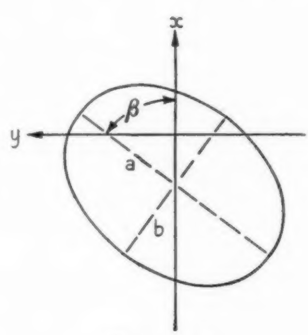

Plane $s = 1$.

FIG. 3.

$$-\frac{1}{2}\int\limits_C \phi_0 \frac{\partial \phi_0}{\partial \nu}\, d\tau = \tfrac{1}{2}\pi\alpha^2(a^2 \sin^2\beta + b^2 \cos^2\beta).$$

Thus the drag coefficient is

$$C_D = \frac{D}{\frac{1}{2}\rho_1 U^2 \pi ab} = C_{D0} + \left(\frac{a}{b}\sin^2\beta + \frac{b}{a}\cos^2\beta\right) + O(t^6\log^2 t), \tag{65}$$

where C_{D0} is the drag coefficient for $\alpha = 0$, from (38). The complex potential $(w)_{s=1}$ is

$$(w)_{s=1} = \tfrac{1}{2}\alpha\left\{\sqrt{(\zeta^2-c^2)} - \zeta + \frac{(a+b)^2}{\sqrt{(\zeta^2-c^2)}+\zeta}\right\},$$

$$\text{where } c^2 = (a^2-b^2)e^{2i\beta},\ \zeta = z - z_g,$$

$$= \tfrac{1}{4}\alpha\{(a+b)^2 - c^2\}\frac{1}{\zeta} + \dots \tag{66}$$

$$= \tfrac{1}{4}\alpha\{(a+b)^2 - (a^2-b^2)e^{2i\beta}\}\frac{1}{z} + \dots .$$

Therefore,

$$\frac{F}{\frac{1}{2}\rho_1 U^2} = \pi\alpha\{(a+b)^2 - (a^2-b^2)e^{2i\beta}\} - 2\pi ab + O(t^5\log^2 t)$$

$$= 2\pi\alpha\{a^2\sin^2\beta + b^2\cos^2\beta - i(a^2-b^2)\sin\beta\cos\beta\} + O(t^5\log^2 t). \tag{67}$$

Thus we have both the components: a lift force in the plane of incidence, giving a lift coefficient

$$C_L = \frac{X}{\frac{1}{2}\rho_1 U^2 \pi ab} = 2\alpha\left(\frac{a}{b}\sin^2\beta + \frac{b}{a}\cos^2\beta\right) + O(t^3\log^2 t), \tag{68}$$

and a force perpendicular to the plane of incidence, giving a force coefficient

$$C_Y = \frac{Y}{\frac{1}{2}\rho_1 U^2 \pi ab} = -2\alpha\left(\frac{a}{b} - \frac{b}{a}\right)\sin\beta\cos\beta + O(t^3\log^2 t). \tag{69}$$

These results are valid when $a/b = O(1)$ from our condition on the curvature of the cross-section. However, by taking α sufficiently small when b/a is small, and if the body has two planes of symmetry, we can keep the velocities at the extremities of the major axis small enough to keep the approximations valid, and we have

$$\left(\frac{\partial C_L}{\partial \alpha}\right)_{\alpha=0} = 2\left(\frac{a}{b}\sin^2\beta + \frac{b}{a}\cos^2\beta\right), \quad \text{etc.} \tag{70}$$

When b/a is small, it is more convenient to take a different lift coefficient C'_L, defined by $C'_L = \text{Lift}/\frac{1}{2}\rho_1 U^2 a^2$, etc., in which case we may write

$$\left(\frac{\partial C'_L}{\partial \alpha}\right)_{\alpha=0} = 2\pi\left(\sin^2\beta + \frac{b^2}{a^2}\cos^2\beta\right) + O(t^2\log^2 t), \tag{71}$$

$$\left(\frac{\partial C'_Y}{\partial \alpha}\right)_{\alpha=0} = -2\pi\left(1 - \frac{b^2}{a^2}\right)\sin\beta\cos\beta + O(t^2\log^2 t), \tag{72}$$

$$C'_D = C'_{D0} + \pi\left(\sin^2\beta + \frac{b^2}{a^2}\cos^2\beta\right)\alpha^2 + O(t^4\log^2 t). \tag{73}$$

Again, it will be seen from (65) and (68) that the direction of the extra force at incidence in the plane of incidence bisects the angle between the normals to the stream direction and the body axis in the plane of incidence.

9. The drag force at incidence

The result noticed at the ends of §§ 7, 8 for special bodies may be shown to be true generally if we define the position of zero incidence to be the position of zero lateral force. Let ϕ_{00} be the potential in the plane $s = 1$ when the body is at zero incidence, so that from (43) we have

$$-2i\int\limits_C \phi_{00}\,dz = 0, \tag{74}$$

and let ϕ_{01} be the extra potential in the plane $s = 1$ due to incidence, so that the lateral force is given by

$$\frac{X+iY}{\frac{1}{2}\rho_1 U^2} = -2i\int\limits_C \phi_{01}\,dz = 2\int\limits_C \phi_{01}\,dy - 2i\int\limits_C \phi_{01}\,dx. \tag{75}$$

If η is the angle made by the tangent to C at any point with the x-axis, and if we take the incidence to be applied in the (x, s)-plane (as we may do without any loss of generality) and to be α, then the boundary conditions give

$$\frac{\partial\phi_{01}}{\partial\nu} = -\alpha\sin\eta \tag{76}$$

on the contour C.

From (37), the drag force is given by

$$\frac{D-D_0}{\frac{1}{2}\rho_1 U^2} = -\int\limits_C \phi_{00}\frac{\partial\phi_{01}}{\partial\nu}\,d\tau - \int\limits_C \phi_{01}\frac{\partial\phi_{00}}{\partial\nu}\,d\tau - \int\limits_C \phi_{01}\frac{\partial\phi_{01}}{\partial\nu}\,d\tau + O(t^6\log^2 t), \tag{77}$$

where D_0 is the drag force at zero incidence.

Consider now the values of the three integrals in (77). We have, for the first integral,

$$\int\limits_C \phi_{00}\frac{\partial\phi_{01}}{\partial\nu}\,d\tau = -\alpha\int\limits_C \phi_{00}\sin\eta\,d\tau = -\alpha\int\limits_C \phi_{00}\,dy = 0 \tag{78}$$

by using (76) and as a result of (74).

For the second integral, we have

$$\int\limits_C \phi_{01}\frac{\partial\phi_{00}}{\partial\nu}\,d\tau = \int\limits_C \left(\phi_{01}\frac{\partial\phi_{00}}{\partial\nu} - \phi_{00}\frac{\partial\phi_{01}}{\partial\nu}\right)d\tau = \int\limits_0^{2\pi}\left(\phi_{01}\frac{\partial\phi_{00}}{\partial r} - \phi_{00}\frac{\partial\phi_{01}}{\partial r}\right)_{r=r_1} r_1\,d\theta \tag{79}$$

from (78) and by applying Green's theorem, since ϕ_{00} and ϕ_{01} both satisfy

Laplace's equation in two dimensions. We may now let $r_1 \to \infty$, and since the series for ϕ_{00} and ϕ_{01} commence with multiples of $\log r$ and $1/r$ respectively, we see that this integral vanishes.

Finally, by using (76) and (75),

$$\int_C \phi_{01} \frac{\partial \phi_{01}}{\partial \nu} d\tau = -\alpha \int_C \phi_{01} \sin \eta \, d\tau = -\alpha \int_C \phi_{01} \, dy = -\frac{\alpha X}{\rho_1 U^2}. \quad (80)$$

Thus, we have $$D = D_0 + \tfrac{1}{2}\alpha X + O(t^6 \log^2 t), \quad (81)$$

which may be written in terms of the force coefficients

$$C_D = C_{D0} + \tfrac{1}{2}(\partial C_L/\partial\alpha)_{\alpha=0}\, \alpha^2 + O(t^4 \log^2 t). \quad (82)$$

10. Flat laminar wings of small aspect ratio

The condition on the maximum curvature of any section of our bodies prevents the study of some very interesting problems, and we now consider the effect on our approximations of removing this condition in certain special cases. Such a special case is that of a flat laminar wing of small aspect ratio with highly swept back leading edges; we will consider this as an illustration.

The flat laminar wing may be taken to be the limiting form of a slender body of elliptical cross-section as the eccentricity of the ellipses tends to unity. As we have seen at the end of § 8, if the eccentricity is not actually unity we can calculate the expressions for C_L and C_D for sufficiently small incidences. Now letting the eccentricity tend to unity, we see that the expressions for the force coefficients tend to definite values, or more precisely, we see that $(\partial C'_L/\partial\alpha)_{\alpha=0}$, $(C'_D)_{\alpha=0}$, and $(\partial^2 C'_D/\partial\alpha^2)_{\alpha=0}$ tend to definite values. If we reverse the order of the above two limiting processes, we find that for finite incidence the velocities become infinite at the points where the curvature becomes infinite. However, the solutions for the potential ϕ_0 and its derivatives are still an approximation to the true potential and its derivatives except in the immediate vicinities of the points of infinite curvature, and so the pressure in particular will be inaccurate only for comparatively small regions on the surface of the body. Since the pressure singularities are integrable, it seems to be a reasonable assumption that the integrated body pressures will give a true approximation to the correct body forces for small incidences.

In what follows, we shall use the above assumption to calculate the body forces when there is no restriction on the curvature of sections, using the formulae obtained previously, but omitting the O-terms as these have lost some of their meaning.

Consider now a flat laminar wing, pointed at the upstream end and with highly swept back leading edges in order to conform with the

condition for a slender body, lying in the plane $x = -\alpha s$, so that its incidence is α. Let a be the semi-span at any section $s =$ constant and let the origin of z_1 ($= x_1+iy_1 = z+\alpha s$) be taken at the centre of the local span. Then the appropriate incompressible flow in two dimensions is that for a flat plate with its edges at $z_1 = \pm ia$, and we have

$$w = \alpha\{\sqrt{(z_1^2+a^2)}-z_1\}. \tag{83}$$

The flow given from this expression for w is appropriate so long as the edges of the wing are 'leading edges'. When the edges are 'trailing edges' this form for w is no longer correct, since a vortex sheet will be formed downstream from the trailing edges: the strength of this sheet must be determined from the condition of Kutta and Joukowski, that the flow leaves the trailing edges smoothly, and from the condition of constant vorticity along each vortex line. Thus, in principle, we must add other terms to (83), representing the motion due to vortices, in order to cancel the singularities in the velocities at $y_1 = \pm a$. If the incidence is small, then these vortices will lie approximately in the plane of the wing (actually we shall find that they do so exactly) and so we shall have $(\partial\phi_0/\partial y_1)_{x_1=0} = 0$ approximately for $|y_1| > a$. Hence the vortex lines, following the streamlines, will extend downstream in straight lines. These conditions are sufficient to determine the strength of the vortex sheet everywhere.

If the maximum span of the wing is $2b$, and the wing is symmetrical, then we have to determine the flow for a plate of width $2a$ with two vortex sheets extending from $y_1 = \pm a$ to $y_1 = \pm b$.

Now if $q = dw/dz_1$, then we must have $\mathrm{Re}(q) =$ constant for $x_1 = 0$, $|y_1| < a$, and $\mathrm{Im}(q) = 0$ for $x_1 = 0$, $|y_1| > a$: hence dq/dz_1 must be a pure imaginary for $|y_1| < a$, and a pure real for $|y_1| > a$ on $x_1 = 0$. Also we should expect that dq/dz_1 will have poles at $z_1 = \pm ib$, and we must have $dq/dz_1 = O(1/z_1^3)$ as $z_1 \to \infty$. Thus a possible form for dq/dz_1 is

$$\frac{dq}{dz_1} = \frac{A}{(z_1^2+b^2)\sqrt{(z_1^2+a^2)}}, \tag{84}$$

where A is a constant to be determined from the boundary conditions. By integrating, we obtain q satisfying the conditions $\mathrm{Re}(q) = -\alpha$ on the wing and $q = 0$ at infinity, viz.

$$q = \alpha\left[\frac{\cosh^{-1}[(b/a)\sqrt{\{(z_1^2+a^2)/(z_1^2+b^2)\}}]}{\cosh^{-1}(b/a)}-1\right]. \tag{85}$$

The strength of the vortex sheet given by (85) is constant and equal to

$$\frac{\pi\alpha}{\cosh^{-1}(b/a)}, \tag{86}$$

which depends upon the value of a. The strength of the vortex sheet must be independent of a since it must be independent of s, and so we must superimpose a certain distribution of flows of the above form in order to satisfy this condition.

If the strength of the vortex sheet is $f(y_1)$ at any point y_1, then the appropriate form for dq/dz_1, from (85) and (86), is

$$\frac{dq}{dz_1} = \int_a^b \frac{\partial}{\partial\beta}\left\{\frac{\beta\sqrt{(\beta^2-a^2)}}{z_1^2+\beta^2}\right\}\frac{f(\beta)\,d\beta}{\sqrt{(z_1^2+a^2)}}, \tag{87}$$

which gives for the velocity $\mathrm{Re}(q)$ on the wing

$$\mathrm{Re}(q) = \int_a^b \frac{\partial}{\partial\beta}\left(\cosh^{-1}\frac{\beta}{a}\right)f(\beta)\,d\beta = \int_a^b \frac{f(\beta)\,d\beta}{\sqrt{(\beta^2-a^2)}}. \tag{88}$$

We must determine $f(\beta)$ as a function of β and b only, so that (88) is independent of a. It is found that the distribution given by

$$f(\beta) = \frac{2\alpha}{\pi}\frac{\beta}{\sqrt{(b^2-\beta^2)}} \tag{89}$$

satisfies this condition and the boundary condition on the wing: this corresponds to an elliptic lift distribution for the wing, and we have finally, from (87) and (89),

$$\frac{dq}{dz_1} = \frac{2\alpha}{\pi}\int_a^b \frac{\partial}{\partial\beta}\left\{\frac{\beta\sqrt{(\beta^2-a^2)}}{z_1^2+\beta^2}\right\}\frac{\beta\,d\beta}{\sqrt{\{(b^2-\beta^2)(z_1^2+a^2)\}}}. \tag{90}$$

This integral can be evaluated to give

$$\frac{dq}{dz_1} = \frac{\alpha b^2}{(z_1^2+b^2)^{\frac{3}{2}}}, \tag{91}$$

and we obtain finally

$$w = \alpha\{\sqrt{(z_1^2+b^2)}-z_1\}. \tag{92}$$

Thus we find that the expression for w downstream from the section of maximum span is the same as that for the flow due to a flat plate of width $2b$, on comparing this result with (83).

We may now put $z_1 = z+\alpha s$ in (83) and (92) and expand in inverse powers of z. The coefficient a_1 of $1/z$ is, for the sections upstream from the maximum span, from (83),

$$a_1 = \tfrac{1}{2}a^2 \quad (da/ds \geqslant 0), \tag{93}$$

and, for the sections downstream from the maximum span, from (92),

$$a_1 = \tfrac{1}{2}b^2 \quad (a \leqslant b). \tag{94}$$

Thus if b is the maximum semi-span (whether it occurs at $s = 1$ with $da/ds \geqslant 0$, or for some $s < 1$), by using (52) we find for the lift coefficient

$$C_L = \frac{\text{Lift}}{\frac{1}{2}\rho_1 U^2 b^2} = 2\pi\alpha, \tag{95}$$

or, referring the lift coefficient to the area of the wing planform S_w,

$$C'_L = \frac{\text{Lift}}{\frac{1}{2}\rho_1 U^2 S_w} = \tfrac{1}{2}\pi A\alpha, \tag{96}$$

where A is the aspect ratio $(= 4b^2/S_w)$.

The drag coefficient is, from (82),

$$C'_D = \frac{\text{Drag}}{\frac{1}{2}\rho_1 U^2 S_w} = \tfrac{1}{4}\pi A\alpha^2. \tag{97}$$

It will be noticed that there is no lift on sections downstream from the maximum span. This is due to the fact that the downwash caused by the vortex sheet is just the velocity required to satisfy the boundary condition on the wing. In fact, the downwash is αU over both the wing and the vortex sheet itself, so that the vortex sheet remains coplanar with the wing everywhere, including the portion downstream from the wing. The shape of the wing planform downstream from the maximum span is thus shown to be immaterial, so that we need not impose upon it the condition of slenderness.

The results of this section were obtained originally by Jones (**5**).

11. Winged bodies of revolution

The appropriate complex potential w for the case of a body of revolution with wings of small aspect ratio may be obtained from the results of the previous section by a simple conformal transformation.

Consider a pointed body of revolution of radius R at any section, at incidence α to the stream so that $z_g = -\alpha s$, and carrying wings symmetrically placed on either side of the body in the plane $x = -\alpha s$. Let the edges of the wings be at a distance a from the body axis at any section (if there are no wings at some given section, then $a = R$). R and a are both functions of s, but the indication of the functional dependence will be omitted.

At zero incidence, when the axis of the body is in the direction of the main stream, the flow is that for the body alone, since the wings lie in stream surfaces. At incidence α we have to add to the complex potential for zero incidence terms due to the cross-flow over the body and wings. These extra terms may be obtained from expressions of the form (83) by replacing z_1 by $z_1 + R^2/z_1$ and a by $a - R^2/a$ in the square root: the origin of z_1 is again taken at $z = -\alpha s$. Thus we have for $w - b_0$

$$w - b_0 = \frac{1}{2\pi} S'(s)\log z_1 + \alpha\left[\sqrt{\left\{\left(z_1 + \frac{R^2}{z_1}\right)^2 + \left(a - \frac{R^2}{a}\right)^2\right\}} - z_1\right]. \tag{98}$$

This form for w is appropriate when the edges of the wings are 'leading edges'. The definition of a leading edge in this case is not quite as simple as it was for the flat wing alone, since the streamlines will be curved if R is not constant. From (98) we find that $\partial\phi_0/\partial y_1$ in the plane of the wings and for $y_1 > a$ is given by

$$\left(\frac{\partial\phi_0}{\partial y_1}\right)_{x_1=0,y_1>a} = \frac{S'(s)}{2\pi y_1}; \tag{99}$$

this quantity is the slope of the projection of the streamlines near to the plane $x_1 = 0$ on to this plane, and so the equations of the streamlines near the plane of the wings are approximately

$$y_1^2 = R^2 + \text{constant}. \tag{100}$$

Equation (100) can be used to find the value of s for which the edge of the wing is tangent to a streamline, and downstream from this section the edge is a 'trailing edge'. As for the case of the wing alone, there will be a vortex sheet extending downstream from the trailing edge, and the strength of this vortex sheet will be determined from the conditions given in § 10. The determination of the distribution of vorticity at any section for a general variation of R with s is very tedious and, in general, the expression for w seems to involve hyperelliptic integrals, so we will be content with the solution of the problem when R is constant downstream from the section of maximum span. If b is the distance of the wing edge from the centre of the body at maximum span, then the expression for w may be obtained from (92) by the same conformal transformation as before, and we have

$$w = \alpha\left[\sqrt{\left\{\left(z_1+\frac{R^2}{z_1}\right)^2+\left(b-\frac{R^2}{b}\right)^2\right\}}-z_1\right] \tag{101}$$

since $S'(s)$ is now zero.

The conformal transformation by means of which (101) is obtained from (92) does not alter the geometry of the vortex system, which still remains coplanar with the wings. Thus the boundary condition on the wing is still satisfied by the downwash from the vortex sheet and again the plan-form of the wings is immaterial downstream from the maximum span, provided that $a \leqslant b$ everywhere. There is, of course, no lift on these sections. These results are true only if $R =$ constant; if R varies, then in general there will be a lift force.

In general the dimensions of the body and wings, i.e. R and a, must be continuous functions of s together with their first derivatives, otherwise we get infinite d^2w/ds^2 and discontinuous pressures everywhere at the section of discontinuity, and the analysis given here breaks down. This

condition has been shown to be unnecessary downstream from the maximum span, and it can be shown that, in addition, it is not necessary on the leading edges when $a = R$, and da/ds may have a discontinuity at this point. By differentiating w, given by (98), it can be shown that dw/ds is continuous and d^2w/ds^2 remains finite when $a = R$ if da/ds is discontinuous there. Thus the leading edges of the wings can come from the body at a finite angle without the necessity for introducing further approximations.

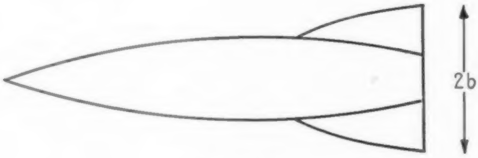

FIG. 4 (*a*).

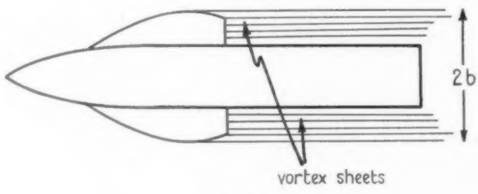

FIG. 4 (*b*).

We are now in a position to determine the lift and drag coefficients for winged bodies of revolution of two different types, (i) a body of revolution of general variation of cross-sectional radius, with wings whose edges are everywhere 'leading edges' upstream from the base (see Fig. 4*a*), and (ii) a body of revolution with a uniform section downstream from the section of maximum wingspan (see Fig. 4*b*).

If $2b$ is the maximum span and R_1 is the radius of the base in each of the two cases, then the lift coefficients and the extra drag coefficients due to incidence have the same form for both. The drag coefficient at zero incidence depends upon the actual body shape, of course. From (98) and (101), by putting $z_1 = z - z_g$ and expanding in the form (10), we find for the coefficient of $1/z$ at $s = 1$

$$a_1 = \frac{b^4+R_1^4}{2b^2}\alpha - \frac{z_g(1)S'(1)}{2\pi} \quad \text{from (98),} \tag{102}$$

and

$$a_1 = \frac{b^4+R_1^4}{2b^2}\alpha \quad \text{from (101).} \tag{103}$$

By substituting these values of a_1 in (51) we find for the lateral force in both cases a lift force given by

$$\frac{X}{\frac{1}{2}\rho_1 U^2} = 2\pi\alpha\frac{b^4-b^2R_1^2+R_1^4}{b^2}. \tag{104}$$

If we take the lift coefficient relative to the base area of the body, we have

$$C_L = 2\alpha\frac{b^4-b^2R_1^2+R_1^4}{b^2R_1^2}. \tag{105}$$

The corresponding drag coefficient is, from (82),

$$C_D = C_{D0}+\frac{b^4-b^2R_1^2+R_1^4}{b^2R_1^2}\alpha^2, \tag{106}$$

where C_{D0} is the drag coefficient at zero incidence.

It may be more convenient sometimes (particularly in case (i) when $R_1 \doteqdot 0$) to refer the lift and drag coefficients to b^2, in which case we have

$$C'_L = 2\pi\alpha\left(1-\frac{R_1^2}{b^2}+\frac{R_1^4}{b^4}\right) \tag{107}$$

and

$$C'_D = C'_{D0}+\pi\left(1-\frac{R_1^2}{b^2}+\frac{R_1^4}{b^4}\right). \tag{108}$$

The lift coefficient given by (107) may be compared with that for a wing of small aspect ratio given by (95), from which it will be seen that, when R_1/b is small, they are very nearly equal, and since $R_1/b < 1$, the lift coefficient for the winged body is always less than that for a flat wing of the same maximum span, showing that the body is less effective in producing lift than a wing of the same projected planform.

We can obtain some interesting results for the magnitude of the interference effects between the wing and the body from a consideration of case (ii) when the wing root lies wholly on the cylindrical portion of the body. The difference between the lift L_{BW} on the combined system and the lift L_B due to the body alone is given by

$$\frac{L_{BW}-L_B}{\frac{1}{2}\rho_1 U^2} = 2\pi\alpha\frac{(b^2-R_1^2)^2}{b^2}. \tag{109}$$

Now the lift L_W on the wing alone (of maximum span $2(b-R_1)$) is given from (95) by

$$\frac{L_W}{\frac{1}{2}\rho_1 U^2} = 2\pi\alpha(b-R_1)^2, \tag{110}$$

so that we have for the extra lift due to the presence of the wing in terms of the lift of the wing by itself

$$L_{BW}-L_B = \left(1+\frac{R_1}{b}\right)^2 L_W. \tag{111}$$

For a very small wing, for which $b-R_1$ is small, we have approximately

$$L_{BW}-L_B \doteqdot 4L_W. \tag{112}$$

From the potential (55) it is easy to show that the upwash near the wing due to the presence of the body is αU, so that a small wing is effectively at incidence 2α; thus we see from (112) that half of the extra lift comes from the wing and half from the body, approximately.

It is suggested that the result (111) will provide a sufficiently exact rule for estimating the effective lift for a wing of any shape attached to a body of revolution. Verification of this hypothesis must await an extended theory or experimental evidence.

REFERENCES

1. T. von Kármán, article in the *Proceedings of the 5th Volta Convention, Rome* (1935).
2. M. J. Lighthill, *Supersonic Flow past Bodies of Revolution*, Aero. Res. Council, R. & M. 2003 (1945).
3. ——, 'Supersonic flow past slender bodies of revolution, the slope of whose meridian section is discontinuous', *Quart. J. Mech. and Applied Math.* **1** (1948), 90.
4. H. S. Tsien, 'Supersonic flow over an inclined body of revolution', *Journal of Aero. Sci.* **5** (1938), 480–3.
5. R. T. Jones, *Properties of Low Aspect Ratio Pointed Wings at Speeds below and above the Speed of Sound*, N.A.C.A., T.N. 1032 (1946).

SUPERSONIC FLOW ROUND POINTED BODIES OF REVOLUTION

By J. B. BRODERICK

(*Department of Mathematics, The University, Manchester*)

[Received 25 November 1947. Revised 27 April 1948.]

SUMMARY

A method is developed for solving approximately the complete equation for isentropic axisymmetrical flow of a gas past bodies of revolution. The potential is expanded in powers of t and $\log t$ (t being the thickness ratio of the body), and the coefficients in this series are then expanded in powers of r and $\log r$ near the body, sufficient terms only being found to give the potential correct to order t^4 on the body. Arbitrary constants are found by the boundary conditions. From the result the pressure and drag coefficients are found correct to order t^4.

Introduction

THIS paper is a development of the work of Th. von Kármán and N. B. Moore (**1**) and M. J. Lighthill (**2**), who considered a linearized theory of supersonic flow past bodies of revolution.

In this paper we consider the general equation for isentropic, irrotational, axially symmetrical flow of a gas, neglecting viscosity and conductivity, past a thin body of revolution placed in a uniform, supersonic stream, with its axis lying in the direction of the undisturbed stream.

The equation of the body is taken in the form $r = tR(x)$, where t is the thickness of the body, its length being taken as unity. The potential at any point will therefore be a function of t, r and x. The potential is assumed to be expanded as a power series in t and $\log t$, whose coefficients are functions of x and r. This expansion is substituted in the differential equation and by equating powers of t and $\log t$, equations to determine the coefficients are obtained. These coefficients are then expanded in series of powers of r and $\log r$ whose coefficients are functions of x. These new coefficients are determined by making use of the differential equation, the boundary condition at the surface of the body, and the condition at infinity.

The first coefficient in the series of powers of t and $\log t$ is the linearized potential. This vanishes at infinity and by making use of its integral form we derive the expansion of this coefficient in powers of r and $\log r$, thereby using the conditions at infinity to fix the series. In deriving these series terms which are of order $t^6 \log^3 t$ or higher order† on the body are everywhere neglected. From the results obtained the pressure distribution on

† Terms containing the sixth or higher powers of t are neglected.

the body and the drag coefficient are each found as a sum of five terms in t^2, $t^2\log t$, t^4, $t^4\log t$ and $t^4\log^2 t$. The pressure coefficient is given by equation (78).

In actual fact the flow is not isentropic and it is necessary to consider to what order change in entropy at the shock-wave might affect the solution found. In other work [Lighthill (**4**), Broderick (**5**)], it has been shown that, for the case of axially symmetrical flow past a cone, the pressure difference everywhere is of order $t^2\log t$; the entropy change at the shock is of order t^{12}, and there is no difference in the drag and pressure coefficients between the complete solution and the isentropic solution if terms in $t^6\log^3 t$ are neglected. It appears probable that this holds in general for bodies of revolution.

Finally, a numerical example is worked out and curves drawn showing the relation between the pressure coefficients at the surfaces of cones with semi-vertical angles of 5°, 10° and 15°, and the Mach number; a comparison is made between the results found from this paper and the numerical results recently computed in America (**6**).

I am indebted to Mr. M. J. Lighthill for suggesting the above problem to me and for much helpful advice and criticism in its solution and in the preparation of this paper.

I. Solution of the equation for isentropic, irrotational flow of a gas past a body of revolution

If V is the velocity of the uniform stream, and $V\left(1+\frac{\partial\phi}{\partial x}\right)$ and $V\frac{\partial\phi}{\partial r}$ are the velocities at the point x, r when the body is placed in the stream, where x and r are cylindrical coordinates, then the equation of motion is

$$\nabla^2\phi = \frac{V^2}{c^2}\left\{2\left(1+\frac{\partial\phi}{\partial x}\right)\frac{\partial\phi}{\partial r}\,\frac{\partial^2\phi}{\partial x\partial r}+\left(1+\frac{\partial\phi}{\partial x}\right)^2\frac{\partial^2\phi}{\partial x^2}+\left(\frac{\partial\phi}{\partial r}\right)^2\frac{\partial^2\phi}{\partial r^2}\right\}, \tag{1}$$

where $c = \sqrt{(\gamma p/\rho)}$ is the local velocity of sound, given by

$$c^2 = c_0^2-\frac{\gamma-1}{2}V^2\left\{2\frac{\partial\phi}{\partial x}+\left(\frac{\partial\phi}{\partial x}\right)^2+\left(\frac{\partial\phi}{\partial r}\right)^2\right\}, \tag{2}$$

and p_0, ρ_0 are the pressure and density in the undisturbed stream.

Denoting V^2/c_0^2 by M^2, we obtain from (1) and (2)

$$\left[M^{-2}-\frac{\gamma-1}{2}\left\{2\frac{\partial\phi}{\partial x}+\left(\frac{\partial\phi}{\partial x}\right)^2+\left(\frac{\partial\phi}{\partial r}\right)^2\right\}\right]\nabla^2\phi$$
$$= \left(1+\frac{\partial\phi}{\partial x}\right)^2\frac{\partial^2\phi}{\partial x^2}+2\left(1+\frac{\partial\phi}{\partial x}\right)\frac{\partial\phi}{\partial r}\,\frac{\partial^2\phi}{\partial x\partial r}+\left(\frac{\partial\phi}{\partial r}\right)^2\frac{\partial^2\phi}{\partial r^2}. \tag{3}$$

The equation of the body of revolution will now be taken as $r = tR(x)$,

where its length is unity and its maximum thickness t, so that by varying t we are able to consider a system of co-axial bodies of revolution. We will assume that $R(x) = 0$ at $x = 0$ and that $R'(x)$ is finite at $x = 0$, so that the bodies of revolution are pointed at the origin. We also assume that $R(x)R'(x)$ is an analytic function† in the region $0 \leqslant x \leqslant 1$.

Since the potential is a function of t, r and x, it is reasonable to assume an expansion for ϕ in the form

$$\begin{aligned}\phi = t^2\phi_2+t^3\phi_3+t^4\phi_4+t^5\phi_5+t^6\phi_6+\ldots \\ +t^4\log t\,\phi_4' +t^6\log t\,\phi_6'+\ldots \\ +t^6\log^2 t\,\phi_6''+\ldots.\end{aligned} \tag{4}$$

(It is important to note that an accent *does not* denote differentiation when it occurs with a term ϕ_k. All derivatives of terms ϕ_k, ϕ_k', etc., will be written in full.)

It is not apparent here why the terms in $\log t$ are included in (4), but the reason will appear later by examining the boundary conditions at the surface of the body. It is found impossible to satisfy these conditions unless the terms in $\log t$ are introduced. Substituting the above expression for ϕ in (3) we obtain

$$\begin{aligned}&\left[M^{-2}-\frac{\gamma-1}{2}\left\{2t^2\frac{\partial\phi_2}{\partial x}+2t^3\frac{\partial\phi_3}{\partial x}+2t^4\log t\frac{\partial\phi_4'}{\partial x}+2t^4\frac{\partial\phi_4}{\partial x}+t^4\left(\frac{\partial\phi_2}{\partial x}\right)^2+\right.\right.\\ &\qquad\left.\left.+t^4\left(\frac{\partial\phi_2}{\partial r}\right)^2+O(t^5)\right\}\right][t^2\nabla^2\phi_2+t^3\nabla^2\phi_3+t^4\log t\,\nabla^2\phi_4'+t^4\nabla^2\phi_4+t^5\nabla^2\phi_5+\\ &\qquad\qquad+t^6\nabla^2\phi_6+t^6\log t\,\nabla^2\phi_6'+t^6\log^2 t\,\nabla^2\phi_6''+O(t^7)]\\ &=\left[1+t^2\frac{\partial\phi_2}{\partial x}+t^3\frac{\partial\phi_3}{\partial x}+t^4\log t\frac{\partial\phi_4'}{\partial x}+t^4\frac{\partial\phi_4}{\partial x}+O(t^5)\right]^2\times\\ &\qquad\times\left[t^2\frac{\partial^2\phi_2}{\partial x^2}+t^3\frac{\partial^2\phi_3}{\partial x^2}+t^4\log t\frac{\partial^2\phi_4'}{\partial x^2}+t^4\frac{\partial^2\phi_4}{\partial x^2}+t^5\frac{\partial^2\phi_5}{\partial x^2}+\right.\\ &\qquad\qquad\left.+t^6\frac{\partial^2\phi_6}{\partial x^2}+t^6\log t\frac{\partial^2\phi_6'}{\partial x^2}+t^6\log^2 t\frac{\partial^2\phi_6''}{\partial x^2}+O(t^7)\right]+\\ &\quad+2\left[1+t^2\frac{\partial\phi_2}{\partial x}+O(t^3)\right]\left[t^2\frac{\partial\phi_2}{\partial r}+t^3\frac{\partial\phi_3}{\partial r}+t^4\log t\frac{\partial\phi_4'}{\partial r}+t^4\frac{\partial\phi_4}{\partial r}+O(t^5)\right]\times\\ &\qquad\times\left[t^2\frac{\partial^2\phi_2}{\partial x\partial r}+t^3\frac{\partial^2\phi_3}{\partial x\partial r}+t^4\log t\frac{\partial^2\phi_4'}{\partial x\partial r}+t^4\frac{\partial^2\phi_4}{\partial x\partial r}+O(t^5)\right]+\\ &\qquad\qquad+t^6\left(\frac{\partial\phi_2}{\partial r}\right)^2\frac{\partial^2\phi_2}{\partial r^2}+O(t^7).\end{aligned} \tag{5}$$

† $R(x)R'(x)$ may be expanded in a Taylor series near each point in the interval.

Equating coefficients of powers of t and $\log t$ in this equation we obtain the following equations:

$$\text{For } t^2:\quad M^{-2}\nabla^2\phi_2-\frac{\partial^2\phi_2}{\partial x^2}=0, \tag{6}$$

$$t^3:\quad M^{-2}\nabla^2\phi_3-\frac{\partial^2\phi_3}{\partial x^2}=0, \tag{7}$$

$$t^4\log t:\quad M^{-2}\nabla^2\phi_4'-\frac{\partial^2\phi_4'}{\partial x^2}=0, \tag{8}$$

$$t^4:\quad M^{-2}\nabla^2\phi_4-\frac{\partial^2\phi_4}{\partial x^2}=(\gamma-1)\frac{\partial\phi_2}{\partial x}\nabla^2\phi_2+2\frac{\partial\phi_2}{\partial x}\frac{\partial^2\phi_2}{\partial x^2}+2\frac{\partial\phi_2}{\partial r}\frac{\partial^2\phi_2}{\partial x\partial r}, \tag{9}$$

$$t^5:\quad M^{-2}\nabla^2\phi_5-\frac{\partial^2\phi_5}{\partial x^2}=(\gamma-1)\frac{\partial\phi_2}{\partial x}\nabla^2\phi_3+(\gamma-1)\frac{\partial\phi_3}{\partial x}\nabla^2\phi_2+$$
$$+2\frac{\partial\phi_2}{\partial x}\frac{\partial^2\phi_3}{\partial x^2}+2\frac{\partial\phi_3}{\partial x}\frac{\partial^2\phi_2}{\partial x^2}+2\frac{\partial\phi_2}{\partial r}\frac{\partial^2\phi_3}{\partial x\partial r}+2\frac{\partial\phi_3}{\partial r}\frac{\partial^2\phi_2}{\partial x\partial r}, \tag{10}$$

$$t^6:\quad M^{-2}\nabla^2\phi_6-\frac{\partial^2\phi_6}{\partial x^2}=(\gamma-1)\frac{\partial\phi_2}{\partial x}\nabla^2\phi_4+(\gamma-1)\frac{\partial\phi_3}{\partial x}\nabla^2\phi_3+$$
$$+(\gamma-1)\frac{\partial\phi_4}{\partial x}\nabla^2\phi_2+\frac{\gamma-1}{2}\left(\frac{\partial\phi_2}{\partial x}\right)^2\nabla^2\phi_2+\frac{\gamma-1}{2}\left(\frac{\partial\phi_2}{\partial r}\right)^2\nabla^2\phi_2+2\frac{\partial\phi_2}{\partial x}\frac{\partial^2\phi_4}{\partial x^2}+$$
$$+2\frac{\partial\phi_3}{\partial x}\frac{\partial^2\phi_3}{\partial x^2}+2\frac{\partial\phi_4}{\partial x}\frac{\partial^2\phi_2}{\partial x^2}+\left(\frac{\partial\phi_2}{\partial x}\right)^2\frac{\partial^2\phi_2}{\partial x^2}+2\frac{\partial\phi_2}{\partial r}\frac{\partial\phi_2}{\partial x}\frac{\partial^2\phi_2}{\partial x\partial r}+$$
$$+2\frac{\partial\phi_2}{\partial r}\frac{\partial^2\phi_4}{\partial x\partial r}+2\frac{\partial\phi_4}{\partial r}\frac{\partial^2\phi_2}{\partial x\partial r}+2\frac{\partial\phi_3}{\partial r}\frac{\partial^2\phi_3}{\partial x\partial r}+\left(\frac{\partial\phi_2}{\partial r}\right)^2\frac{\partial^2\phi_2}{\partial r^2}, \tag{11}$$

$$t^6\log t:\quad M^{-2}\nabla^2\phi_6'-\frac{\partial^2\phi_6'}{\partial x^2}=(\gamma-1)\frac{\partial\phi_2}{\partial x}\nabla^2\phi_4'+(\gamma-1)\frac{\partial\phi_4'}{\partial x}\nabla^2\phi_2+$$
$$+2\frac{\partial\phi_2}{\partial x}\frac{\partial^2\phi_4'}{\partial x^2}+2\frac{\partial\phi_4'}{\partial x}\frac{\partial^2\phi_2}{\partial x^2}+2\frac{\partial\phi_2}{\partial r}\frac{\partial^2\phi_4'}{\partial x\partial r}+2\frac{\partial\phi_4'}{\partial r}\frac{\partial^2\phi_2}{\partial x\partial r}, \tag{12}$$

$$t^6\log^2 t:\quad M^{-2}\nabla^2\phi_6''-\frac{\partial^2\phi_6''}{\partial x^2}=0. \tag{13}$$

Kármán and Moore (**1**), and M. J. Lighthill (**2**), have shown that the solution of equation (6), applicable to the case of flow round a body of revolution, is

$$\phi_2=-\int\limits_0^{x-\alpha r}\frac{f(y)\,dy}{\sqrt{\{(x-y)^2-\alpha^2r^2\}}} \tag{14}$$

$$=-K_0(\alpha pr)f(x) \tag{15}$$

in the Heaviside notation, with p^{-1} written for $\int\limits_0^x dx$ and α for $\sqrt{(M^2-1)}$;

$f(x)$ is an arbitrary function which, however, is zero for $x \leqslant 0$ and for $x > 1$, and K_0 is the modified Bessel function of order zero. Expanding the Bessel function we have

$$\phi_2 = -\sum_{n=0}^{\infty} [b_n(\alpha pr)^{2n} - a_n(\alpha pr)^{2n}\log(\alpha pr)]\, f(x), \tag{16}$$

which is a series involving powers of r and $\log r$ times a series in powers of r. The first few terms of (16) can be written

$$K + A\log r + Br^2 + Cr^2\log r + \ldots, \tag{17}$$

where

$$A = f(x), \tag{18}$$

$$K = (\log\tfrac{1}{2}\alpha p + \gamma)f(x) = f(x)\log\tfrac{1}{2}\alpha - \int_0^x f'(y)\log(x-y)\,dy, \tag{19}$$

by the formula $\log x = -\log p - \gamma$ and the Heaviside representation of a Faltung integral,

$$C = \tfrac{1}{4}\alpha^2 p^2 f(x) = \tfrac{1}{4}\alpha^2 f''(x), \tag{20}$$

and

$$B = \tfrac{1}{4}\alpha^2 p^2(\log\tfrac{1}{2}\alpha p + \gamma - 1)f(x) = \tfrac{1}{4}\alpha^2[K''(x) - f''(x)], \tag{21}$$

where an accent denotes differentiation with respect to x.

Subsequent terms in the series (17) could be similarly found, or alternatively by substituting (17) in equation (6). However, the next term in (17) is $O(r^4\log r)$ which on the body is $O(t^4\log t)$, and thus, in the term $t^2\phi_2$ in the expansion (4) for ϕ, terms $O(t^6\log t)$ have been neglected. It will be seen later that $f(x)$ is determined by the boundary condition and hence that the series (17) is determined uniquely. The series (17) is valid in the region $0 \leqslant x \leqslant 1$ and by obtaining it as above from the integral form (14), we ensure that the boundary condition at infinity is satisfied. The expression (14) gives the value of ϕ_2 everywhere inside the Mach cone $x = \alpha r$ while $\phi_2 = 0$ in the region in front of this cone.

Since ϕ_3 and ϕ_4' satisfy the same equation as ϕ_2 we may assume that

$$\left.\begin{aligned} \phi_3 &= K_1 + A_1\log r + B_1 r^2 + \ldots \\ \text{and} \qquad \phi_4' &= k + a\log r + br^2 + \ldots. \end{aligned}\right\} \tag{22}$$

It will later become apparent from the boundary condition at $r = tR(x)$ that $\phi_3 \equiv 0$. Using this fact and equation (10) we see that ϕ_5 has also the form

$$k_1 + a_1\log r + b_1 r^2 + \ldots, \tag{23}$$

and ϕ_5 will also be seen to vanish identically by considering the boundary condition.

Now equation (9) may be written

$$\frac{\partial^2\phi_4}{\partial r^2}+\frac{1}{r}\frac{\partial\phi_4}{\partial r}-\alpha^2\frac{\partial^2\phi_4}{\partial x^2} = \{2M^2+(\gamma-1)M^4\}\frac{\partial\phi_2}{\partial x}\frac{\partial^2\phi_2}{\partial x^2}+2M^2\frac{\partial\phi_2}{\partial r}\frac{\partial^2\phi_2}{\partial x\partial r}$$
$$= F(x,r), \text{ say.} \tag{24}$$

When r is small and $0 \leqslant x \leqslant 1$, we have

$$\left.\begin{aligned}\frac{\partial\phi_2}{\partial r} &= \frac{A}{r}+(2B+C)r+2Cr\log r+O(r^3\log r),\\ \text{and}\quad \frac{\partial^2\phi_2}{\partial x\partial r} &= \frac{A'}{r}+(2B'+C')r+2C'r\log r+O(r^3\log r).\end{aligned}\right\} \tag{25}$$

Hence

$$\frac{\partial\phi_2}{\partial r}\frac{\partial^2\phi_2}{\partial x\partial r} = \frac{AA'}{r^2}+A(2B'+C')+A'(2B+C)+$$
$$+2(AC'+A'C)\log r+O(r^2\log^2 r), \tag{26}$$

and

$$\frac{\partial\phi_2}{\partial x}\frac{\partial^2\phi_2}{\partial x^2} = \{K'+A'\log r+O(r^2\log r)\}\{K''+A''\log r+O(r^2\log r)\}. \tag{27}$$

Hence from equation (24) we may write, *when r is small and $0 \leqslant x \leqslant 1$*,

$$F(x,r) = \frac{P}{r^2}+Q\log^2 r+R\log r+S+O(r^2\log^2 r), \tag{28}$$

where $P = 2M^2AA'$ and we do not need the values of the other coefficients.

We solve equation (24) by Heaviside operators and, since $\phi_4 = 0$ and $\partial\phi_4/\partial x = 0$ when $x = 0$, the equation becomes

$$\frac{\partial^2\phi_4}{\partial r^2}+\frac{1}{r}\frac{\partial\phi_4}{\partial r}-\alpha^2p^2\phi_4 = F(x,r). \tag{29}$$

If $F(x,r)$ is replaced by zero then two independent solutions of (29) are $I_0(\alpha pr)$ and $K_0(\alpha pr)$, where I_0 and K_0 are the modified Bessel functions of zero order. Now denoting $I_0(\alpha pr)$ by $l(r)$ and $K_0(\alpha pr)$ by $m(r)$, and putting $l'm-lm' = w$, the general solution of (29) is given by

$$\phi_4 = l(r)\int^r \frac{m(r)}{w}F\,dr-m(r)\int^r \frac{l(r)}{w}F\,dr, \tag{30}$$

where $w = 1/r$, and hence we may write

$$\phi_4 = -K_0(\alpha pr)\int_a^r sI_0(\alpha ps)F(x,s)\,ds-I_0(\alpha pr)\int_r^\infty sK_0(\alpha ps)F(x,s)\,ds, \tag{31}$$

where a is independent of r. The limits have been chosen so that ϕ_4 represents a disturbance travelling in such a manner that x increases with r, which is easily seen by considering the asymptotic expansions of I_0 and

K_0. Also ϕ_4 is zero in the region $x \leqslant \alpha r$. To find the form of ϕ_4 when r is small we have

$$\left.\begin{aligned} I_0(\alpha pr) &= 1+O(r^2),\\ \text{and}\qquad K_0(\alpha pr) &= \left(\log\frac{2}{\alpha pr}-\gamma\right)+O(r^2\log r).\end{aligned}\right\} \tag{32}$$

Hence, neglecting terms of order $r^2\log^3 r$, we have from (31)

$$\phi_4 = -\left(\log\frac{2}{\alpha pr}-\gamma\right)\int\limits_a^r \frac{P}{s}\,ds-\left(\log\frac{2}{\alpha pr}-\gamma\right)C-$$
$$-\int\limits_r^\infty K_0(\alpha ps)\frac{P}{s}\,ds-\int\limits_0^\infty sK_0(\alpha ps)\left\{F(x,s)-\frac{P}{s^2}\right\}ds, \tag{33}$$

where C is a function of a.

Now

$$-\int\limits_0^\infty sK_0(\alpha ps)\left\{F(x,s)-\frac{P}{s^2}\right\}ds-\int\limits_r^\infty K_0(\alpha ps)\frac{P}{s}\,ds$$
$$= -\int\limits_0^\infty du\int\limits_0^{x/\alpha(\cosh u+1)} s\left\{F(x-\alpha s\cosh u,s)-\frac{P(x-\alpha s\cosh u)}{s^2}\right\}ds-$$
$$-\int\limits_0^{\cosh^{-1}[(x/\alpha r)-1]} du\int\limits_r^{x/\alpha(\cosh u+1)} \frac{P(x-\alpha s\cosh u)}{s}\,ds, \tag{34}$$

and

$$-\int\limits_0^{\cosh^{-1}[(x/\alpha r)-1]} du\int\limits_r^{x/\alpha(\cosh u+1)} \frac{P(x-\alpha s\cosh u)}{s}\,ds$$
$$= -\int\limits_0^{\cosh^{-1}[(x/\alpha r)-1]} du\int\limits_r^{x/\alpha(\cosh u+1)} \sum_{n=0}^{\infty}(-1)^n\frac{P^{(n)}(x)\alpha^n s^n\cosh^n u}{n!\,s}\,ds$$
$$= -\int\limits_0^{\cosh^{-1}[(x/\alpha r)-1]} du\left[P(x)\log\frac{x}{\alpha r(\cosh u+1)}+\sum_{n=1}^{\infty}(-1)^n\frac{P^{(n)}(x)x^n\cosh^n u}{n!\,n(\cosh u+1)^n}+\right.$$
$$\left.+P'(x)\alpha r\cosh u+O(r^2)\right], \tag{35}$$

where $P^{(n)}(x)$ denotes the nth derivative of $P(x)$.

When r is small

$$\cosh^{-1}\left(\frac{x}{\alpha r}-1\right)\sim\log\frac{2x}{\alpha r}-\frac{\alpha r}{x}+O(r^2),$$

and therefore

$$-\int\limits_0^{\cosh^{-1}[(x/\alpha r)-1]} \frac{\cosh^n u}{(1+\cosh u)^n}\,du$$

$$= -\log\frac{2x}{\alpha r} - \int\limits_0^{\infty} \frac{\cosh^n u-(1+\cosh u)^n}{(1+\cosh u)^n}\,du+O(r). \qquad (36)$$

Also

$$-\int\limits_0^{\cosh^{-1}[(x/\alpha r)-1]} P'(x)\alpha r\cosh u\,du = -P'(x)\alpha r\sqrt{\left\{\left(\frac{x}{\alpha r}-1\right)^2-1\right\}}$$

$$= -xP'(x)+O(r), \qquad (37)$$

and

$$-\int\limits_0^{\cosh^{-1}[(x/\alpha r)-1]} P(x)\log\frac{x}{\alpha r(1+\cosh u)}\,du$$

$$= -P(x)\log\frac{x}{\alpha r}\left[\log\frac{2x}{\alpha r}-\frac{\alpha r}{x}+O(r^2)\right]+P(x)\left[\int\limits_0^{\cosh^{-1}[(x/\alpha r)-1]} (u-\log 2)\,du+\right.$$

$$+\int\limits_0^{\infty}\{\log(1+\cosh u)-u-\log 2\}\,du-$$

$$\left.-\int\limits_{\cosh^{-1}[(x/\alpha r)-1]}^{\infty}\{\log(1+\cosh u)-u-\log 2\}\,du\right]$$

$$= -P(x)\log\frac{x}{\alpha r}\left[\log\frac{2x}{\alpha r}-\frac{\alpha r}{x}+O(r^2)\right]+P(x)\left[\tfrac{1}{2}\log^2\frac{2x}{\alpha r}-\frac{\alpha r}{x}\log\frac{2x}{\alpha r}+\right.$$

$$\left.+O(r^2\log r)-\log 2\log\frac{2x}{\alpha r}+\frac{\alpha r}{x}\log 2+O(r^2)+\tfrac{1}{6}\pi^2+O(r)\right]$$

$$= P(x)\left[\tfrac{1}{6}\pi^2-\tfrac{1}{2}\log^2\frac{2x}{\alpha r}+O(r)\right]. \qquad (38)$$

Finally, from (35), (36), (37) and (38) we deduce that

$$-\int\limits_0^{\cosh^{-1}[(x/\alpha r)-1]} du \int\limits_r^{x/\alpha(\cosh u+1)} \frac{P(x-\alpha s\cosh u)}{s}\,ds$$

$$= P(x)\left[\tfrac{1}{6}\pi^2-\tfrac{1}{2}\log^2\frac{2x}{\alpha r}\right]-xP'(x)+$$

$$+\sum_{n=1}^{\infty}(-1)^{n+1}\frac{P^{(n)}(x)x^n}{n!\,n}\left[\log\frac{2x}{\alpha r}+\int\limits_0^{\infty}\frac{\cosh^n u-(1+\cosh u)^n}{(1+\cosh u)^n}\,du\right]+O(r).$$

$$(39)$$

Therefore, neglecting terms in $r^2\log^3 r$, we write from (33) and (39)

$$\phi_4 = -\Big(\log\frac{2}{\alpha pr}-\gamma\Big)(\log r-\log a)P-\Big(\log\frac{2}{\alpha pr}-\gamma\Big)C-$$

$$-\int\limits_0^\infty du \int\limits_0^{x/\alpha(\cosh u+1)} s\Big\{F(x-\alpha s\cosh u, s)-\frac{P(x-\alpha s\cosh u)}{s^2}\Big\}\, ds+$$

$$+P(x)\Big[\tfrac{1}{6}\pi^2-\tfrac{1}{2}\log^2\frac{2x}{\alpha}-\tfrac{1}{2}\log^2 r+\log\frac{2x}{\alpha}\log r\Big]-xP'(x)+$$

$$+\sum_{n=1}^\infty(-1)^{n+1}\frac{P^{(n)}(x)x^n}{n!\,n}\Big[\log\frac{2x}{\alpha}-\log r+$$

$$+\int\limits_0^\infty\frac{\cosh^n u-(1+\cosh u)^n}{(1+\cosh u)^n}\,du\Big]+O(r), \tag{40}$$

and hence ϕ_4 has the form

$$\begin{aligned}&\alpha_1\log^2 r+\beta_1 r^2\log^2 r+O(r^4\log^2 r)+\\&+\gamma_1\log r+\delta_1 r^2\log r+O(r^4\log r)+\\&+\epsilon_1 \qquad +\eta_1 r^2 \qquad +O(r^4)\end{aligned} \tag{41}$$

(since the terms in $r^2\log^3 r$ and r must vanish as ϕ_4 satisfies equation (24) when $F(x,r)$ is given by (28)).

From (40) and (41) we deduce that

$$\alpha_1 = \tfrac{1}{2}P, \tag{42}$$

$$\begin{aligned}\gamma_1 &= C-P\log a+P(\gamma+\log\tfrac{1}{2}\alpha p)+P\log\frac{2x}{\alpha}-\sum_{n=1}^\infty(-1)^{n+1}\frac{P^{(n)}(x)x^n}{n!\,n}\\&= C-P\log a,\end{aligned} \tag{43}$$

from the interpretation of the operational forms and since

$$P(x)\log x-\int\limits_0^x P'(x-y)\log y\,dy = \sum_{n=1}^\infty(-1)^{n+1}\frac{P^{(n)}(x)x^n}{n!\,n},$$

and

$$\epsilon_1 = (C-P\log a)(\log\tfrac{1}{2}\alpha p+\gamma)-\int\limits_0^\infty du\int\limits_0^{x/\alpha(\cosh u-1)} s\Big\{F(x-\alpha s\cosh u, s)-$$

$$-\frac{P(x-\alpha s\cosh u)}{s^2}\Big\}\,ds+P(x)\Big(\tfrac{1}{6}\pi^2-\tfrac{1}{2}\log^2\frac{2x}{\alpha}\Big)-xP'(x)+$$

$$+\Big\{P(x)\log x-\int\limits_0^x P'(y)\log(x-y)\,dy\Big\}\log\frac{2x}{\alpha}+$$

$$+\sum_1^\infty(-1)^{n+1}\frac{P^{(n)}(x)x^n}{n!\,n}\int\limits_0^\infty\frac{\cosh^n u-(1+\cosh u)^n}{(1+\cosh u)^n}\,du. \tag{44}$$

Eliminating C and a from (43) and (44) we find that

$$\epsilon_1 = \gamma_1(x)\log\tfrac{1}{2}\alpha - \int\limits_0^x \gamma_1'(y)\log(x-y)\,dy + P(x)\left(\tfrac{1}{6}\pi^2 - \tfrac{1}{2}\log^2\frac{2x}{\alpha}\right) - xP'(x) -$$

$$- \int\limits_0^\infty du \int\limits_0^{x/\alpha(\cosh u+1)} s\left\{F(x-\alpha s\cosh u, s) - \frac{P(x-\alpha s\cosh u)}{s^2}\right\} ds +$$

$$+ \left\{P(x)\log x - \int\limits_0^x P'(y)\log(x-y)\,dy\right\}\log\frac{2x}{a} +$$

$$+ \int\limits_0^\infty du\left[\int\limits_{x\cosh u/(1+\cosh u)}^x P'(x-y)\log y\,dy + P(x)\log\frac{\cosh u}{1+\cosh u} -\right.$$

$$\left. - P\left(\frac{x}{1+\cosh u}\right)\log\frac{x\cosh u}{1+\cosh u}\right]. \quad (45)$$

Hence in the solution (41), α_1 and ϵ_1 have been determined and later γ_1 will be determined by the boundary condition at the surface of the body, thus making the solution unique. The terms neglected in (41) are $O(t^2\log^2 t)$ on the body, and the corresponding terms in the expansion for ϕ are $O(t^6\log^2 t)$.

The next step is to solve equation (11) for ϕ_6. Using the fact that ϕ_3 and ϕ_5 vanish identically, (11) may be written

$$M^{-2}\nabla^2\phi_6 - \frac{\partial^2\phi_6}{\partial x^2} = (\gamma-1)\frac{\partial\phi_2}{\partial x}\nabla^2\phi_4 + (\gamma-1)\frac{\partial\phi_4}{\partial x}\nabla^2\phi_2 + \frac{\gamma-1}{2}\left(\frac{\partial\phi_2}{\partial x}\right)^2\nabla^2\phi_2 +$$

$$+ \frac{\gamma-1}{2}\left(\frac{\partial\phi_2}{\partial r}\right)^2\nabla^2\phi_2 + 2\frac{\partial\phi_2}{\partial x}\frac{\partial^2\phi_4}{\partial x^2} + 2\frac{\partial\phi_4}{\partial x}\frac{\partial^2\phi_2}{\partial x^2} + \left(\frac{\partial\phi_2}{\partial x}\right)^2\frac{\partial^2\phi_2}{\partial x^2} +$$

$$+ 2\frac{\partial\phi_2}{\partial r}\frac{\partial\phi_2}{\partial x}\frac{\partial^2\phi_2}{\partial x\partial r} + 2\frac{\partial\phi_2}{\partial r}\frac{\partial^2\phi_4}{\partial x\partial r} + 2\frac{\partial\phi_4}{\partial r}\frac{\partial^2\phi_2}{\partial x\partial r} + \left(\frac{\partial\phi_2}{\partial r}\right)^2\frac{\partial^2\phi_2}{\partial r^2}. \quad (46)$$

Since $\nabla^2\phi_2 = M^2\dfrac{\partial^2\phi_2}{\partial x^2}$, (46) may be written

$$\frac{\partial^2\phi_6}{\partial r^2} + \frac{1}{r}\frac{\partial\phi_6}{\partial r} - \alpha^2\frac{\partial^2\phi_6}{\partial x^2} = (\gamma-1)M^2\frac{\partial\phi_2}{\partial x}\nabla^2\phi_4 + (\gamma-1)M^4\frac{\partial\phi_4}{\partial x}\frac{\partial^2\phi_2}{\partial x^2} +$$

$$+ \frac{\gamma-1}{2}M^4\left(\frac{\partial\phi_2}{\partial x}\right)^2\frac{\partial^2\phi_2}{\partial x^2} + \frac{\gamma-1}{2}M^4\left(\frac{\partial\phi_2}{\partial r}\right)^2\frac{\partial^2\phi_2}{\partial x^2} + 2M^2\left(\frac{\partial\phi_2}{\partial x}\frac{\partial^2\phi_4}{\partial x^2} + \frac{\partial\phi_4}{\partial x}\frac{\partial^2\phi_2}{\partial x^2}\right) +$$

$$+ M^2\left(\frac{\partial\phi_2}{\partial x}\right)^2\frac{\partial^2\phi_2}{\partial x^2} + 2M^2\frac{\partial^2\phi_2}{\partial x\partial r}\frac{\partial\phi_2}{\partial x}\frac{\partial\phi_2}{\partial r} + 2M^2\left(\frac{\partial\phi_2}{\partial r}\frac{\partial^2\phi_4}{\partial x\partial r} + \frac{\partial\phi_4}{\partial r}\frac{\partial^2\phi_2}{\partial x\partial r}\right) +$$

$$+ M^2\left(\frac{\partial\phi_2}{\partial r}\right)^2\frac{\partial^2\phi_2}{\partial r^2}. \quad (47)$$

Now we have

$$\left.\begin{aligned}
\nabla^2\phi_4 &= \frac{2\alpha_1}{r^2}+O(\log^2 r), \qquad \frac{\partial^2\phi_4}{\partial x^2} = O(\log^2 r),\\
\frac{\partial^2\phi_4}{\partial x\partial r} &= \frac{2\alpha_1'\log r}{r}+\frac{\gamma_1'}{r}+O(r\log^2 r),\\
\frac{\partial\phi_2}{\partial x} &= A'\log r+K'+O(r^2\log r),\\
\frac{\partial\phi_2}{\partial r} &= \frac{A}{r}+(2B+C)r+2Cr\log r+O(r^3\log r),\\
\frac{\partial^2\phi_2}{\partial r^2} &= -\frac{A}{r^2}+(2B+3C)+2C\log r+O(r^2\log r).
\end{aligned}\right\} \tag{48}$$

Substituting these values in equation (47) we obtain

$$\begin{aligned}
&\frac{\partial^2\phi_6}{\partial r^2}+\frac{1}{r}\frac{\partial\phi_6}{\partial r}-\alpha^2\frac{\partial^2\phi_6}{\partial x^2}\\
&= (\gamma-1)M^2\{A'\log r+K'+O(r^2\log r)\}\left\{\frac{2\alpha_1}{r^2}+O(\log^2 r)\right\}+\\
&\quad+(\gamma-1)M^4O(\log^3 r)+\frac{\gamma-1}{2}M^4O(\log^3 r)+\\
&\quad+\frac{\gamma-1}{2}M^4\left\{\frac{A^2}{r^2}+O(\log r)\right\}\{A''\log r+K''+O(r^2\log r)\}+2M^2O(\log^3 r)+\\
&\quad+2M^2\{A'\log r+K'+O(r^2\log r)\}\left\{\frac{A}{r}+O(r\log r)\right\}\left\{\frac{A'}{r}+O(r\log r)\right\}+\\
&\quad+2M^2\left\{\frac{2\alpha_1\log r}{r}+\frac{\gamma_1}{r}+O(r\log^2 r)\right\}\left\{\frac{A'}{r}+O(r\log r)\right\}+\\
&\quad+M^2\left\{\frac{A^2}{r^2}+2(2B+C)A+4AC\log r+O(r^2\log^2 r)\right\}\times\\
&\qquad\qquad\times\left\{-\frac{A}{r^2}+(2B+3C)+2C\log r+O(r^2\log r)\right\}+\\
&\quad+2M^2\left\{\frac{A}{r}+O(r\log r)\right\}\left\{\frac{2\alpha_1'\log r}{r}+\frac{\gamma_1'}{r}+O(r\log^2 r)\right\},
\end{aligned} \tag{49}$$

which, on collecting terms, becomes

$$\frac{\partial^2\phi_6}{\partial r^2}+\frac{1}{r}\frac{\partial\phi_6}{\partial r}-\alpha^2\frac{\partial^2\phi_6}{\partial x^2}$$

$$\begin{aligned}
&= -\frac{A^3M^2}{r^4}+\frac{1}{r^2}\Big[(\gamma-1)M^2 2\alpha_1 K'+\frac{\gamma-1}{2}M^4A^2K''+2M^2AA'K'+\\
&\qquad +2M^2A\gamma_1'+2M^2A'\gamma_1+M^2\{A^2(2B+C)-2A^2(2B+C)\}\Big]+\\
&\quad +\frac{\log r}{r^2}\Big[(\gamma-1)M^2 2\alpha_1 A'+\frac{\gamma-1}{2}M^4A^2A''+2M^2AA'^2+4M^2A\alpha_1'+\\
&\qquad +4M^2A'\alpha_1-2M^2A^2C\Big]+O(\log^3 r),\\
&= \frac{P_2}{r^4}+\frac{Q_2}{r^2}+\frac{R_2\log r}{r^2}+O(\log^3 r),
\end{aligned} \tag{50}$$

where $$P_2 = -A^3M^2 = -M^2f^3, \tag{51}$$

and we do not need the values of the other coefficients.

To solve equation (50) put

$$\phi_6 = \frac{\alpha_2}{r^2}+\beta_2+O(r^2)+\gamma_2\log r+O(r^2\log r)+\delta_2\log^2 r+O(r^2\log^2 r)+$$
$$+\epsilon_2\log^3 r+O(r^2\log^3 r). \tag{52}$$

Then
$$\left.\begin{aligned}
\frac{\partial\phi_6}{\partial r} &= -\frac{2\alpha_2}{r^3}+O(r)+\frac{\gamma_2}{r}+O(r\log r)+\\
&\quad +2\delta_2\frac{\log r}{r}+O(r\log^2 r)+\frac{3\epsilon_2\log^2 r}{r}+O(r\log^3 r),\\
\text{and}\quad &\\
\frac{\partial^2\phi_6}{\partial r^2} &= \frac{6\alpha_2}{r^4}-\frac{\gamma_2}{r^2}-\frac{2\delta_2\log r}{r^2}+\frac{2\delta_2}{r^2}+\frac{6\epsilon_2\log r}{r^2}-\frac{3\epsilon_2\log^2 r}{r^2}+O(\log^3 r).
\end{aligned}\right\} \tag{53}$$

Hence $$\frac{\partial^2\phi_6}{\partial r^2}+\frac{1}{r}\frac{\partial\phi_6}{\partial r}-\alpha^2\frac{\partial^2\phi_6}{\partial r^2} = \frac{4\alpha_2}{r^4}+\frac{2\delta_2}{r^2}+\frac{6\epsilon_2\log r}{r^2}-\frac{\alpha^2\alpha_2''}{r^2}+O(\log^3 r), \tag{54}$$

and, comparing (50) and (54), we obtain

$$4\alpha_2 = P_2, \qquad 2\delta_2-\alpha^2\alpha_2'' = Q_2, \qquad 6\epsilon_2 = R_2. \tag{55}$$

These equations determine α_2, δ_2, and ϵ_2 uniquely. By proceeding further it can be shown that γ_2 and β_2 are completely arbitrary, and that all the other coefficients are determined in terms of γ_2 and β_2 and known quantities. Later we shall see that γ_2 is determined by the boundary condition at the surface of the body and β_2 could then be obtained in terms of γ_2 as ϵ_1 was obtained in terms of γ_1, by using the condition at infinity. The only coefficient in ϕ_6 which we require is α_2 which is given by

$$\alpha_2 = \frac{P_2}{4} = -\frac{M^2f^3}{4}. \tag{56}$$

Terms neglected in (52) are then $O(\log^3 t)$ on the body and the corresponding terms in ϕ are $O(t^6 \log^3 t)$.

Equation (12) for ϕ_6' may be written

$$\frac{\partial^2\phi_6'}{\partial r^2}+\frac{1}{r}\frac{\partial\phi_6'}{\partial r}-\alpha^2\frac{\partial^2\phi_6'}{\partial x^2} = (\gamma-1)M^2\frac{\partial\phi_2}{\partial x}\nabla^2\phi_4'+(\gamma-1)M^4\frac{\partial\phi_4'}{\partial x}\frac{\partial^2\phi_2}{\partial x^2}+$$

$$+2M^2\frac{\partial^2\phi_4'}{\partial x^2}\frac{\partial\phi_2}{\partial x}+2M^2\frac{\partial\phi_4'}{\partial x}\frac{\partial^2\phi_2}{\partial x^2}+2M^2\frac{\partial\phi_2}{\partial r}\frac{\partial^2\phi_4'}{\partial x\partial r}+2M^2\frac{\partial^2\phi_2}{\partial x\partial r}\frac{\partial\phi_4'}{\partial r}. \quad (57)$$

From the values of ϕ_2 and ϕ_4' already found it is clear that the right-hand side of (57), when expanded in powers of r, has the same form as the right-hand side of (24), and hence

$$\phi_6' = \alpha_3\log^2 r+O(r^2\log^2 r)+\beta_3+O(r^2)+\gamma_3\log r+O(r^2\log r), \quad (58)$$

where, exactly as in the case of ϕ_4, γ_3 is determined by the boundary condition at the surface of the body, and β_3 by the condition at infinity, and all the other coefficients are then fixed uniquely. Since none of these coefficients are required in the following work we shall not determine them. The lowest order term in ϕ due to ϕ_6' is $O(t^6\log^3 t)$ on the body which we neglect.

Finally, the solution of equation (13) is evidently of the form

$$\phi_6'' = K_2+A_2\log r+B_2 r^2+C_2 r^2\log r+O(r^4\log r), \quad (59)$$

where A_2 is determined by the boundary condition at the body, and K_2 in terms of A_2 by the condition at infinity.

This completes the useful information we can find from equations (6) to (13). To determine the coefficients in the previous series which are still arbitrary it is necessary to consider the boundary condition at the surface of the body $r = tR(x)$. This boundary condition is

$$\frac{\partial\phi/\partial r}{1+\partial\phi/\partial x} = tR'(x), \quad (60)$$

when $r = tR(x)$.

Substituting the expression (4) for ϕ in (60) the boundary condition becomes

$$\Big[t^2\frac{\partial\phi_2}{\partial r}+t^3\frac{\partial\phi_3}{\partial r}+t^4\log t\frac{\partial\phi_4'}{\partial r}+t^4\frac{\partial\phi_4}{\partial r}+t^5\frac{\partial\phi_5}{\partial r}+t^6\frac{\partial\phi_6}{\partial r}+$$

$$+t^6\log t\frac{\partial\phi_6'}{\partial r}+t^6\log^2 t\frac{\partial\phi_6''}{\partial r}+\ldots\Big]\div$$

$$\div\Big[1+t^2\frac{\partial\phi_2}{\partial x}+t^3\frac{\partial\phi_3}{\partial x}+t^4\log t\frac{\partial\phi_4'}{\partial x}+t^4\frac{\partial\phi_4}{\partial x}+t^5\frac{\partial\phi_5}{\partial x}+t^6\frac{\partial\phi_6}{\partial x}+$$

$$+t^6\log t\frac{\partial\phi_6'}{\partial x}+t^6\log^2 t\frac{\partial\phi_6''}{\partial x}+\ldots\Big] = tR'(x). \quad (61)$$

which, on substituting the values for the potentials, becomes

$$\begin{aligned}
&\Big[t^2\Big\{\frac{A}{r}+(2B+C)r+2Cr\log r+O(r^3\log r)\Big\}+t^3\Big\{\frac{A_1}{r}+O(r\log r)\Big\}+\\
&\quad+t^4\log t\Big\{\frac{a}{r}+O(r\log r)\Big\}+t^4\Big\{\frac{2\alpha_1\log r}{r}+\frac{\gamma_1}{r}+O(r\log^2 r)\Big\}+\\
&\qquad+t^5\Big\{\frac{a_1}{r}+O(r\log r)\Big\}+t^6\Big\{-\frac{2\alpha_2}{r^3}+\frac{\gamma_2}{r}+O\Big(\frac{\log^2 r}{r}\Big)\Big\}+\\
&\qquad\qquad+t^6\log t\Big\{\frac{2\alpha_3\log r}{r}+\frac{\gamma_3}{r}+O(r\log^2 r)\Big\}+\\
&\qquad\qquad\qquad+t^6\log^2 t\Big\{\frac{A_2}{r}+O(r\log r)\Big\}+\ldots\Big]\div\\
&\div\Big[1+t^2\{K'+A'\log r+O(r^2\log r)\}+t^3\{A_1'\log r+K_1'+O(r^2\log r)\}+\\
&\quad+t^4\log t\{k'+a'\log r+O(r^2\log r)\}+t^4\{\alpha_1'\log^2 r+\gamma_1'\log r+\epsilon_1'+O(r^2\log^2 r)\}+\\
&\qquad+t^5\{a_1'\log r+k_1'+O(r^2\log r)\}+t^6\Big\{\frac{\alpha_2'}{r^2}+O(\log^3 r)\Big\}+\\
&\qquad\qquad+t^6\log t\,O(\log^2 r)+t^6\log^2 t\,O(\log r)+\ldots\Big]=tR'(x). \qquad (62)
\end{aligned}$$

Now, putting $r = tR(x)$ and equating coefficients of powers of t and $\log t$ in the equation (62), we obtain the following equations:

$$\left.\begin{aligned}
&\text{Coefficient of } t\text{:} && A = RR',\\
&t^2\text{:} && \frac{A_1}{R} = 0, && \text{giving}\quad \phi_3 \equiv 0,\\
&t^3\text{:} && (2B+C)R+2CR\log R+\frac{2\alpha_1\log R}{R}+\frac{\gamma_1}{R}-\frac{2\alpha_2}{R^3}-\\
& && \quad-\frac{AK'}{R}-\frac{AA'\log R}{R}=0, && \text{giving } \gamma_1,\\
&t^3\log t\text{:} && 2CR+\frac{a}{R}+\frac{2\alpha_1}{R}-\frac{AA'}{R}=0, && \text{giving } a,\\
&t^4\text{:} && \frac{a_1}{R}=0 && \text{giving}\quad \phi_5\equiv 0.
\end{aligned}\right\} \qquad (63)$$

It is unnecessary to write down the remaining coefficients. However, we note that the quantities γ_2, γ_3 and A_2 are determined by equating to zero the coefficients of t^5, $t^5\log t$ and $t^5\log^2 t$ respectively, and thus the boundary condition at the surface of the body is satisfied if we neglect terms in $t^6\log^3 t$.

One further point has to be considered here. It seems possible, *a priori*, that by continuing the expansion for ϕ further, a term such as $t^8\phi_8$ might

be of order t^4 on the body, in which case an approximate solution for ϕ_8 would have to be determined. To investigate this, assume that a longer expansion for ϕ has been substituted in (3) and consider the coefficient of t^8. Clearly the important terms are

$$\left(\frac{\partial\phi_2}{\partial r}\right)^2\frac{\partial^2\phi_4}{\partial r^2}+2\frac{\partial\phi_2}{\partial r}\frac{\partial\phi_4}{\partial r}\frac{\partial^2\phi_2}{\partial r^2}=O\left(\frac{\log r}{r^4}\right). \tag{64}$$

Therefore
$$M^{-2}\nabla^2\phi_8-\frac{\partial^2\phi_8}{\partial x^2}=O\left(\frac{\log r}{r^4}\right), \tag{65}$$

and hence $\phi_8 = O(r^{-2}\log r)$, and $t^8\phi_8 = O(t^6\log t)$ on the body.

If we consider the coefficient of t^{10} in (5) we deduce that

$$M^{-2}\nabla^2\phi_{10}-\frac{\partial^2\phi_{10}}{\partial x^2}=O\left(\frac{1}{r^6}\right),$$

and hence that $t^{10}\phi_{10} = O(t^6)$ on the body. Similarly

$$M^{-2}\nabla^2\phi_{12}-\frac{\partial^2\phi_{12}}{\partial x^2}=O\left(\frac{\log r}{r^6}\right)$$

and therefore $t^{12}\phi_{12} = O(t^8\log t)$ on the body. From these the following results can be proved by induction:

$$\left.\begin{aligned}\phi_{4p-2}&=O(r^{-2p+2}), & \phi_{4p}&=O(r^{-2p+2}\log r)\quad (p\geqslant 2),\\ \phi_2&=O(\log r), & \phi_4&=O(\log^2 r).\end{aligned}\right\} \tag{66}$$

Again, it is easy to show that $\phi_8' = O(1/r^2)$ and $\phi_{10}' = O(r^{-2}\log r)$. These results suggest that $\phi_{2n}^{(p)}$ and ϕ_{2n-2p} are of the same order and this can be proved by induction. Finally, a complete statement on the orders of magnitude on the body of all the terms $t^{2n}\log^p t\,\phi_{2n}^{(p)}$ is contained in the following equations:

$$\left.\begin{aligned}t^{2n}\log^p t\,\phi_{2n}^{(p)}&=O(t^{n+p+2}\log^{p+1}t)\quad(\text{for } n+p \text{ even and } p<n-2),\\ &=O(t^{n+p+1}\log^p t)\quad(\text{for } n+p \text{ odd and } p<n-1),\\ t^{2n}\log^{n-1}t\,\phi_{2n}^{(n-1)}&=O(t^{2n}\log^n t),\\ t^{2n}\log^{n-2}t\,\phi_{2n}^{(n-2)}&=O(t^{2n}\log^n t).\end{aligned}\right\} \tag{66a}$$

Since p is always less than or equal to $n-1$ we immediately see that no term $t^{2n}\log^p t\,\phi_{2n}^{(p)}$ can contribute a term of order t^4 or lower order to ϕ when $n+p > 3$, and hence the only terms affecting ϕ to order t^4, are ϕ_2, ϕ_4, ϕ_6 and ϕ_4', all of which have been considered. Hence every term in the expansion for ϕ of order t^4 or lower order has been found, and all terms of order $t^6\log^3 t$ or higher order have been neglected.

II. Evaluation of the drag coefficient of bodies of revolution

The drag coefficient C_D may be defined as the total drag divided by the product of $\frac{1}{2}\rho_0 V^2$ and the maximum cross-sectional area of the body. Therefore

$$C_D = \frac{4}{\pi t^2}\int\limits_0^1 \frac{p-p_0}{\frac{1}{2}\rho_0 V^2} 2\pi t^2 RR'\,dx = 8\int\limits_0^1 \frac{p-p_0}{\frac{1}{2}\rho_0 V^2} f\,dx. \tag{67}$$

To find the value of the pressure coefficient $(p-p_0)/\frac{1}{2}\rho_0 V^2$ we have from equation (2),

$$\gamma\frac{p}{\rho} = \gamma\frac{p_0}{\rho_0} - \frac{\gamma-1}{2}V^2\left\{2\frac{\partial\phi}{\partial x}+\left(\frac{\partial\phi}{\partial x}\right)^2+\left(\frac{\partial\phi}{\partial r}\right)^2\right\}, \tag{68}$$

i.e.

$$\frac{p}{p_0}\frac{\rho_0}{\rho} = 1-\frac{\gamma-1}{2\gamma}V^2\frac{\rho_0}{p_0}\left\{2\frac{\partial\phi}{\partial x}+\left(\frac{\partial\phi}{\partial x}\right)^2+\left(\frac{\partial\phi}{\partial r}\right)^2\right\}. \tag{69}$$

Since $p/\rho^\gamma = p_0/\rho_0^\gamma$, (69) becomes

$$\left(\frac{p}{p_0}\right)^{(\gamma-1)/\gamma} = 1-\frac{\gamma-1}{2\gamma}V^2\frac{\rho_0}{p_0}\left\{2\frac{\partial\phi}{\partial x}+\left(\frac{\partial\phi}{\partial x}\right)^2+\left(\frac{\partial\phi}{\partial r}\right)^2\right\}, \tag{70}$$

and hence

$$\frac{p}{p_0} = \left[1-\frac{\gamma-1}{2\gamma}V^2\frac{\rho_0}{p_0}\left\{2\frac{\partial\phi}{\partial x}+\left(\frac{\partial\phi}{\partial x}\right)^2+\left(\frac{\partial\phi}{\partial r}\right)^2\right\}\right]^{\gamma/(\gamma-1)}, \tag{71}$$

which on expansion becomes

$$\frac{p-p_0}{p_0} = -\frac{1}{2}\frac{\rho_0}{p_0}V^2\left\{2\frac{\partial\phi}{\partial x}+\left(\frac{\partial\phi}{\partial x}\right)^2+\left(\frac{\partial\phi}{\partial r}\right)^2\right\}+$$
$$+\frac{1}{8\gamma}\left(\frac{\rho_0}{p_0}\right)^2V^4\left\{2\frac{\partial\phi}{\partial x}+\left(\frac{\partial\phi}{\partial x}\right)^2+\left(\frac{\partial\phi}{\partial r}\right)^2\right\}^2+O\left(\frac{\partial\phi}{\partial x}\right)^3, \tag{72}$$

and therefore

$$\frac{p-p_0}{\frac{1}{2}\rho_0 V^2} = -2\frac{\partial\phi}{\partial x}-\left(\frac{\partial\phi}{\partial x}\right)^2-\left(\frac{\partial\phi}{\partial r}\right)^2+$$
$$+\frac{M^2}{4}\left\{4\left(\frac{\partial\phi}{\partial x}\right)^2+4\frac{\partial\phi}{\partial x}\left(\frac{\partial\phi}{\partial r}\right)^2+\left(\frac{\partial\phi}{\partial r}\right)^4\right\}+O\left(\frac{\partial\phi}{\partial x}\right)^3. \tag{73}$$

On the body $\partial\phi/\partial x = O(t^2\log t)$, so that we may write from equation (73)

$$\frac{p-p_0}{\frac{1}{2}\rho_0 V^2} = -2\frac{\partial\phi}{\partial x}+\alpha^2\left(\frac{\partial\phi}{\partial x}\right)^2-\left(\frac{\partial\phi}{\partial r}\right)^2+M^2\frac{\partial\phi}{\partial x}\left(\frac{\partial\phi}{\partial r}\right)^2+$$
$$+\frac{M^2}{4}\left(\frac{\partial\phi}{\partial r}\right)^4+O(t^6\log^3 t). \tag{74}$$

On substituting the expression for ϕ, (74) becomes

$$\frac{p-p_0}{\frac{1}{2}\rho_0 V^2} = -2\left\{t^2\frac{\partial\phi_2}{\partial x}+t^4\log t\frac{\partial\phi_4'}{\partial x}+t^4\frac{\partial\phi_4}{\partial x}+t^6\frac{\partial\phi_6}{\partial x}+O(t^6\log t\log^2 r)\right\}+$$
$$+\alpha^2\left\{t^2\frac{\partial\phi_2}{\partial x}+t^4\log t\frac{\partial\phi_4'}{\partial x}+t^4\frac{\partial\phi_4}{\partial x}+t^6\frac{\partial\phi_6}{\partial x}+O(t^6\log t\log^2 r)\right\}^2-$$
$$-\left\{t^2\frac{\partial\phi_2}{\partial r}+t^4\log t\frac{\partial\phi_4'}{\partial r}+t^4\frac{\partial\phi_4}{\partial r}+t^6\frac{\partial\phi_6}{\partial r}+O\left(t^6\log t\frac{\log r}{r}\right)\right\}^2+$$
$$+M^2\left\{t^2\frac{\partial\phi_2}{\partial x}+O(t^4\log t\log r)\right\}\times$$
$$\times\left\{t^2\frac{\partial\phi_2}{\partial r}+t^4\frac{\partial\phi_4}{\partial r}+t^4\log t\frac{\partial\phi_4'}{\partial r}+t^6\frac{\partial\phi_6}{\partial r}+O\left(t^6\log t\frac{\log r}{r}\right)\right\}^2+$$
$$+\frac{M^2}{4}\left\{t^2\frac{\partial\phi_2}{\partial r}+O\left(\frac{t^4\log r}{r}\right)\right\}^2, \tag{75}$$

and, substituting the series for the potentials in (75), we find that

$$\frac{p-p_0}{\frac{1}{2}\rho_0 V^2} = -2t^2\{K'+A'\log r+B'r^2+C'r^2\log r+O(r^4\log r)\}-$$
$$-2t^4\log t\{k'+a'\log r+O(r^2\log r)\}-$$
$$-2t^4\{\alpha_1'\log^2 r+\gamma_1'\log r+\epsilon_1'+O(r^2\log^2 r)\}-2t^6\left\{\frac{\alpha_2'}{r^2}+O(\log^3 r)\right\}+$$
$$+\alpha^2t^4\{K'^2+2K'A'\log r+A'^2\log^2 r+O(r^2\log^2 r)\}-$$
$$-t^4\left\{\frac{A^2}{r^2}+2A(2B+C)+4AC\log r+O(r^2\log^2 r)\right\}-$$
$$-2t^6\log t\left\{\frac{Aa}{r^2}+O(\log^2 r)\right\}-2t^6\left\{\frac{A}{r}\left(\frac{\gamma_1}{r}+\frac{2\alpha_1\log r}{r}\right)+O(\log^2 r)\right\}-$$
$$-2t^8\left\{\frac{A}{r}+O(r\log r)\right\}\left\{-\frac{2\alpha_2}{r^3}+O\left(\frac{1}{r}\right)\right\}+$$
$$+M^2t^6\left\{(A'\log r+K')\frac{A^2}{r^2}+O(\log r)\right\}+\frac{M^2}{4}t^8\left(\frac{A^4}{r^4}\right)+$$
$$+M^2t^2[A'\log r+K'+O(r^2\log r)]\left[2\left\{\frac{A}{r}+O(r\log r)\right\}\right]\times$$
$$\times\left[t^6\left\{\frac{\gamma_1}{r}+\frac{2\alpha_1\log r}{r}+O(r\log^2 r)\right\}+t^6\log t\left\{\frac{a}{r}+O(r\log r)\right\}+\right.$$
$$\left.+t^8\left\{-\frac{2\alpha_2}{r^3}+O\left(\frac{1}{r}\right)\right\}\right]+$$

$$+\frac{M^2}{4}t^8\left[\left\{\frac{4A^3}{r^2}(2B+C)+\frac{4A^2}{r^2}2AC\log r+O(\log r)\right\}+\right.$$

$$+4t^2\left\{\frac{A^3}{r^3}+O\left(\frac{1}{r}\right)\right\}\left\{\frac{\gamma_1}{r}+\frac{2\alpha_1\log r}{r}+O(r\log^2 r)\right\}+$$

$$+4t^2\log t\left\{\frac{A^3}{r^3}+O\left(\frac{1}{r}\right)\right\}\left\{\frac{a}{r}+O(r\log r)\right\}+$$

$$+4t^4\left\{\frac{A^3}{r^3}+\frac{3A^2(2B+C)}{r}+\frac{6A^2C\log r}{r}+O(r\log r)\right\}\times$$

$$\left.\times\left\{-\frac{2\alpha_2}{r^3}+O\left(\frac{1}{r}\right)\right\}\right]. \quad (76)$$

It is to be noted that the terms in square brackets in equation (76) are of order $t^6\log^q t$ (or higher order) on the body and are therefore taken to be negligible. They have been written out because they contain squares and higher powers of $1/r$ and therefore might possibly tend to infinity as r tends to zero. However, their coefficients contain powers of $f(x)$ which are $O(r)$ as $r\to 0$ *on the body* and by examination we can see that the coefficient of $t^6\log^q t$ in (76) is of order $\log^s r$. Hence, the corresponding integral in (67) converges giving a term genuinely $O(t^6\log^q t)$ in the drag coefficient.

Therefore, from (76) we have, on the body,

$$\frac{p-p_0}{\frac{1}{2}\rho_0 V^2} = -t^2\left[2K'+2A'\log R+\frac{A^2}{R^2}\right]-2A'\,t^2\log t-$$

$$-t^4\left[2B'R^2+2C'R^2\log R+2\alpha_1'\log^2 R+2\gamma_1'\log R+\right.$$

$$+2\epsilon_1'+\frac{2\alpha_2'}{R^2}-\alpha^2(K'^2+2K'A'\log R+A'^2\log R)+$$

$$+2A(2B+C)+4AC\log R+\frac{2A\gamma_1}{R^2}+\frac{4\alpha_1 A\log R}{R^2}-$$

$$\left.-\frac{4\alpha_2 A}{R^4}-M^2(A'\log R+K')\frac{A^2}{R^2}-\frac{M^2A^4}{4R^4}\right]-$$

$$-t^4\log t\left[2C'R^2+2k'+2a'\log R+4\alpha_1'\log R+2\gamma_1'-\right.$$

$$\left.-\alpha^2(2K'A'+2A'^2\log R)+4AC+\frac{2Aa}{R^2}+\frac{4\alpha_1 A}{R^2}-\frac{M^2A'A^2}{R^2}\right]-$$

$$-t^4\log^2 t[2\alpha_1'+2a'-\alpha^2A'^2]+O(t^6\log^3 t). \quad (77)$$

Substituting the values for A, B and C this expression may be written

$$
\begin{aligned}
\frac{p-p_0}{\frac{1}{2}\rho_0 V^2} = & -t^2\left[\frac{f^2}{R^2}+2f'\log R+2K'\right]-2f't^2\log t- \\
& -t^4\left[-\tfrac{1}{2}\alpha^2 f''' R^2-\tfrac{1}{2}\alpha^2 ff''-\frac{M^2}{4}\frac{f^4}{R^4}+\right. \\
& +\left(\tfrac{1}{2}\alpha^2 f''' R^2+\alpha^2 ff''-\frac{M^2 f^2 f'}{R^2}\right)\log R-\alpha^2 f'^2\log^2 R+\tfrac{1}{2}\alpha^2 R^2 K'''+ \\
& +\alpha^2 fK''-\frac{M^2 f^2 K'}{R^2}-2\alpha^2 f'K'\log R-\alpha^2 K'^2+\frac{4f\alpha_1\log R}{R^2}+ \\
& \left.+\frac{2f\gamma_1}{R^2}+2\alpha_1'\log^2 R+2\gamma_1'\log R+2\epsilon_1'-\frac{4\alpha_2 f}{R^4}+\frac{2\alpha_2'}{R^2}\right]- \\
& -t^4\log t\left[\tfrac{1}{2}\alpha^2 f''' R^2+\alpha^2 ff''-\frac{M^2 f^2 f'}{R^2}-2\alpha^2 f'^2\log R-2\alpha^2 f'K'+\right. \\
& \left.+\frac{2fa}{R^2}+2a'\log R+2k'+\frac{4f\alpha_1}{R^2}+4\alpha_1'\log R+2\gamma_1'\right]- \\
& -t^4\log^2 t[-\alpha^2 f'^2+2a'+2\alpha_1']+O(t^6\log^3 t),
\end{aligned}
\tag{78}
$$

where

$$
\left.
\begin{aligned}
& f = RR', \qquad K = f(x)\log\tfrac{1}{2}\alpha-\int_0^x f'(y)\log(x-y)\,dy, \\
& \alpha_1 = M^2 ff', \qquad \alpha_2 = -\tfrac{1}{4}M^2 f^3, \qquad P(x) = 2M^2 ff', \\
& \gamma_1 = \tfrac{1}{4}\alpha^2 f'' R^2+ff'\log R-\tfrac{1}{2}\alpha^2 f'' R^2\log R+fK'- \\
& \qquad -\tfrac{1}{2}\alpha^2 R^2 K''+2\alpha_2/R^2-2\alpha_1\log R, \\
& \epsilon_1 = \gamma_1(x)\log\tfrac{1}{2}\alpha-\int_0^x \gamma_1'(y)\log(x-y)\,dy+ \\
& \qquad +P(x)\{\tfrac{1}{6}\pi^2-\tfrac{1}{2}\log^2(2x/\alpha)\}-xP'(x)- \\
& -\int_0^\infty du\int_0^{x/\alpha(\cosh u+1)} s\left\{F(x-\alpha s\cosh u,s)-\frac{P(x-\alpha s\cosh u)}{s^2}\right\}ds+ \\
& +\left\{P(x)\log x-\int_0^x P'(y)\log(x-y)\,dy\right\}\log\frac{2x}{\alpha}+ \\
& +\int_0^\infty du\left[\int_{x\cosh u/(1+\cosh u)}^{x} P'(x-y)\log y\,dy+P(x)\log\frac{\cosh u}{1+\cosh u}-\right. \\
& \qquad \left.-P\left(\frac{x}{1+\cosh u}\right)\log\frac{x\cosh u}{1+\cosh u}\right],
\end{aligned}
\right\}
\tag{79}
$$

$$\left.\begin{aligned} a &= ff'-2\alpha_1-\tfrac{1}{2}\alpha^2 f'' R^2, \\ k &= a(x)\log\tfrac{1}{2}\alpha-\int\limits_0^x a'(y)\log(x-y)\,dy, \\ F(x,r) &= \{2M^2+(\gamma-1)M^4\}\frac{\partial\phi_2}{\partial x}\frac{\partial^2\phi_2}{\partial x^2}+2M^2\frac{\partial\phi_2}{\partial r}\frac{\partial^2\phi_2}{\partial x\partial r}. \end{aligned}\right|$$

The pressure coefficient is given by equation (78) and the drag coefficient is found by substituting (78) in (67).

III. Comparison of the analytical and numerical solutions for the pressure coefficient of a cone

Using numerical integration, Taylor and Maccoll (**3**) found solutions for supersonic flow past three cones, and recently tables of solutions for supersonic flow past a variety of cones have been published in America (**6**). These are the only solutions by exact computation for supersonic flow past bodies of revolution which have been published and it is interesting to compare the approximate analytical solution developed in this paper with those of (**6**), in order to judge to what extent the present theory may be applied to general bodies of revolution.

For a cone t is the tangent of the semi-vertical angle and $R(x) = x$. We find the following results from equation (79):

$$\left.\begin{aligned} f &= x, \\ K &= x\log\tfrac{1}{2}\alpha-x\log x+x, \\ \alpha_1 &= M^2 x, \\ \alpha_2 &= -\tfrac{1}{4}M^2x^3, \\ \gamma_1 &= x\log\tfrac{1}{2}\alpha-\tfrac{1}{2}x-2M^2x\log x, \\ a &= x(1-2M^2), \\ k &= x(1-2M^2)\log\tfrac{1}{2}\alpha-(1-2M^2)(x\log x-x), \\ F(x,r) &= \{2M^2+(\gamma-1)M^4\}\frac{1}{\sqrt{(x^2-\alpha^2r^2)}}\cosh^{-1}\frac{x}{\alpha r}+2M^2\frac{x}{r^2}, \\ \epsilon_1 &= M^2x\log^2x+(\tfrac{1}{2}-\log\tfrac{1}{2}\alpha)x\log x- \\ &\qquad -x\{\alpha^2\log^2\tfrac{1}{2}\alpha+(2M^2-\tfrac{1}{2})\log\tfrac{1}{2}\alpha+2M^2+\tfrac{1}{2}\}- \\ &\qquad\qquad -\frac{2M^2+(\gamma-1)M^4}{2\alpha^2}x. \end{aligned}\right\} \quad (80)$$

Substituting these results in (78), we deduce that

$$C_p = -t^2-2t^2\log\tfrac{1}{2}t\alpha+3\alpha^2t^4\log^2\tfrac{1}{2}t\alpha+(5M^2-1)t^4\log\tfrac{1}{2}t\alpha+ \\ +t^4\left[3\tfrac{1}{4}M^2+\tfrac{1}{2}+\frac{(\gamma+1)M^4}{\alpha^2}\right], \quad (81)$$

neglecting terms in $t^6\log^3 t$.

We call the terms in t^2 and $t^2 \log t$ in equation (81) the first approximation to the pressure coefficient and the whole expression the second approximation. For comparison, one other form of the pressure coefficient for a cone is of interest, that one found by solving the linearized equation for flow past a cone, satisfying the boundary condition exactly and using the exact form of Bernoulli's equation. Doing this we find that

$$C_p = \frac{2}{\gamma M^2}\left[1-\frac{\gamma-1}{2}M^2\left\{\frac{-2t^2\cosh^{-1}(1/\alpha t)}{\sqrt{(1-\alpha^2t^2)}+t^2\cosh^{-1}(1/\alpha t)}+\right.\right.$$
$$+\left(\frac{t^2\cosh^{-1}(1/\alpha t)}{\sqrt{(1-\alpha^2t^2)}+t^2\cosh^{-1}(1/\alpha t)}\right)^2+$$
$$\left.\left.+\left(\frac{t\sqrt{(1-\alpha^2t^2)}}{\sqrt{(1-\alpha^2t^2)}+t^2\cosh^{-1}(1/\alpha t)}\right)^2\right\}\right]^{\gamma/(\gamma-1)}-\frac{2}{\gamma M^2}. \tag{82}$$

Comparison of the numerical solutions (**6**) and the analytical solutions

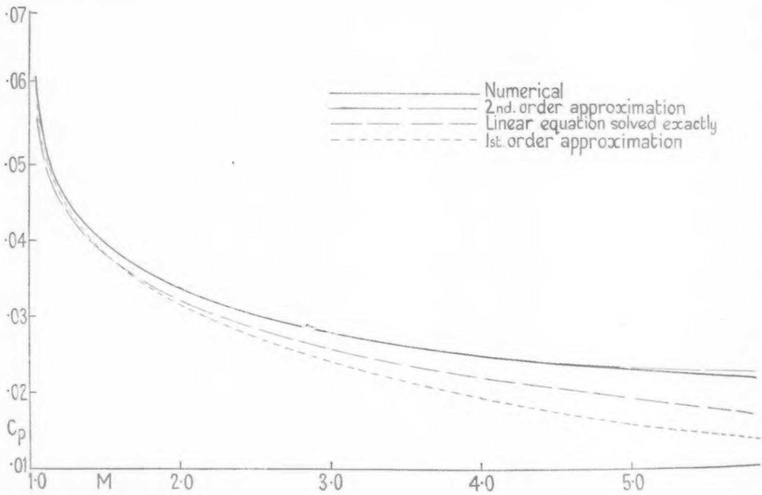

FIG. 1. Graph showing the relation between the pressure coefficient at the surface of a 5° cone and the Mach number.

for pressure coefficients at the surface has been made for cones with semi-vertical angles of 5°, 10°, and 15°, and the results of plotting C_p against M are shown in Figs. 1, 2, and 3.

In the case of the 5° cone it is not possible on the scale of the figure to show any difference in C_p between the numerical results and the second analytical approximation up to a Mach number near 5. Indeed, the difference between these two values for C_p is about 0·4 per cent. at a Mach number of 1·04, and about 0·04 per cent. at a Mach number of 3.

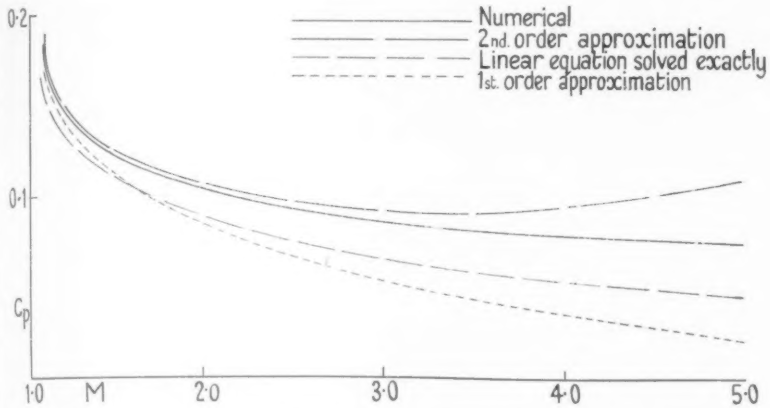

FIG. 2. Graph showing the relation between the pressure coefficient at the surface of a 10° cone and the Mach number.

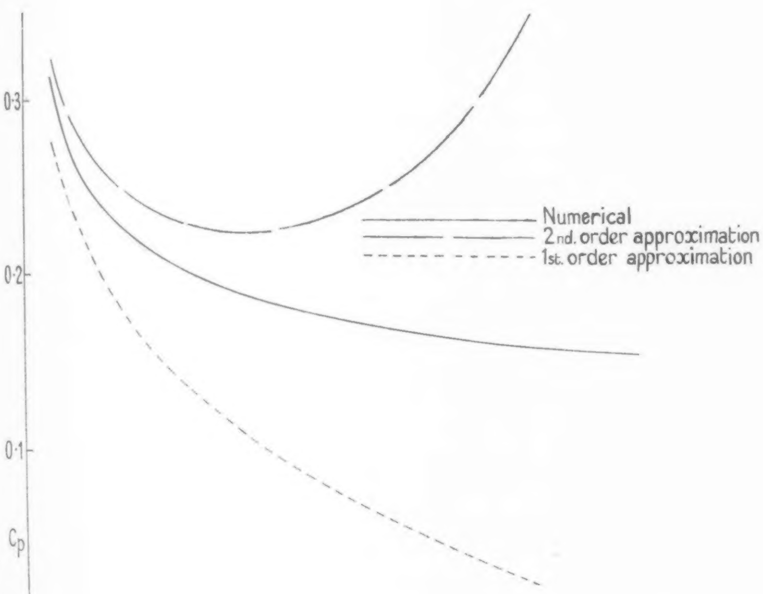

FIG. 3. Graph showing the relation between the pressure coefficient at the surface of a 15° cone and the Mach number.

For the 10° cone the second approximation is good up to Mach number about 3, while in the case of the 15° cone the agreement is not good except for very small Mach numbers.

We can state that the second approximation is a great improvement on linear theory for thin cones and the same is no doubt true for all bodies of revolution.

REFERENCES

1. TH. VON KÁRMÁN and N. B. MOORE, 'Resistance of slender bodies moving with supersonic velocities with special reference to projectiles', *Trans. of the Amer. Soc. of Mech. Engineers*, 1932.
2. M. J. LIGHTHILL, *Supersonic Flow past Bodies of Revolution*. Aero. Res. Counc. R. & M. No. 2003, January 1945.
3. G. I. TAYLOR and J. W. MACCOLL, 'The air pressure on a cone moving at high speeds', *Proc. Roy. Soc.* A **139** (1933), 278–311.
4. M. J. LIGHTHILL, 'The position of the shock wave in certain aerodynamic problems', to be published in *Quart. J. Mech. and Applied Math.*
5. J. B. BRODERICK, 'Supersonic flow past a semi-infinite cone', see below, pp. 121–8.
6. Massachusetts Institute of Technology, Technical Report No. I, *Tables of Supersonic Flow Around Cones*, The Murray Printing Company, Cambridge, Massachusetts, 1947.

SUPERSONIC FLOW PAST A SEMI-INFINITE CONE

By J. B. BRODERICK

(*Department of Mathematics, The University, Manchester*)

[Received 13 December 1947. Revised 27 April 1948]

SUMMARY

An approximate analytical solution of the problem of supersonic flow past pointed bodies of revolution was recently given by the author (**1**). In deriving this solution isentropic, irrotational flow was assumed and no account was taken of the shock-wave. It does not seem possible to extend the solution when the shock-wave is taken into account in general, but for the particular case of axially symmetrical flow past a cone the extension can be made. The purpose of this paper is to show that the extended solution gives the same approximate value for the pressure coefficient as that found in the earlier paper for flow past a cone. We may infer that this result holds for all convex bodies of revolution.

Introduction

In a recent paper (**1**) the author developed a method for solving the non-linear partial differential equation for isentropic, irrotational flow past bodies of revolution, by expanding the potential in powers of t and $\log t$ (t being the thickness ratio of the body), and thus reducing the non-linear equation to a series of linear equations. It was found that the solution obtained differs from uniform flow only inside the Mach cone and hence can give no approximation to the position of the shock-wave; furthermore, it can be shown that the series diverges on the Mach cone. However, it appears to give correct results near the body and the pressure and drag coefficients were found to order t^4.

It would be desirable to extend this previous work in order to find a solution which would hold also in the neighbourhood of the shock-wave and which would give the position of the shock-wave and the pressure and drag coefficients when the shock-wave is taken into consideration. One would then know definitely whether the solution already obtained for the drag coefficient to order t^4 was correct. However, it does not appear possible to carry out this work for bodies of revolution in general. Hence the extension has been made in this paper for the particular case of axially symmetrical flow past a semi-infinite cone, as this case can be dealt with analytically. We find that the pressure coefficient for a cone obtained by using the complete equations is the same as that found in the earlier paper to order t^4; a first approximation to the position of the shock-wave is also deduced. We may infer that the expression for the pressure coefficient given in the earlier paper is correct to order t^4 for all convex bodies of revolution. This paper has not been written in order

to determine a solution to the problem of supersonic flow past a cone. This problem has already been considered numerically by Taylor and Maccoll (**2**) for three particular cones, and further exhaustive numerical results have been published in America (**3**). The first analytical approximation to the position of the shock-wave has also lately been found by Lighthill (**4**), who used another method of solution.

Comparisons of the analytical solution and the numerical solutions are made in the author's earlier paper to which the reader is referred.

In conclusion, I wish to thank Professor Goldstein and Mr. Lighthill for their very helpful advice and suggestions.

The following notation is used throughout this paper:

$$V = \text{velocity of main stream.}$$

$$V\left(1+\frac{\partial\phi}{\partial x}\right) = \text{velocity parallel to axis of cone.}$$

$$V\frac{\partial\phi}{\partial r} = \text{velocity perpendicular to axis of cone.}$$

$$\frac{\partial\phi}{\partial x_1}, \frac{\partial\phi}{\partial r_1} = \text{values of } \frac{\partial\phi}{\partial x}, \frac{\partial\phi}{\partial r} \text{ at the shock-wave.}$$

$$c = \text{local velocity of sound.}$$

$$c_0 = \text{velocity of sound in main stream.}$$

$$M = \frac{V}{c_0}.$$

$$\alpha = \sqrt{(M^2-1)}.$$

$$\mu = \text{Mach angle.}$$

$$\eta = \text{angle between shock-wave and axis of cone.}$$

$$t = \text{tangent of semi-vertical angle of cone.}$$

$$\frac{1}{\alpha} = \alpha_1 = \tan\mu.$$

$$\frac{1}{\beta} = \beta_1 = \tan\eta.$$

I. Hydrodynamical equations

The general equation for the flow of a gas with axial symmetry in cylindrical polar coordinates is

$$\frac{c^2}{V^2}\nabla^2\phi = \left(1+\frac{\partial\phi}{\partial x}\right)^2\frac{\partial^2\phi}{\partial x^2}+2\left(1+\frac{\partial\phi}{\partial x}\right)\frac{\partial^2\phi}{\partial x\partial r}\frac{\partial\phi}{\partial r}+\left(\frac{\partial\phi}{\partial r}\right)^2\frac{\partial^2\phi}{\partial r^2}. \tag{1}$$

For flow past a cone the variables such as pressure and density will be functions of r/x only. Thus $\partial\phi/\partial x_1$ and $\partial\phi/\partial r_1$ are constant along the

shock-wave and we may put $\phi = xf(r/x)$. Then using the Rankine shock-wave equation, Bernoulli's equation, and (1) we deduce that f satisfies the equation

$$\left[M^{-2}-\frac{\gamma-1}{2}\{2(f-yf')+(f-yf')^2+f'^2\}\right][y^2f''+y^{-1}f'+f'']$$
$$= \{y(1+f-yf')-f'\}^2f'', \quad (2)$$

where $r/x = y$, and dashes denote derivatives.

The boundary condition at the cone is† $\phi_r/(1+\phi_x) = r/x = t$ which becomes

$$t+tf(t) = (1+t^2)f'(t), \quad (3)$$

and using again the shock-wave equations we deduce two conditions at the shock-wave which may be written

$$f(\beta_1) = 0, \quad (4)$$

and
$$f'(\beta_1) = \frac{4}{\gamma+1}\frac{1}{(1+\alpha_1^2)^2}(\beta_1-\alpha_1)+O(\beta_1-\alpha_1)^2. \quad (5)$$

We have then to solve equation (2) with boundary conditions given by equations (3), (4), and (5). Since equation (2) is of the second order the boundary conditions determine the relation between β_1 and α_1.

II. Solution of the equation of motion near the body

Following the method developed in (**1**) we substitute

$$f = t^2f_2+t^4f_4+t^6f_6+...+f_{41}t^4\log\tfrac{1}{2}t\alpha+f_{61}t^6\log\tfrac{1}{2}t\alpha+...+f_{62}t^6\log^2\tfrac{1}{2}t\alpha+... \quad (6)$$

in equation (2), and equating powers of t and $\log\frac{1}{2}t\alpha$ we deduce a series of linear equations for the functions $f_2, f_4, f_{41},...$. The solution for f_2 is

$$f_2 = A\left[\log\left\{\frac{1}{y\alpha}+\frac{1}{y\alpha}\sqrt{(1-\alpha^2y^2)}\right\}-\sqrt{(1-\alpha^2y^2)}\right], \quad (7)$$

except for the addition of an arbitrary constant. It will be seen later from the boundary conditions that this arbitrary constant is zero, so we neglect it at this stage in order to save unnecessary terms in f_4. The arbitrary constant A will be fixed by the boundary conditions at the surface of the cone. The solution for f_4 is also found and f_2 and f_4 are then expanded in powers of y (since y is small near the cone). The results are

$$f_2 = -A[1+\log\tfrac{1}{2}y\alpha-\tfrac{1}{4}\alpha^2y^2+O(y^4)] \quad (8)$$

and

$$f_4 = M^2A^2\log^2\tfrac{1}{2}y\alpha+M^2A^2\left\{1+\frac{M^2(\gamma+1)}{2\alpha^2}\right\}\log\tfrac{1}{2}y\alpha+O(y^2\log\tfrac{1}{2}y\alpha)-$$
$$-B\{1+\log\tfrac{1}{2}y\alpha+O(y^2)\}, \quad (9)$$

† Suffixes denote partial derivatives, and t is the value of y at the boundary of the cone.

where B is another arbitrary constant. Making use of these expansions we then deduce

$$f_6 = \frac{M^2A^3}{4y^2} + O(\log^3 \tfrac{1}{2}y\alpha), \tag{10}$$

and

$$f_{41} = -C[1+\log \tfrac{1}{2}y\alpha + O(y^2)], \tag{11}$$

where C, again, is an arbitrary constant.

It can then be shown (**1**) that no term, other than f_2, f_4, f_6 and f_{41}, can affect the value of f to order t^4, so we need not consider any other term in the expansion (6) in order to find f correct to order t^4 *near the body*.

From the solution (7) it appears that $y = 1/\alpha$ (which gives the position of the Mach cone) is a singularity of f. We next consider the behaviour of the solution near this point. Using (7) and, putting $z = (1/\alpha)-y$, we deduce

$$f_2'(y) = -f_2'(z) = -A\sqrt{2}\,\alpha^{\frac{3}{2}}z^{\frac{1}{2}}\{1+O(z)\}, \tag{12}$$

where the positive sign of the square root has to be taken to agree with equation (8). Then from a consideration of equation (2) we can see that, to obtain the asymptotic form of f_{2n+2}' near $z = 0$, we have only to consider the equation

$$2zf_{2n+2}''(z) - f_{2n+2}'(z) = \frac{(\gamma+1)M^4}{\alpha^4}\sum_{p=1}^{n} f_{2p}'(z)f_{2n+2-2p}''(z). \tag{13}$$

From (13) we find

$$-f_4'(z) = \frac{(\gamma+1)M^4A^2}{\alpha} + O(z^{\frac{1}{2}}),$$

which suggests in general

$$f_{2n}'(z) = \frac{A_n(\gamma+1)^{n-1}\alpha^2M^{4(n-1)}}{\alpha^{3(n-1)}}\left(\frac{z}{\alpha}\right)^{1-\frac{1}{2}n} + O(z^{\frac{3}{2}-\frac{1}{2}n}). \tag{14}$$

Substituting (14) in (13) we find

$$-nA_{n+1} = \sum_{p=1}^{n} A_p(1-\tfrac{1}{2}p)A_{n+1-p}. \tag{15}$$

In a similar manner the form, near $z = 0$, of other terms in f' such as f_{41}' and f_{61}' may be determined and the solution near $z = 0$ may be written

$$f'(z) = \sum_{n=1}^{\infty} t^{2n}\left[\frac{A_n\,\alpha^2(\gamma+1)^{n-1}M^{4(n-1)}}{\alpha^{3(n-1)}}\left(\frac{z}{\alpha}\right)^{1-\frac{1}{2}n} + O(z^{\frac{3}{2}-\frac{1}{2}n})\right] + \\ + O\left\{t^{2n+2}\log t\left(\frac{z}{\alpha}\right)^{1-\frac{1}{2}n}\right\}, \tag{16}$$

and this expansion diverges at $z = 0$ (the Mach cone). Furthermore, the expansion found for f does not exist outside the Mach cone. To find the value of f in this region it is therefore necessary to consider a solution near the shock-wave. This is done in the next section.

III. Solution of the equation of motion near the shock-wave

Substituting equations (4) and (5) in (2) we deduce that

$$f''(\beta_1) = -\frac{2}{(\gamma+1)(1+\alpha_1^2)^2}+O(\beta_1-\alpha_1). \tag{17}$$

Similarly
$$f'''(\beta_1) = \frac{\text{constant}}{\beta_1-\alpha_1}+O(1),$$

and we infer that a series exists of the form

$$f(y) = \left[\frac{4}{\gamma+1}\,\frac{\beta_1-\alpha_1}{(1+\alpha_1^2)^2}+O(\beta_1-\alpha_1)^2\right](y-\beta_1)+$$
$$+\left[-\frac{1}{\gamma+1}\,\frac{1}{(1+\alpha_1^2)^2}+O(\beta_1-\alpha_1)\right](y-\beta_1)^2+$$
$$+\left[\frac{\text{constant}}{\beta_1-\alpha_1}+O(1)\right](y-\beta_1)^3+\dots, \tag{18}$$

which may be regrouped as

$$f(y) = (\beta_1-\alpha_1)^2 g\left(\frac{y-\beta_1}{\beta_1-\alpha_1}\right)+(\beta_1-\alpha_1)^3 h\left(\frac{y-\beta_1}{\beta_1-\alpha_1}\right)+\dots, \tag{19}$$

where
$$g(w) = \frac{4}{\gamma+1}\,\frac{1}{(1+\alpha_1^2)^2}w-\frac{1}{\gamma+1}\,\frac{1}{(1+\alpha_1^2)^2}w^2+\dots. \tag{20}$$

Put then

$$\left.\begin{aligned}\beta_1-\alpha_1 = \xi,\qquad w = \frac{y-\beta_1}{\beta_1-\alpha_1},\qquad y = \alpha_1+\xi(1+w),\\ f(w) = \xi^2 g(w)+\xi^3 h(w)+\dots,\end{aligned}\right\} \tag{21}$$

and equate powers of ξ in equation (2).

The term independent of ξ vanishes identically, and equating coefficients of ξ we deduce that

$$(\gamma+1)(1+\alpha_1^2)g'g''+\frac{g'}{1+\alpha_1^2}-\frac{2(1+w)g''}{1+\alpha_1^2} = 0. \tag{22}$$

The solution is

$$g'^2 = \frac{16}{3(\gamma+1)^2(1+\alpha_1^2)^4}\{(\gamma+1)(1+\alpha_1^2)^2 g'-(1+w)\}, \tag{23}$$

using the fact that $g' = \dfrac{4}{\gamma+1}\,\dfrac{1}{(1+\alpha_1^2)^2}$ when $w = 0$ to fix the arbitrary constant. From (23) we deduce that

$$g' = \frac{8}{3(\gamma+1)(1+\alpha_1^2)^2}+\frac{4}{3(\gamma+1)(1+\alpha_1^2)^2}\sqrt{(1-3w)}. \tag{24}$$

Since w is negative in the field of flow, g' is regular therein and g itself is obtained as $\int\limits_0^w g'(w)\,dw$. Other terms in equation (21) could be found in

a similar manner, and then equation (21) gives the value of f near the shock-wave. We now determine the value of f' at a point near the shock-wave and inside the Mach cone. Put $w = -(k+1)$, where k is an arbitrary positive constant (noticing $w = -1$ on the Mach cone, from equation (21)). Then $-z = y-\alpha_1 = k(\alpha_1-\beta_1)$ from equation (21). At this point from (24) and (21) we deduce that

$$f'(y) = \left\{\frac{8}{3(\gamma+1)(1+\alpha_1^2)^2}+\frac{4}{3(\gamma+1)(1+\alpha_1^2)^2}\sqrt{(4+3k)}\right\}(\beta_1-\alpha_1)+O(\beta_1-\alpha_1)^2. \tag{25}$$

IV. Boundary conditions

The boundary conditions at the shock-wave have already been satisfied. The two values for f' are now equated when $z = k(\beta_1-\alpha_1)$. With this value of z, we have from (16), if k be chosen large enough to secure convergence ($k > \frac{4}{3}$ is sufficient),

$$f'(z) = \sum_{n=1}^{\infty} t^{2n}\left[\frac{A_n\,\alpha^2(\gamma+1)^{n-1}M^{4(n-1)}}{\alpha^{3(n-1)}}\left\{\frac{k(\beta_1-\alpha_1)}{\alpha}\right\}^{1-\frac{1}{2}n}+O\{(\beta_1-\alpha_1)^{\frac{3}{2}-\frac{1}{2}n}\}\right]+$$
$$+O\{t^{2n+2}\log t(\beta_1-\alpha_1)^{1-\frac{1}{2}n}\}, \tag{26}$$

and putting $\beta_1-\alpha_1 = O(t^r)$ we see immediately from (25) and (26) that $r = 4$.

Put then
$$\left\{\frac{k(\beta_1-\alpha_1)}{\alpha}\right\}^{\frac{1}{2}} = K\,\frac{(\gamma+1)M^4}{\alpha^3}t^2\{1+O(t^2\log t)\}, \tag{27}$$

where K is a constant, and substitute (27) in (25) and (26) and equate the results; we obtain

$$-\sum_{n=1}^{\infty} A_n K^{-n} = \frac{1}{k}\left\{\frac{8}{3}+\frac{8}{3}\sqrt{\left(1+\frac{3k}{4}\right)}\right\}. \tag{28}$$

Now put $F(u) = \sum_{n=1}^{\infty} A_n u^n$; from equation (15) we find

$$F(u)-uF'(u) = F(u)[F(u)-\tfrac{1}{2}uF'(u)]. \tag{29}$$

Solving (29), we have

$$-F(u) = \frac{A_1^2u^2+\sqrt{(A_1^4u^4+4A_1^2u^2)}}{2}, \tag{30}$$

the arbitrary constant and radical sign being fixed by the fact that $F(u)/u \to A_1$ as $u \to 0$. Now, from (30),

$$-F(K^{-1}) = \frac{A_1^2}{2K^2}\left\{1+\sqrt{\left(1+\frac{4K^2}{A_1^2}\right)}\right\}, \tag{31}$$

and, comparing (28) and (31), we see that

$$\frac{K^2}{k} = \tfrac{3}{16}A_1^2 = \tfrac{3}{8}A^2, \tag{32}$$

from equation (12). Then, from (27),

$$\beta_1-\alpha_1 = \tfrac{3}{8}A^2\frac{(\gamma+1)^2M^8}{\alpha^5}t^4+O(t^6\log t). \tag{33}$$

This equation determines the first approximation to the position of the shock-wave when A is known.

A further boundary condition remains to be satisfied, that given by equation (3). Substituting the expansion (6) in (3), after replacing f_2, f_4, f_6, and f_{41} by their power series in y and $\log y$ near the body, and equating powers of t and $\log \frac{1}{2}\alpha t$ we deduce the following values for the arbitrary constants

$$\left.\begin{aligned} A &= -1,\\ B &= \tfrac{1}{2}+M^2+\frac{M^4(\gamma+1)}{2\alpha^2},\\ C &= 2M^2-1. \end{aligned}\right\} \tag{34}$$

It can also be shown that by continuing the solution the boundary condition at the surface of the body can be satisfied theoretically to any degree of approximation. Other arbitrary constants in the solution for f are obtained by integrating equation (16), to give f, and then introducing the result into (21) with $z = k(\beta_1-\alpha_1)$ and $w = -(k+1)$. Since f in (21) is $O(t^8)$, this shows that the arbitrary constants which may be added to f_2 and f_4 in (8) and (9) must vanish, otherwise there would be terms in t^2 and t^4 in the value of f obtained by integrating (16). Similarly the arbitrary constant which may be added to f_{41} in (11) is zero. Thus the statement made after equation (7) is justified. The solution for f near the body may now be written

$$\begin{aligned} f = {} & t^2[1+\log\tfrac{1}{2}y\alpha-\tfrac{1}{4}\alpha^2y^2+O(y^4)]+\\ & +t^4\left[M^2\log^2\tfrac{1}{2}y\alpha-\tfrac{1}{2}\log\tfrac{1}{2}y\alpha-\tfrac{1}{2}-M^2-\frac{M^4(\gamma+1)}{2\alpha^2}+O(y^2\log\tfrac{1}{2}y\alpha)\right]+\\ & +t^6\left[-\frac{M^2}{4y^2}+O(\log^3\tfrac{1}{2}y\alpha)\right]+t^4\log\tfrac{1}{2}t\alpha[-(2M^2-1)\{1+\log\tfrac{1}{2}y\alpha+O(y^2)\}]+\\ & +O(t^6\log^2\tfrac{1}{2}y\alpha). \end{aligned} \tag{35}$$

V. Derivation of angle of shock-wave, entropy change at shock, strength of shock, and pressure coefficient

The angle of the shock-wave is given from (33) and

$$\eta-\mu = \tfrac{3}{8}(\gamma+1)^2\frac{M^6}{\alpha^3}t^4+O(t^6\log t). \tag{36}$$

Using the shock-wave equations, we deduce that the change of entropy is proportional to $M^{18}t^{12}/\alpha^6$, and hence that the strength of shock is proportional to M^6t^4/α^2. These results agree with those obtained by

Lighthill (**4**). Using again the shock-wave equations and Bernoulli's equation, we may write the pressure coefficient in the following form:

$$C_p = \frac{p-p_0}{\frac{1}{2}\rho_0 V^2} = -2(f-yf')+\alpha^2(f-yf')^2-f'^2+M^2(f-yf')^2f'^2+\tfrac{1}{4}M^2f'^2, \tag{37}$$

if we neglect terms in $t^6\log^3 t$ on the cone. Substituting (35), with $y=t$, in (37) we find

$$C_p = -t^2-2t^2\log\tfrac{1}{2}t\alpha+3\alpha^2t^4\log^2\tfrac{1}{2}t\alpha+(5M^2-1)t^4\log\tfrac{1}{2}t\alpha+ \\ +t^4\left[3\tfrac{1}{4}M^2+\tfrac{1}{2}+\frac{M^4(\gamma+1)}{\alpha^2}\right]. \tag{38}$$

This equation gives the first and second approximations to the pressure coefficient at the surface of the cone, and it is the same as that found in the author's paper (**1**) where the effect of the shock-wave was completely neglected. Thus it has been demonstrated in this paper that, for the case of supersonic flow past a cone, the additional effect of the shock-wave does not alter the value of the pressure coefficient to order t^4. It is reasonable to infer that this result holds in general for pointed bodies of revolution which have a convex surface. For a comparison of the analytic and numerical solutions the reader is referred to the earlier paper mentioned above.

REFERENCES

1. J. B. Broderick, 'Supersonic flow round pointed bodies of revolution', see above, pp. 98–120.

2. G. I. Taylor and J. W. Maccoll, 'The air pressure on a cone moving at high speeds', *Proc. Roy. Soc.* A **139** (1933), 278–311.

3. Massachusetts Institute of Technology, Technical Report No. I. *Tables of Supersonic Flow around Cones*, The Murray Press Company, Cambridge, Massachusetts, 1947.

4. M. J. Lighthill, 'The position of the shock wave in certain aerodynamic problems', to be published in *Quart. J. Mech. and Applied Math.*

13

oulli's
rm:

$^2f'^2,$

(37)

$y = l,$

(38)

ressure
found
s com-
at, for
shock-
. It is
dies of
nalytic
r men-

on', see

at high

ables of
nbridge,

lynamic